DESIGN AND CHARACTERIZATION OF GELATIN HYDROGELS INCORPORATING LOW-MOLECULAR-WEIGHT DRUGS FOR TISSUE REGENERATION

TAKASHI SAITO

2015

Chapter 2

Enhancement of gene suppression by controlled release of small interfering RNA from gelatin hydrogels

PART II
DESIGN OF GELATIN HYDROGELS INCORPORATING WATER-INSOLUBLE LOW MOLECULAR WEIGHT DRUGS

Chapter 4
Enhancement of in vivo macrophage recruitment by Controlled release of sphingosine-1-phosphate agonist from gelatin hydrogels

ABBREVIATIONS

1,25-D_3	Active vitamin D_3
ALP	Alkaline phosphatase
ANGPT2	Angiopoietin-2
Asc2P	Ascorbic acid 2-phosphate
BCA	Bicinchonic acid
cDNA	Complimentary DNA
CG	Cationized gelatin
CMC	Critical micellar concentration
Colon26-Luc	A luciferase-expressing cell line derived from colon 26
DAB	3,3-diaminobenzidine
DDS	Drug delivery system
DDW	Double distilled water
DMAP	4-dimethylaminopyridine
DMB	1,9-dimethylmethylene blue
DMSO	Dimethyl sulfoxide
DSC	Disuccimidyl carbonate
DSW	Deionized and sterilized water
Dex	Dexamethasone
DFO	Deferoxiamine
DLS	Dynamic light scattering
DMEM	Dulbecco's modified Eagle medium
EBM-2	Endothelial cell basal medium-2
ECM	Extracellular matrix
EDA	Ethylenediamine
EGF	Epidermal growth factor
ELISA	Enzyme-linked immunosorbent assay
ELS	Electrophoretic light scattering
EOG	Ethylene oxide gas
EtOH	Ethanol

β-GP	β-glycerophosphate
HCl	Hydrogen chloride
HIFs	Hypoxia-inducible factors
hMSC	Human mesenchymal stem cells
H&E	Hematoxylin and eosin
HRE	Hypoxia-responsive element
HUVEC	Human umbilical vein endothelial cells
LA-Gelatin	L-lactic acid oligomer grafted gelatin
LLAo	L-lactic acid oligomer
LMWH	Low-molecular-weight heparin
Luc siRNA	siRNA targeted at the firefly luciferase gene
N/P	Amino group number of CG per the phosphate group number of Luc siRNA
p300/CBP	p300/cyclic adenosine monophosphate response element binding protein
PBS	Phosphate-buffered saline
PDGF-B	Platelet-derived growth factor-B
pI5 gelatin	Gelatin with an isoelectric point of 5.0
pI9 gelatin	Gelatin with an isoelectric point of 9.0
pO_2	Partial pressure of oxygen
RNAi	RNA interference
SDS	Sodium dodecyl sulfate
SEW2871	5-[4-phenyl-5-(trifluoromethyl) thiophen-2-yl]-3-[3-(trifluoromethyl) phenyl] 1,2,4-oxadiazole
siRNA	small interfering RNA
α-SMA	α-smooth muscle actin
TNBS	2,4,6-trinitrobenzene sulfonic acid
VEGF	Vascular endothelial growth factor
WST-8	2-(2-methoxy-4-nitrophenyl)-3-(4-nitrophenyl)-5-(2,4-disulfophenyl)-2H-tetrazolium)

GENERAL INTRODUCTION

Advanced surgical therapies currently available, such as reconstructive surgery, endoscopic surgery, and organ/cell transplantation, have undoubtedly saved and improved many lives of patients and their quality of life. On the other hand, several new drugs other than the conventional low-molecular-weight drugs have been developed. However, there are still technical and methodological limitations in their clinical use. One trial of the therapeutic strategies for diseases treatment is called as “regenerative medicine” [1] where the natural-healing potential of patients themselves is utilized to allow the regeneration of autologous tissues. There are two approaches to achieve regenerative medicine; “cell transplantation” and “tissue engineering”. The essential concept of tissue engineering was originally suggested by R. Langer and J. Vacanti in 1993 [2]. In the former case, the transplantation of matured cells of terminal differentiation, precursor or stromal/stem cells are transplanted to induce cell-based tissue regeneration. However, the cells transplantation has not been always of great success, because the survival rate of cells transplanted is poor and consequently their biological function cannot be expected.

The tissue engineering is a biomedical technology or methodology which allows cells to enhance their potential of proliferation and differentiation. Three components are proposed to induce tissue engineering-based tissue regeneration: cells, their scaffolds, and growth factors to accelerate their proliferation and differentiation. At present, the latter two components have been widely investigated to achieve tissue regeneration based on the cells potential. With the development of tissue engineering, the present advantage, disadvantage, and future aspects of tissue engineering are made

clear and summarized by A. Mikos *et al*. in 2006 [3]. The key aspects of tissue engineering are shown in Table 1.

Table 1. key aspects of tissue engineering.

Tissue Engineering Aspect	Challenge
Wound healing environment	Regeneration of lost tissues in essentially "contaminated" conditions.
Scaffold design requirements	Injectability.
	Ability to encapsulate cells.
	Ability to harden to a state which mimics the mechanical properties of bone.
	Degradation at a rate fast enough to allow the in-growth of surrounding tissue.
Cell-surface interactions	Ability to selectively promote the adhesion of specific cell populations while excluding the invasion of others.
Growth-factor delivery	Increased efficiency by loading physiological amounts of growth factors into a scaffold allowing for improved cost-effectiveness.
	Spatial and temporal control over the release of multiple growth factors using multiple kinetic rates.
Assessment	Development of clinically-relevant animal models for in vivo qualitative and quantitative assessment of implanted materials.
Scale-up	Ability to use tissue engineered constructs in large defects where diffusional limitations may limit the viability of encapsulated cells.
	Ability to determine the translatability of results seen with in vivo animal models in the clinical setting.
Specific clinical issues which remain unaddressed	Control over the morphology of regenerated bone.
	Periodontal ligament anchorage and effective gingival seal around titanium dental implants.
	Regeneration of entire teeth with supporting structures in extraction sockets.

As one of the possible ways to realize tissue regeneration application, drug delivery system (DDS) to enhance the biological action of growth factor for cell-based tissue regeneration is practically promising. There are four purposes of DDS: the controlled release of drugs, the stability enhancement of drugs, the absorption acceleration of drugs, and the drugs targeting at the site of action [4]. Previously, the therapeutic effects of drugs with different physicochemical and biological properties have been investigated [5-7]. However, drugs often show their side-effects. To reduce

the side-effects, DDS is expected as a promising technology to modify the biodistribution of drugs and consequently their increasing therapeutic effects. Although some drugs have a highly therapeutic potential, they cannot be used because of the severe side-effects at the site other than the action one upon administering systemically. In this case, the local and controlled release of drugs will dissolve the problems. The DDS technology enables the drugs of low-molecular-weight compounds [7-16], genes [17-20], peptide [21-23], antibody [24, 25], and proteins [26-28] to efficiently enhance the biological effects *in vivo*. Other application of DDS technology are for diagnosis [29], imaging [30], and cell culture technique [31]. This is because it facilitates drug molecules at the right site, the appropriate time, and suitable concentration. As the DDS carriers for drugs release, a variety of materials, such as polymer, ceramics, and metal have been investigated [32-40]. Each of the materials has advantages and disadvantages. Therefore, their combinations have been also investigated to compensate their features [41-43]. For the drugs release of DDS technology, there is one problem to be improved. That is the remaining of release carrier material after drug release. The remaining materials often cause inflammation and therapeutically undesirable responses [44, 45]. Therefore, for the practical use, it is indispensable to develop a carrier material for drug release systems which does not induce the materials-induced responses. It is well recognized that, compared with hydrophobic polymer materials, hydrophilic materials of hydrogels show weaker the foreign body responses. Based on this idea, several hydrogels and their combination with other materials have been investigated [46-65].

Gelatin is a protein which is prepared through an acid and alkaline process of collagen. Gelatin is a biodegradable material and has been extensively used for food, drug ingredients, cosmetics, and medical purposes. Gelatin has various side chains

which can be chemically modified with ease. Dehydrothermal or chemical treatment enables gelatin to intermolecularly cross-link to obtain the hydrogel. The gelatin hydrogel can be enzymatically degraded and the degradability can be changed by altering the cross-linking condition. The biosafety of gelatin has been proven through its long practical applications [66-68]. In addition, the hydrogel system is also applicable for the controlled release of low-molecular-weight drugs [54, 69-72]. Many types of drugs can be released from the hydrogel. The release mechanism is that the drug immobilized on gelatin molecules can be released when gelatin is water-solubilized to generate the water-soluble fragments [8, 73-75]. However, most of low-molecular-weight drugs are not always strongly interacted with gelatin molecules for their immobilization, resulting in the initial rapid release. Therefore, it is necessary to create a methodology how to decrease the initial burst release of drugs. To enhance the interaction of drugs with gelatin molecules, first the drugs were modified with micelles of gelatin, and then the drugs-gelatin micelles were incorporated into the gelatin hydrogel. By this technology, the controlled release of drugs from the gelatin hydrogel was achieved. In addition, as one trial to achieve the higher efficiency of drugs, various components and shapes of the gelatin hydrogels were designed and prepared. Another thing is that in this series of research, the drugs were applied for tissue regeneration. The drugs directly act on cells to allow to activate their biological function. The activated cells enhance the natural-healing potential of body, resulting in promoted tissue regeneration and repairing.

The objective of this thesis is to design and prepare gelatin hydrogels incorporating various types of low-molecular-weight drugs for their controlled and local release of the drugs, and evaluate the efficacy of drugs released from gelatin hydrogels

comparing with free drugs. In PART I, gelatin hydrogels incorporating water-soluble low-molecular-weight drugs were designed. The release profile of the drugs was evaluated. Then, the biological characterizations of drugs released from gelatin hydrogels were performed by evaluating their actions with disease animal models.

Chapter 1 is concerned with the hypoxia-induced angiogenesis by the controlled release of deferoxiamine (DFO) from gelatin hydrogels *in vivo*. The time profile of DFO release from the hydrogels incorporating DFO and the hydrogel degradation were examined. Following the intramuscular implantation of hydrogels incorporating DFO into a mouse model of ischemic leg, the angiogenic effect was evaluated in comparison to that obtained with free DFO injection. Biodegradable gelatin hydrogels could release DFO for an enhanced *in vivo* biological activity, resulting in promoted angiogenesis.

Chapter 2 is concerned with small interfering RNA (siRNA) transfection efficacy by gelatin hydrogels incorporating siRNA and cationized gelatin (CG) complex. Gelatin was cationized by chemically introducing ethylene diamine into the carboxyl groups in different conditions to obtain CG. The CG was mixed with siRNA in double distilled water (DDW) to form polyion complexes. The complex was mixed with gelatin in DDW, followed by the chemical crosslinking to prepare gelatin hydrogels incorporating the complex of siRNA and CG. The siRNA release profile from the hydrogel was investigated while the activity of siRNA released was evaluated.

Chapter 3 is concerned with a gelatin hydrogel system for the controlled release of low-molecular-weight heparin (LMWH). CG was mixed in DDW to form the complex of LMWH. The complex was mixed with gelatin, followed by the dehydrothermal cross-linking to prepare gelatin hydrogels incorporating the complex of

LMWH and cationized gelatin. The profile of LMWH release from the hydrogel and the hydrogel degradation were examined. When applied to the mouse model of abdominal membrane fibrosis, the hydrogel system of LMWH release showed a promising anti-fibrotic effect.

In PART II, gelatin hydrogels incorporating water-insoluble low-molecular-weight drugs were designed. As one of the amphiphilic polymers, L-lactic acid oligomer grafted gelatin (LA-Gelatin) was prepared. The water-insoluble drugs were water-solubilized by the micelle of LA-Gelatin. The drugs water-solubilized were homogeneously incorporated into gelatin hydrogels. The biological characterizations of drugs released from gelatin hydrogels were performed with cell culture experiments *in vitro* as well as some disease animal models *in vivo*.

Chapter 4 is concerned with a gelatin hydrogel system for the controlled release of a water-insoluble agonist of sphingosine-1-phosphate type 1 receptor agonist (SEW2871). SEW2871 (SEW) was water-solubilized by the micelle formation with LA-Gelatin (SEW-micelle). SEW-micelle were mixed with gelatin, followed by the dehydrothermal crosslinking of gelatin to obtain gelatin hydrogels incorporating SEW-micelle. SEW was released from the hydrogels incorporating SEW-micelle *in vitro* and *in vivo*. The water-solubilized SEW showed *in vitro* macrophage migration activity. When implanted into the back subcutis or the skin wound defect of mice, the hydrogel incorporating SEW-micelle promoted macrophage migration toward the tissue around the implanted site to a significantly great extent compared with SEW-free hydrogel and that mixed with SEW-micelle.

Chapter 5 is concerned with gelatin sponges for the controlled release of dexamethasone (Dex) and active vitamin D_3 (1,25-D_3). The Dex and 1,25-D_3 were

water-solubilized by the micelle formation with LA-Gelatin (Dex-micelle and D_3-micelle). Three dimensional sponge scaffolds of gelatin hydrogel incorporating Dex- and 1,25-D_3-micelle were prepared. The human mesenchymal stem cells (hMSC) were seeded into the sponge by an agitated seeding method. When the Dex and 1,25-D_3 were added to an osteogenic differentiation medium, the level of alkaline phosphatase (ALP) activity and the amount of mineralization of hMSC increased to a significantly great extent compared with those of 1,25-D_3-free medium. Moreover, gelatin sponges incorporating Dex- and D_3-micelle showed the highest amount of mineralization compared with gelatin sponges, gelatin sponges incorporating Dex-micelle, and gelatin sponges incorporating D_3-micelle.

In summary, this thesis describes the importance and necessity of controlled release system of low-molecular-weight drugs for tissue regeneration. It is concluded that the appropriate release profile of drugs is key to effectively achieve the drugs-based applications of tissue regeneration.

REFERENCES

[1] D.L. Stocum, Regenerative biology and medicine, Journal of musculoskeletal & neuronal interactions, 2 (2002) 270-273.

[2] R. Langer, J.P. Vacanti, Tissue engineering, Science, 260 (1993) 920-926.

[3] A.G. Mikos, S.W. Herring, P. Ochareon, J. Elisseeff, H.H. Lu, R. Kandel, F.J. Schoen, M. Toner, D. Mooney, A. Atala, M.E. Van Dyke, D. Kaplan, G. Vunjak-Novakovic, Engineering complex tissues, Tissue engineering, 12 (2006) 3307-3339.

[4] Y. Kimura, Y. Tabata, Experimental tissue regeneration by DDS technology of bio-signaling molecules, Journal of dermatological science, 47 (2007) 189-199.

[5] R.M. Pearson, V.V. Juettner, S. Hong, Biomolecular corona on nanoparticles: a survey of recent literature and its implications in targeted drug delivery, Frontiers in chemistry, 2 (2014) 108.

[6] G. Saravanakumar, V.G. Deepagan, R. Jayakumar, J.H. Park, Hyaluronic acid-based conjugates for tumor-targeted drug delivery and imaging, Journal of biomedical nanotechnology, 10 (2014) 17-31.

[7] M.C. Rodriguez, M. Cudic, Optimization of physicochemical and pharmacological properties of peptide drugs by glycosylation, Methods Mol Biol, 1081 (2013) 107-136.

[8] T. Tanigo, R. Takaoka, Y. Tabata, Sustained release of water-insoluble simvastatin from biodegradable hydrogel augments bone regeneration, J Control Release, 143 (2010) 201-206.

[9] T. Saito, Y. Tabata, Preparation of gelatin hydrogels incorporating low-molecular-weight heparin for anti-fibrotic therapy, Acta biomaterialia, 8 (2012) 646-652.

[10] A. Hokugo, T. Saito, A. Li, K. Sato, Y. Tabata, R. Jarrahy, Stimulation of bone regeneration following the controlled release of water-insoluble oxysterol from biodegradable hydrogel, Biomaterials, 35 (2014) 5565-5571.

[11] T. Matsuzaki, T. Matsushita, Y. Tabata, T. Saito, T. Matsumoto, K. Nagai, R. Kuroda, M. Kurosaka, Intra-articular administration of gelatin hydrogels incorporating rapamycin-micelles reduces the development of experimental osteoarthritis in a murine model, Biomaterials, 35 (2014) 9904-9911.

[12] B.S. Wong, S.L. Yoong, A. Jagusiak, T. Panczyk, H.K. Ho, W.H. Ang, G. Pastorin, Carbon nanotubes for delivery of small molecule drugs, Adv Drug Deliv Rev, 65 (2013) 1964-2015.

[13] M. Casolaro, R. Cini, B. Del Bello, M. Ferrali, E. Maellaro, Cisplatin/hydrogel complex in cancer therapy, Biomacromolecules, 10 (2009) 944-949.

[14] J. Cha, W. Lee, C. Park, Y. Cho, C.-H. Ahn, I. Kwon, Preparation and characterization of cisplatin-incorporated chitosan hydrogels, microparticles, and nanoparticles, Macromolecular Research, 14 (2006) 573-578.

[15] M. Konishi, Y. Tabata, M. Kariya, A. Suzuki, M. Mandai, K. Nanbu, K. Takakura, S. Fujii, In vivo anti-tumor effect through the controlled release of cisplatin from biodegradable gelatin hydrogel, J Control Release, 92 (2003) 301-313.

[16] J.R. Tauro, R.A. Gemeinhart, Extracellular protease activation of chemotherapeutics from hydrogel matrices: a new paradigm for local chemotherapy, Molecular pharmaceutics, 2 (2005) 435-438.

[17] P.L. Felgner, G.M. Ringold, Cationic liposome-mediated transfection, Nature, 337 (1989) 387-388.

[18] T. Nishi, K. Yoshizato, S. Yamashiro, H. Takeshima, K. Sato, K. Hamada, I.

Kitamura, T. Yoshimura, H. Saya, J. Kuratsu, Y. Ushio, High-efficiency in vivo gene transfer using intraarterial plasmid DNA injection following in vivo electroporation, Cancer research, 56 (1996) 1050-1055.

[19] H. Cabral, K. Kataoka, Progress of drug-loaded polymeric micelles into clinical studies, J Control Release, 190 (2014) 465-476.

[20] D. Oupicky, C. Konak, K. Ulbrich, M.A. Wolfert, L.W. Seymour, DNA delivery systems based on complexes of DNA with synthetic polycations and their copolymers, J Control Release, 65 (2000) 149-171.

[21] H. Nakagami, T. Nishikawa, N. Tamura, A. Maeda, H. Hibino, M. Mochizuki, T. Shimosato, T. Moriya, R. Morishita, K. Tamai, K. Tomono, Y. Kaneda, Modification of a novel angiogenic peptide, AG30, for the development of novel therapeutic agents, Journal of cellular and molecular medicine, 16 (2012) 1629-1639.

[22] D.J. Craik, D.P. Fairlie, S. Liras, D. Price, The future of peptide-based drugs, Chemical biology & drug design, 81 (2013) 136-147.

[23] S. Majumdar, T.J. Siahaan, Peptide-mediated targeted drug delivery, Medicinal research reviews, 32 (2012) 637-658.

[24] W. Ding, Risk-based scientific approach for determination of extractables/leachables from biomanufacturing of antibody-drug conjugates (ADCs), Methods Mol Biol, 1045 (2013) 303-311.

[25] M.A. Firer, G. Gellerman, Targeted drug delivery for cancer therapy: the other side of antibodies, Journal of hematology & oncology, 5 (2012) 70.

[26] X. Guo, J. Liao, H. Park, A. Saraf, R.M. Raphael, Y. Tabata, F.K. Kasper, A.G. Mikos, Effects of TGF-beta3 and preculture period of osteogenic cells on the chondrogenic differentiation of rabbit marrow mesenchymal stem cells encapsulated in

a bilayered hydrogel composite, Acta biomaterialia, 6 (2010) 2920-2931.

[27] M. Matsui, Y. Tabata, Enhanced angiogenesis by multiple release of platelet-rich plasma contents and basic fibroblast growth factor from gelatin hydrogels, Acta biomaterialia, 8 (2012) 1792-1801.

[28] H. Wang, O.C. Boerman, K. Sariibrahimoglu, Y. Li, J.A. Jansen, S.C. Leeuwenburgh, Comparison of micro- vs. nanostructured colloidal gelatin gels for sustained delivery of osteogenic proteins: Bone morphogenetic protein-2 and alkaline phosphatase, Biomaterials, 33 (2012) 8695-8703.

[29] S. Bhaskar, F. Tian, T. Stoeger, W. Kreyling, J.M. de la Fuente, V. Grazu, P. Borm, G. Estrada, V. Ntziachristos, D. Razansky, Multifunctional Nanocarriers for diagnostics, drug delivery and targeted treatment across blood-brain barrier: perspectives on tracking and neuroimaging, Particle and fibre toxicology, 7 (2010) 3.

[30] M. Longmire, P.L. Choyke, H. Kobayashi, Clearance properties of nano-sized particles and molecules as imaging agents: considerations and caveats, Nanomedicine (Lond), 3 (2008) 703-717.

[31] E.J. Carbone, T. Jiang, C. Nelson, N. Henry, K.W. Lo, Small molecule delivery through nanofibrous scaffolds for musculoskeletal regenerative engineering, Nanomedicine : nanotechnology, biology, and medicine, 10 (2014) 1691-1699.

[32] S.W. Kim, Y.H. Bae, T. Okano, Hydrogels: swelling, drug loading, and release, Pharm Res, 9 (1992) 283-290.

[33] W.J. Habraken, J.G. Wolke, J.A. Jansen, Ceramic composites as matrices and scaffolds for drug delivery in tissue engineering, Adv Drug Deliv Rev, 59 (2007) 234-248.

[34] S. Ganta, H. Devalapally, A. Shahiwala, M. Amiji, A review of stimuli-responsive

nanocarriers for drug and gene delivery, J Control Release, 126 (2008) 187-204.

[35] R.C. Mundargi, V.R. Babu, V. Rangaswamy, P. Patel, T.M. Aminabhavi, Nano/micro technologies for delivering macromolecular therapeutics using poly(D,L-lactide-co-glycolide) and its derivatives, J Control Release, 125 (2008) 193-209.

[36] M. Prabaharan, Review paper: chitosan derivatives as promising materials for controlled drug delivery, J Biomater Appl, 23 (2008) 5-36.

[37] E.A. Simone, T.D. Dziubla, V.R. Muzykantov, Polymeric carriers: role of geometry in drug delivery, Expert Opin Drug Deliv, 5 (2008) 1283-1300.

[38] A.J. Halliday, M.J. Cook, Polymer-based drug delivery devices for neurological disorders, CNS Neurol Disord Drug Targets, 8 (2009) 205-221.

[39] D. Costa, M.G. Miguel, B. Lindman, Swelling properties of cross-linked DNA gels, Adv Colloid Interface Sci, 158 (2010) 21-31.

[40] C. Kojima, Design of stimuli-responsive dendrimers, Expert Opin Drug Deliv, 7 (2010) 307-319.

[41] C. Foss, E. Merzari, C. Migliaresi, A. Motta, Silk fibroin/hyaluronic acid 3D matrices for cartilage tissue engineering, Biomacromolecules, 14 (2013) 38-47.

[42] U. Freymann, M. Endres, K. Neumann, H.J. Scholman, L. Morawietz, C. Kaps, Expanded human meniscus-derived cells in 3-D polymer-hyaluronan scaffolds for meniscus repair, Acta biomaterialia, 8 (2012) 677-685.

[43] K.C. Kavya, R. Jayakumar, S. Nair, K.P. Chennazhi, Fabrication and characterization of chitosan/gelatin/nSiO2 composite scaffold for bone tissue engineering, International journal of biological macromolecules, 59 (2013) 255-263.

[44] M. Amon, R. Menapace, U. Radax, H. Freyler, In vivo study of cell reactions on

poly(methyl methacrylate) intraocular lenses with different surface properties, J Cataract Refract Surg, 22 Suppl 1 (1996) 825-829.

[45] P.S. Stayton, M.E. El-Sayed, N. Murthy, V. Bulmus, C. Lackey, C. Cheung, A.S. Hoffman, 'Smart' delivery systems for biomolecular therapeutics, Orthod Craniofac Res, 8 (2005) 219-225.

[46] J. Choi, T. Konno, M. Takai, K. Ishihara, Regulation of cell proliferation by multi-layered phospholipid polymer hydrogel coatings through controlled release of paclitaxel, Biomaterials, 33 (2012) 954-961.

[47] J. Hurler, O.A. Berg, M. Skar, A.H. Conradi, P.J. Johnsen, N. Skalko-Basnet, Improved burns therapy: Liposomes-in-hydrogel delivery system for mupirocin, Journal of pharmaceutical sciences, (2012).

[48] H. Kumar Singh Yadav, H.G. Shivakumar, In Vitro and In Vivo Evaluation of pH-Sensitive Hydrogels of Carboxymethyl Chitosan for Intestinal Delivery of Theophylline, ISRN pharmaceutics, 2012 (2012) 763127.

[49] W.G. Sanders, P.C. Hogrebe, D.W. Grainger, A.K. Cheung, C.M. Terry, A biodegradable perivascular wrap for controlled, local and directed drug delivery, J Control Release, 161 (2012) 81-89.

[50] E. Khodaverdi, F.S. Tekie, S.A. Mohajeri, F. Ganji, G. Zohuri, F. Hadizadeh, Preparation and investigation of sustained drug delivery systems using an injectable, thermosensitive, in situ forming hydrogel composed of PLGA-PEG-PLGA, AAPS PharmSciTech, 13 (2012) 590-600.

[51] J. Li, C. Gong, X. Feng, X. Zhou, X. Xu, L. Xie, R. Wang, D. Zhang, H. Wang, P. Deng, M. Zhou, N. Ji, Y. Zhou, Y. Wang, Z. Wang, G. Liao, N. Geng, L. Chu, Z. Qian, Q. Chen, Biodegradable thermosensitive hydrogel for SAHA and DDP delivery:

therapeutic effects on oral squamous cell carcinoma xenografts, PloS one, 7 (2012) e33860.

[52] G.E. Rooney, A.M. Knight, N.N. Madigan, L. Gross, B. Chen, C.V. Giraldo, S. Seo, J.J. Nesbitt, M. Dadsetan, M.J. Yaszemski, A.J. Windebank, Sustained delivery of dibutyryl cyclic adenosine monophosphate to the transected spinal cord via oligo [(polyethylene glycol) fumarate] hydrogels, Tissue engineering. Part A, 17 (2011) 1287-1302.

[53] M. Dadsetan, Z. Liu, M. Pumberger, C.V. Giraldo, T. Ruesink, L. Lu, M.J. Yaszemski, A stimuli-responsive hydrogel for doxorubicin delivery, Biomaterials, 31 (2010) 8051-8062.

[54] S. Gordon, E. Teichmann, K. Young, K. Finnie, T. Rades, S. Hook, In vitro and in vivo investigation of thermosensitive chitosan hydrogels containing silica nanoparticles for vaccine delivery, European journal of pharmaceutical sciences : official journal of the European Federation for Pharmaceutical Sciences, 41 (2010) 360-368.

[55] M. Shibayama, T. Norisuye, Gel formation analyses by dynamic light scattering, B Chem Soc Jpn, 75 (2002) 641-659.

[56] H. Sa-Lima, K. Tuzlakoglu, J.F. Mano, R.L. Reis, Thermoresponsive poly(N-isopropylacrylamide)-g-methylcellulose hydrogel as a three-dimensional extracellular matrix for cartilage-engineered applications, Journal of biomedical materials research. Part A, 98 (2011) 596-603.

[57] K. Nagase, J. Kobayashi, A. Kikuchi, Y. Akiyama, H. Kanazawa, T. Okano, Preparation of thermoresponsive cationic copolymer brush surfaces and application of the surface to separation of biomolecules, Biomacromolecules, 9 (2008) 1340-1347.

[58] H. Tokuyama, T. Iwama, Temperature-swing solid-phase extraction of heavy

metals on a poly(N-isopropylacrylamide) hydrogel, Langmuir : the ACS journal of surfaces and colloids, 23 (2007) 13104-13108.

[59] P. Froimowicz, D. Klinger, K. Landfester, Photoreactive nanoparticles as nanometric building blocks for the generation of self-healing hydrogel thin films, Chemistry, 17 (2011) 12465-12475.

[60] S. Matsumoto, S. Yamaguchi, S. Ueno, H. Komatsu, M. Ikeda, K. Ishizuka, Y. Iko, K.V. Tabata, H. Aoki, S. Ito, H. Noji, I. Hamachi, Photo gel-sol/sol-gel transition and its patterning of a supramolecular hydrogel as stimuli-responsive biomaterials, Chemistry, 14 (2008) 3977-3986.

[61] T.Y. Liu, S.H. Hu, K.H. Liu, D.M. Liu, S.Y. Chen, Study on controlled drug permeation of magnetic-sensitive ferrogels: effect of Fe3O4 and PVA, J Control Release, 126 (2008) 228-236.

[62] F. Corrente, P. Paolicelli, P. Matricardi, B. Tita, F. Vitali, M.A. Casadei, Novel pH-sensitive physical hydrogels of carboxymethyl scleroglucan, Journal of pharmaceutical sciences, 101 (2012) 256-267.

[63] P. Sun, P. Li, Y.M. Li, Q. Wei, L.H. Tian, A pH-sensitive chitosan-tripolyphosphate hydrogel beads for controlled glipizide delivery, Journal of biomedical materials research. Part B, Applied biomaterials, 97 (2011) 175-183.

[64] M. Bahram, F. Keshvari, P. Najafi-Moghaddam, Development of cloud point extraction using pH-sensitive hydrogel for preconcentration and determination of malachite green, Talanta, 85 (2011) 891-896.

[65] A.W. Chan, R.A. Whitney, R.J. Neufeld, Semisynthesis of a controlled stimuli-responsive alginate hydrogel, Biomacromolecules, 10 (2009) 609-616.

[66] D.L. Heene, D. Zekorn, H.G. Lasch, Gelatine plasma volume expanders: chemistry,

biological activities and clinical experiences, Bibliotheca haematologica, 29 (1968) 907-913.

[67] Y. Marois, N. Chakfe, X. Deng, M. Marois, T. How, M.W. King, R. Guidoin, Carbodiimide cross-linked gelatin: a new coating for porous polyester arterial prostheses, Biomaterials, 16 (1995) 1131-1139.

[68] D. Zekorn, Intravascular retention, dispersal, excretion and break-down of gelatin plasma substitutes, Bibliotheca haematologica, 33 (1969) 131-140.

[69] D. Sivakumaran, D. Maitland, T. Hoare, Injectable microgel-hydrogel composites for prolonged small-molecule drug delivery, Biomacromolecules, 12 (2011) 4112-4120.

[70] M.C. Chen, H.W. Tsai, C.T. Liu, S.F. Peng, W.Y. Lai, S.J. Chen, Y. Chang, H.W. Sung, A nanoscale drug-entrapment strategy for hydrogel-based systems for the delivery of poorly soluble drugs, Biomaterials, 30 (2009) 2102-2111.

[71] L. Indolfi, F. Causa, C. Giovino, F. Ungaro, F. Quaglia, P.A. Netti, Microsphere-integrated drug-eluting stents: PLGA microsphere integration in hydrogel coating for local and prolonged delivery of hydrophilic antirestenosis agents, Journal of biomedical materials research. Part A, 97 (2011) 201-211.

[72] R.S. Navath, A.R. Menjoge, H. Dai, R. Romero, S. Kannan, R.M. Kannan, Injectable PAMAM dendrimer-PEG hydrogels for the treatment of genital infections: formulation and in vitro and in vivo evaluation, Molecular pharmaceutics, 8 (2011) 1209-1223.

[73] M. Yamamoto, Y. Tabata, Y. Ikada, Ectopic bone formation induced by biodegradable hydrogels incorporating bone morphogenetic protein, Journal of biomaterials science. Polymer edition, 9 (1998) 439-458.

[74] M. Yamamoto, Y. Tabata, L. Hong, S. Miyamoto, N. Hashimoto, Y. Ikada, Bone

regeneration by transforming growth factor beta1 released from a biodegradable hydrogel, J Control Release, 64 (2000) 133-142.

[75] T. Kushibiki, K. Matsumoto, T. Nakamura, Y. Tabata, Suppression of the progress of disseminated pancreatic cancer cells by NK4 plasmid DNA released from cationized gelatin microspheres, Pharm Res, 21 (2004) 1109-1118.

PART I

DESIGN OF GELATIN HYDROGELS INCORPORATING WATER-SOLUBLE LOW-MOLECULAR-WEIGHT DRUGS

Chapter 1

Enhancement of in vivo hypoxia-induced angiogenesis by controlled release of deferoxiamine from gelatin hydrogels

INTRODUCTION

In healthy tissues, the partial pressure of oxygen (pO_2) varies from tissue to tissue in the microenvironment. Oxygen diffuses passively across the capillary wall from the blood to the tissue according to its concentration gradient. The oxygen tension of arterial blood is 100 mmHg (pO_2 = 13.2%). While that of venous blood is 40 mmHg (pO_2 = 5.3%) [1]. The tissue pO_2 ranges from 2.5% to 9.5% (20–72 mmHg). The pO_2 of healthy brain [2], lung [3], liver [4], kidney [5], muscle [6], bone marrow [7] and cell [1] are 4.4%, 5.6%, 5.4%, 9.5%, 3.8%, 6.4% and 2.5%, respectively. On the other hand, the inadequate perfusion of body fluid in diseased tissues causes the formation of multiple temporary or chronic areas at low pO_2 (hypoxia). Hypoxia is usually defined as pO_2 < 2.0%, and severe hypoxia (anoxia) is defined as pO_2 < 0.02% [8] and [9]. Hypoxia is often observed in regions of intense inflammation, such as within arthritic joints, atherosclerotic plaques and, notably, domains within solid tumors [10]. Hypoxia is an essential initial process of inflammation and generally induced when tissues are injured and damaged. Hypoxia naturally induces the production of hypoxia-inducible factors (HIFs) in the body. Three isoforms of HIF (HIF-1, -2 and -3) have been reported [11]. HIF-1 was discovered in 1995 [12] and normally consists of HIF-1α and HIF-1β subunits [13]. HIF-1α can recruit the transcriptional coactivator of p300/cyclic adenosine monophosphate response element binding protein (p300/CBP) in the nucleus. The active HIF-complex (i.e. HIF-1α, -β or p300/CBP complex) binds to the

hypoxia-responsive element (HRE), which can induce several proteins and enzymes involved in glucose uptake and metabolism, angiogenesis, erythropoiesis, cell proliferation and the control of apoptosis [13-20]. HIF-1α is very unstable under normal pO_2 (normoxia), and the half-life period in the cells is <5 min [21]. This turnover is controlled by the post-translational modifications of the degradation and inactivation pathways [22, 23]. On the other hand, the production of HIF-1α is increased under hypoxic conditions. The exposure of cells to nickel(II) and cobalt(II) ions stabilizes HIF-1α protein because the HIF-1α degradation and inactivation pathways can be suppressed [24] and [25]. In addition, the HIF-1α level is increased by the Fe(II) chelator which inhibits prolyl hydroxylase domain containing enzyme and factor inhibiting HIF-1, which are involved in tagging HIF-1α for proteosomal degradation. The Fe(II) chelators desferal, exjade and ferriprox are clinically used. Deferoxiamine mesilate (DFO) is the desferal of an Fe(II) ion chelator and is widely used as a research and clinical drug. Generally, DFO is used for hypoferremia treatment. DFO can change the intracellular condition to hypoxic by removing Fe(II) ions [24] and [26] and stabilizing the intracellular HIF-1□. Therefore, if DFO is used efficiently, angiogenesis can be expected. The induction of angiogenesis by DFO treatment has been reported in the literature [27, 28]. However, DFO is a water-soluble, low-molecular-weight drug and the time period of vascular retention is very short [29]. Hence, systemic administration tends to result in Fe(II) ions being removed randomly from the body. As one trial to tackle the problems, it is necessary to develop a local release system for DFO. Local DFO release will induce angiogenesis as a result of HIF-1 upregulation.

The objective of this chapter is to design a gelatin hydrogel for the controlled release of DFO. Gelatin and DFO have being used clinically as drug carriers/medical

materials and as a therapeutic agent, respectively. The time profile of DFO release from hydrogels incorporating DFO and hydrogel degradation was examined. Following the intramuscular implantation of hydrogel incorporating DFO into a mouse model of ischemic leg, the angiogenic effect was evaluated in comparison to that obtained with free DFO injection.

EXPERIMENTAL

Materials

Gelatin with an isoelectric point (pI) of 9.0 (weight-average molecular weight (Mw) = 100,000), prepared through acid processing of pig skin (pI9 gelatin), and collagenase L were kindly supplied from Nitta Gelatin Co., Osaka, Japan. Normal human umbilical vein endothelial cells (HUVEC), endothelial cell basal medium-2 (EBM-2) and EGM-2 BulletKit (EGM-2) were purchased from Takara Bio Inc., Shiga, Japan. Cell Count Reagent SF was purchased from Nacalai Tesque Inc., Kyoto, Japan to examine

(2-(2-methoxy-4-nitrophenyl)-3-(4-nitrophenyl)-5-(2,4-disulfophenyl)-2H-tetrazolium) (WST-8) assay. Dulbecco's phosphate-buffered saline was purchased from Nissui Pharmaceutical Co. Ltd., Tokyo, Japan to prepare 1× phosphate-buffered saline aqueous solution (PBS, pH 7.4).

HIF-1α immnoassay

An HIF-1α immnoassay was performed to check the biological activity of DFO. HUVECs were cultured in EBM-2 and EGM-2, and used at the passages 2–4. The cells (1×10^4 cells/100 μl) were seeded into each well of a 96-well black microplate with a

clear bottom (#3603, Corning Inc., New York) and incubated overnight at 37 °C and 20% O_2 in an O_2-controllable incubator (O_2/CO_2 incubator 9200E, Wakenyaku Co. Ltd., Kyoto, Japan). Next, the medium was changed to that containing different concentrations of DFO, while cell culture continued in the medium which had been preincubated at 1.0%, 5.0% and 20% O_2 for 24 hr. Next, the HIF-1α immunoassay of cells was carried out by cell-based enzyme-linked immunosorbent assay (ELISA) human total HIF-1α kit (R&D Systems Inc., Minneapolis, MN) according to the manufacturer's protocol. Briefly, the medium was removed, and the well was washed with PBS (100 μl) three times. The cells were fixed with 100 μl of 4 vol% paraformaldehyde in PBS for 20 min at room temperature. The formaldehyde solution was removed and the well was washed three times with 200 μl of a buffered solution containing preservatives (wash buffer) for 5 min with gentle shaking. The wash buffer was removed and 100 μl of a quenching buffer (0.6% H_2O_2) was added while the plate was incubated for 20 min at room temperature. The quenching buffer was removed, and the well was washed three times with 200 μl of the wash buffer. Then, 100 μl of 10% fetal bovine serum in wash buffer (blocking buffer) was added into the well, and the plate was incubated for 1 hr at room temperature. After removing the blocking buffer, the well was washed three times with 200 μl of the wash buffer. Next, a primary antibody mixture (100 μl) was added to each well, followed by incubation for 16 hr at 4 °C. Following the removal of primary antibody mixture and washing the well three times, a secondary antibody mixture (100 μl) was added to each well, followed by 2 hr incubation at room temperature. The secondary antibody mixture was removed, and the well was washed twice with the wash buffer and PBS. Then, a sensitive and stable fluorogenic substrate for horseradish-peroxidase (substrate F1, 75 μl) was added to each

well and the incubation was continued for 30 min at room temperature protected from direct light. Next, a sensitive and stable fluorogenic substrate for alkaline phosphatase (substrate F2, 75 μl) was added and similar procedure was done. The fluorescence of mixed substrate F1 and F2 solution was measured at room temperature on a SpectraMax Gemini EM (Molecular Device, Osaka, Japan) at excitation and emission wavelengths of 540 and 600 nm or 360 and 450 nm. The amount of total HIF-1α in the cells was assessed from the fluorescent intensity at 600 nm, while that of total cytochrome c in the cells was done from that at 450 nm. The amount of total HIF-1α was normalized to that of the total cytochrome c.

Vascular endothelial growth factor immnoassay

HUVECs (1×10^4 cells/100 μl) were seeded into each well of a 96-well black microplate with a clear bottom and incubated overnight at 37 °C and 20% O_2 in an O_2-controllable incubator. Next, the medium was exchanged by that containing different concentrations of DFO, while cell culture continued in medium which had been preincubated at 1.0% and 5.0% O_2 for 24 hr at O_2 percentages of 1.0 and 5.0 for 24 hr. Next, vascular endothelial growth factor (VEGF) immunoassay was carried out by VEGF ELISA Quantikine kit (#DVE00, R&D Systems Inc., Minneapolis, MN) according to the manufacturer's protocol. Briefly, assay diluent RD1W (50 μl) and the cell culture supernatant collected (100 μl) were added to each well of a 96-well multiwell microplate coated with a mouse monoclonal antibody against VEGF, while the plate was incubated for 2 hr at room temperature. The solution was removed, and the well was washed times with 400 μl of the wash buffer. Then, polyclonal antibody against VEGF conjugated to horseradish peroxidase (200 μl) was added to each well

while the plate was incubated for 2 hr at room temperature. The solution was removed, and the well was washed three times. A stabilized hydrogen peroxide and chromogen solution (200 μl) was added to each well, followed by incubation for 20 min at room temperature, protecting the plate from direct light. A sulfuric acid solution (2 N, 50 μl) was added to each well. The absorbance of medium was measured at 450 nm by a VERSAmax microplate reader (Molecular Devices, Sunnyvale, CA).

Quantitative real-time reverse-transcription polymerase chain reaction (qPCR) assay

Total RNA was collected from HUVECs using the RNAeasy Plus Mini kit (Qiagen, Hilden, Germany) according to the manufacturer's protocol. The cells were prepared by the same procedure as described above. Complimentary DNA (cDNA) was prepared from 1 ng of whole RNA by use of the SuperScript VILO cDNA synthesis kit (Invitrogen, Carlsbad, CA), and analyzed with the SYBR-Green based, quantitative fluorescent PCR method (Applied Biosystems, Foster City, CA). Fluorescence was detected with an Applied Biosystems 7500 real-time PCR system (Applied Biosystems, Foster City, CA, USA). The primers of *angiopoietin-2* (*ANGPT2*), *epidermal growth factor* (*EGF*), *platelet-derived growth factor-B* (*PDGF-B*) and *β-actin* as a housekeeping gene are summarized in Table 1. The following PCR conditions were used: 95 °C for 15 min, followed by 40 cycles of 94 °C for 15 s, 60 °C for 30 s, and 72 °C for 1 min, followed by 72 °C for a final 10 min. Fold-induction was calculated using the Ct method, $\Delta\Delta Ct = (Ct^{target} - Ct^{housekeeping})^{infected} - (Ct^{target} - Ct^{housekeeping})^{uninfected}$, and the final data were derived from $2^{-\Delta\Delta Ct}$. The value obtained was normalized to that of cells cultured at 5.0% O_2 as 1.0.

Table 1
Primers used in Real-time rt-PCR analysis.

Gene	Forward	Reverse	Tm[a]
Angiopoietin-2 (ANGPT2) NM_001118887.1	5'-ggatggagacaacgacaaatg-3'	5'-ggaccacatgcatcaaacc-3'	60
Epidermal growth factor (EGF) NM_001178130.1	5'-aagaatgggggtcaaccagt-3'	5'-tgaagttggttgcattgacc-3'	60
Platelet-Derived Growth Factor-B (PDGF-B) NM_002608.2	5'-ctggcatgcaagtgtgagac-3'	5'-cgaatggtcacccgagttt-3'	60
β-actin NM_001101.2	5'-ccaaccgcgagaagatga-3'	5'-ccagaggcgtacagggatag-3'	59

[a] The melting temperature at which 50% of double-stranded DNA is separated into single-stranded DNA

Evaluation of DFO cytotoxicity

The cytotoxicity of DFO was evaluated by the conventional WST-8 assay. Briefly, HUVECs (5×10^3 cells) were cultured in each well of a 96-well multiwell culture plate (#3595, Corning Inc., NY) using medium (100 μl) which had been preincubated at 5.0% O_2 for 24 hr. The medium was exchanged for 100 μl of medium with or without DFO at different concentrations, followed by incubation for 24, 48 and 72 hr. After removal of the medium, 100 μl of medium containing WST-8 was added, and the cells were incubated for a further 2 hr. The absorbance of medium was measured at 450 nm. The percentage of cell viability was expressed as 100% for cells cultured without DFO for 24 hr. The experiment was repeated five times independently for each sample.

The cells (3×10^4 cells/ml medium) were cultured in each well of a 24-well multiwell culture plate (#3526, Corning Inc., NY), and treated by the similar condition to the WST-8 assay. The cells were rinsed gently with PBS and detached with trypsin/EDTA (100 μl) solution in PBS. The cell suspension (95 μl) was mixed with trypan blue solution (5 μl) and the number of viable cells was counted using a hemocytometer (Sigma–Aldrich Japan KK, Tokyo, Japan).

Preparation of gelatin hydrogels incorporating DFO

An aqueous solution of pI9 gelatin (20 wt%, 1.0 ml) was added to 5.0 mg/ml DFO (1.0 ml) in double-distilled water at 37 °C. The mixed solution was poured into a polytetrafluoroethylene mold and frozen in liquid nitrogen, followed by freeze-drying. The hydrogels prepared were treated in a drying oven (AURORA DN-305, Sato Vacuum Inc., Japan) for 24 hr at 140 °C to allow the gelatin to dehydrothermally crosslink.

Evaluation of DFO release from gelatin hydrogels incorporating DFO and hydrogel degradation

Hydrogels of 5.0–7.0 mg in dry weight were placed in PBS (500 μl) and agitated at 37 °C. The PBS supernatant was collected 1, 2, 4, 8 and 24 hr later, while the same volume of free PBS was added to continue the agitation. PBS was then exchanged for PBS containing collagenase (50 μg/μl) and the release test was performed for the same duration. The amount of DFO in PBS solution was determined by conventional Fe(II) chelate activity assay. Briefly, ammonium iron(III) sulfate 12-hydrate (48 μg) was dissolved in 0.1 N of hydrogen chloride (HCl) solution (24 μl). The solution was mixed with 25 mM thioglycolic acid solution (28 μl) and 7.0 wt% ammonia solution (28 μl). The mixed solution (80 μl) was added to the PBS supernatant. The absorbance of medium was measured at 560 nm to calculate the DFO amount from the calibration curve. Next, the absorbance of the supernatant was measured at 280 nm to calculate the amount of hydrogel degraded.

In vivo angiogenesis evaluation

BALB/c mice (8 week old males weighing 20 g) were purchased from Shimizu Laboratory Supplies Co., Kyoto, Japan. The animal experimentation was conducted according to the guidance of the Institute for Frontier Medical Sciences, Kyoto University. To evaluate the *in vivo* angiogenesis of gelatin hydrogels incorporating DFO, a hind limb ischemia model was created. Briefly, mice were anesthetized by an intraperitoneal pentobarbital (0.65 mg/kg) injection and isoflurane inhalation, and the right groin area was shaved. The entire right saphenous artery and vein, right external iliac artery and vein, and deep femoral and circumflex arteries and vein were ligated, cut and excised to obtain a model of severe hind limb ischemia. The mice were classified into four groups (n = 4–5 per group): intramuscular injection of PBS or DFO solution (1.0 mg/ml, 50 μl), and intramuscular implantation of gelatin hydrogels (2.0–2.2 mg) without DFO into the muscles of the groin, or gelatin hydrogels (2.0–2.2 mg) incorporating DFO (50 μg). The mice were killed either 3 or 7 days later. The muscular-specimen whole-thigh tissues were fixed with 4 wt% paraformaldehyde solution in PBS overnight at 4 °C, and then decalcified with Plank–Rychlo's solution overnight at room temperature. After decalcification, the samples were embedded in paraffin. Each specimen was cross-sectioned into slices 4 μm thick with a rotary microtome (RM2125RT, Leica Microsystems Inc., Osaka, Japan). For histological analysis, sections were stained with hematoxylin and eosin (H&E) dyes, and the number of blood vessels was counted for all sections using a microscope (PROVIS AX80, Olympus Co., Japan).

Paraffin sections (5 μm thick) of tissues were stained with a mouse monoclonal anti-α-smooth muscle actin (α-SMA) antibody (1:100, Sigma–Aldrich Japan KK, Tokyo,

Japan). Briefly, the sections were incubated with the anti-α-SMA antibody for 1 hr at room temperature. After washing, the sections were stained with a Simple Stain Mouse MAX-PO (Histofine, Nichirei Biosciences Inc., Tokyo, Japan) for 45 min at room temperature. Then, DAKO EnVision horseradish peroxidase and 3,3-diaminobenzidine (DAB) substrate kit (Vector Laboratories, Burlingame, CA) were added to the antibody-treated section to view the primary antibody by bright-field microscopy (DP-72, Olympus Corporation, Tokyo, Japan). For nuclear staining, Mayer's hematoxylin was applied to the incubate at room temperature for 30 s. The sections were mounted with an aqueous mounting medium (MGK-S, Matsunami Glass Ind. Ltd., Osaka, Japan) for microscopic observation. The number of α-SMA-positive vessels was counted in all sections to evaluate the number of matured blood vessels.

Statistical analysis

All the results were expressed as the mean ± standard deviation (SD). Significant analysis was done based on the one-way ANOVA, and the difference was considered to be significant at $P < 0.05$.

RESULTS

The effect of DFO on the in vitro production of HIF-1α and VEGF

Figure 1A shows the HIF-1α production from HUVECs cultured with different concentrations of DFO at various O_2 levels. In the absence of DFO, the HIF-1α level was significantly high at 1.0% O_2 compared with that at 5.0% and 20% O_2. When the DFO was added to the 5.0% O_2 culture, the HIF-1α level increased with an increase in the DFO concentration to be significantly higher at DFO concentrations of 50 μM or higher compared with that without DFO addition.

Figire 1B shows the VEGF production from HUVECs cultured with different concentrations of DFO at various O_2 levels. In the absence of DFO, the VEGF level was significantly high at 1.0% O_2 compared with that at 5.0% and 20% O_2. At the 5.0% O_2 culture with DFO, the VEGF level increased with an increase in the DFO concentration and was significantly higher at DFO concentrations of 100 μM or higher compared with that without DFO addition. The VEGF level was gradually decreased in the cells cultured with 1.0% O_2 at higher concentrations of DFO.

Effect of DFO concentration on HUVEC gene expression

Figures 2A–C show the relative mRNA expression of ANGPT2, EGF and PDGF-B, respectively. The level of ANGPT2, EGF and PDGF-B expression for cells cultured at 1.0% O_2 was significantly high compared with that at 5.0% O_2. When DFO was added to the 5.0% O_2 culture, the level of ANGPT2 expression was increased with an increase in the DFO concentration to be significantly higher at DFO concentrations of 50 μM or higher compared with that without DFO addition. When DFO was added to

the 5.0% O_2 culture, the level of EGF expression was significantly higher at DFO concentrations of 50 μM or higher compared with that without DFO addition. When DFO was added to the 5.0% O_2 culture, the level of PDGF-B expression was significantly higher at DFO concentrations of 10 μM or higher compared with that without DFO addition, respectively. Expression of hypoxia-mimicking deriving protein was not observed for cells cultured with 1.0% O_2 when DFO was added.

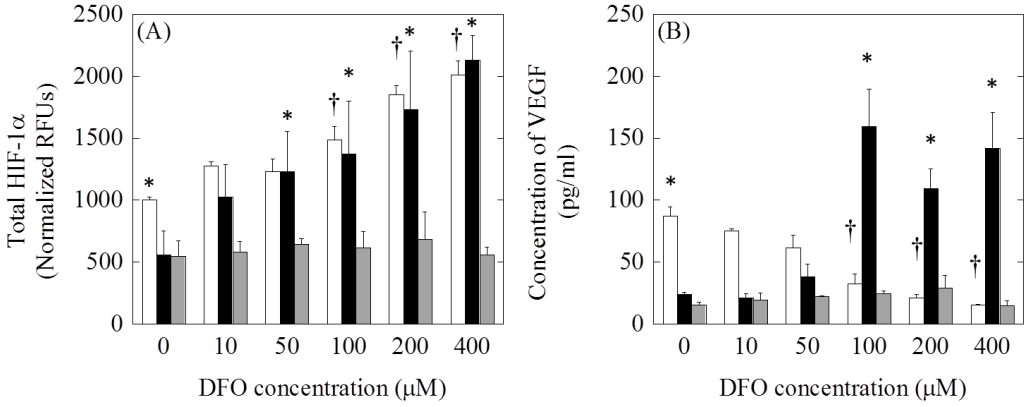

Figure 1. HIF-1α (A) and VEGF secretion (B) from HUVECs cultured with different concentrations of DFO at O_2 levels of 1.0% (□), 5.0% (■) and 20% (■). ∗$P < 0.05$; significant vs. the value in culture at 5.0% O_2 without DFO. †$P < 0.05$; significant vs. the value in culture at 1.0% O_2 without DFO.

Cytotoxicity evaluation of DFO

Figures 3A and B show the WST-8 activity and cell viability of HUVECs cultured at different concentrations of DFO. The WST-8 activity was significantly higher in the presence of DFO compared with that without DFO addition. However, the cell number decreased with an increase in the DFO concentration.

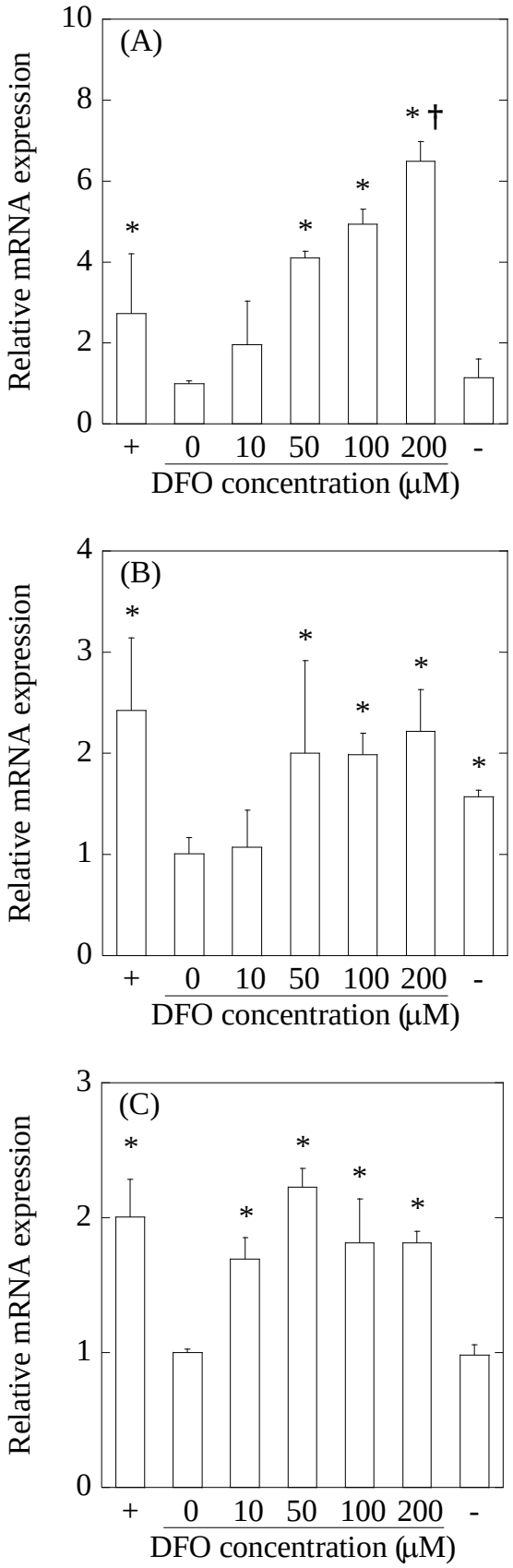

Figure 2. Relative mRNA expression of *ANGPT2* (A), *EGF* (B) and *PDGF-B* (C) for HUVECs cultured with or without different concentrations of DFO at O_2 levels of 1.0% without DFO (as a positive control, +), 5.0% and 20% without DFO (as a negative control, −). *β-actin* mRNA of every culture sample was used as an internal standard to normalize the level of total mRNA. The value obtained was normalized by that of cells cultured at 5.0% O_2 without DFO. $*P < 0.05$; significant vs. the value in culture at 5.0% O_2 without DFO. $†P < 0.05$; significant vs. the value in culture at 1.0% O_2 without DFO.

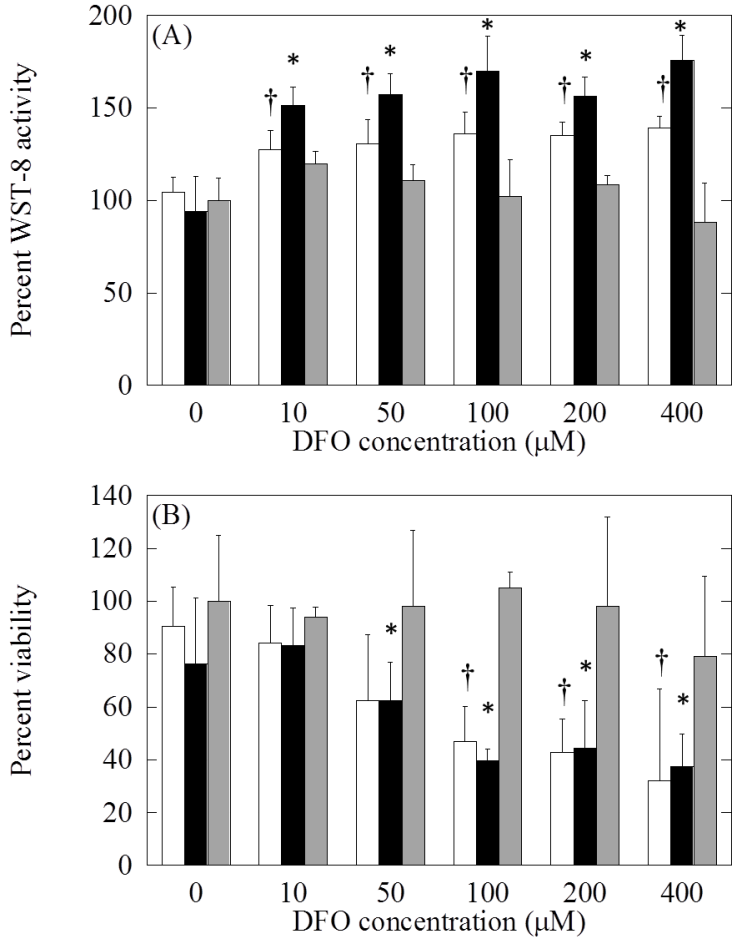

Figure 3. WST-8 activity (A) and cell viability (B) of HUVECs cultured at different concentrations of DFO at O_2 levels of 1.0 (□), 5.0 (■) and 20% (■). ∗$P < 0.05$; significant vs. the value in culture at 5.0% O_2 without DFO. †$P < 0.05$; significant vs. the value in culture at 1.0% O_2 without DFO.

Time profiles of DFO release from hydrogels incorporating DFO and hydrogel degradation

Figures 4A and B show the *in vitro* time profiles of DFO release from gelatin hydrogels incorporating DFO and hydrogel degradation in PBS with or without collagenase. In the collagenase-free PBS, ~61% of incorporated DFO was initially released, but thereafter no release was observed, while 44.3% of hydrogels was initially degraded. However, in the PBS containing collagenase, the DFO was released over time and a similar time profile of hydrogel degradation was observed.

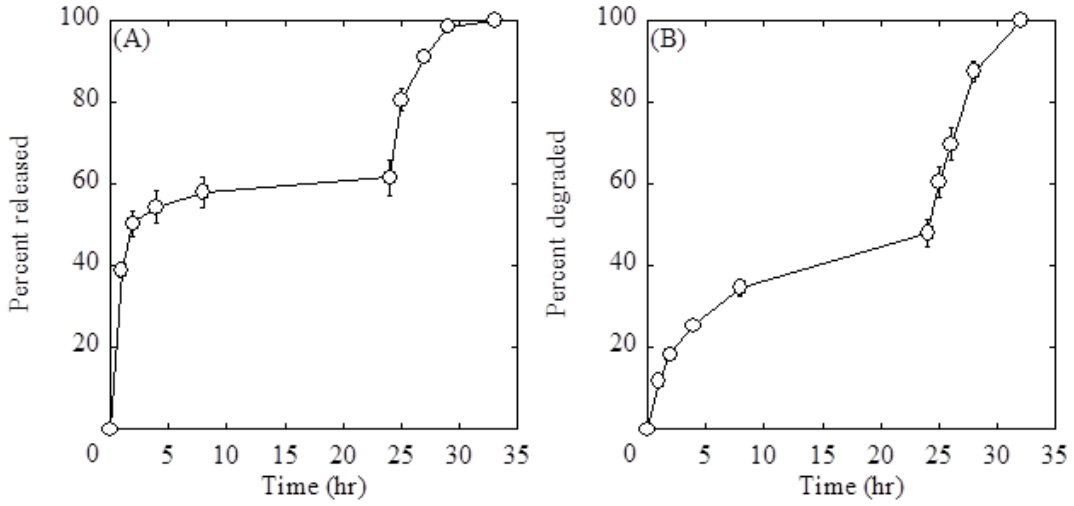

Figure 4. *In vitro* time profiles of DFO release from gelatin hydrogels (A) and hydrogel degradation (B). The hydrogels were dehydrothermally cross-linked at 140 °C for 24 hr. The release test was performed in PBS for an initial 24 hr, and thereafter in collagenase solution in PBS at 37 °C.

In vivo angiogenesis of gelatin hydrogel incorporating DFO

Figure 5A shows histological sections of H&E staining and anti-α-SMA immunohistochemical staining. **Figure 5B** shows the number of total blood vessels for a mouse ischemia model. H&E and anti-α -SMA immunohistochemical images allow counting of the number of total blood vessels and vascular smooth muscle positive blood vessels, respectively. Angiogenesis was observed 3 and 7 days after application of hydrogels incorporating DFO to a significantly stronger extent compared with other groups. Significantly high angiogenesis was observed 7 days after application of the hydrogels compared with that for 3 days. Moreover, angiogenesis was observed 7 days after implantation of hydrogels significantly more compared with that of free DFO. **Figure 5C** shows the anti-α-SMA-positive blood vessel for a mouse model of hind limb ischemia. The number of α-SMA-positive cells was significantly larger for the gelatin hydrogel incorporating DFO 7 days after application than that of other groups.

(A)

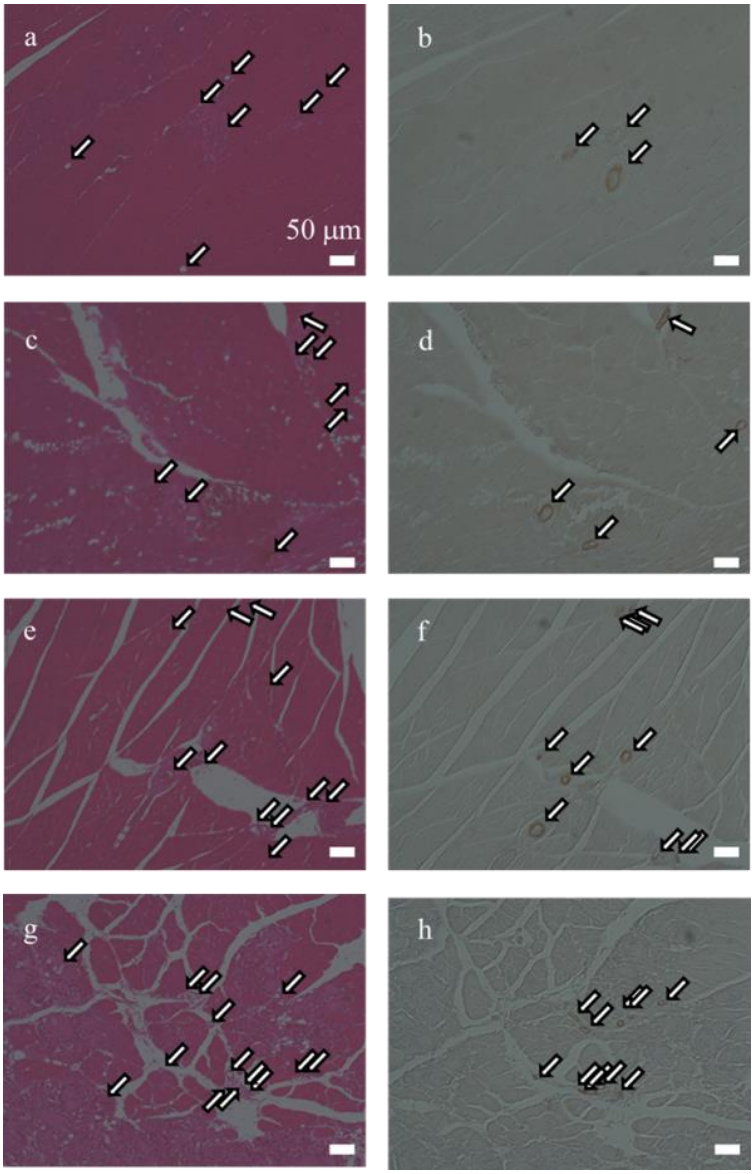
a
50 μm
b
c
d
e
f
g
h

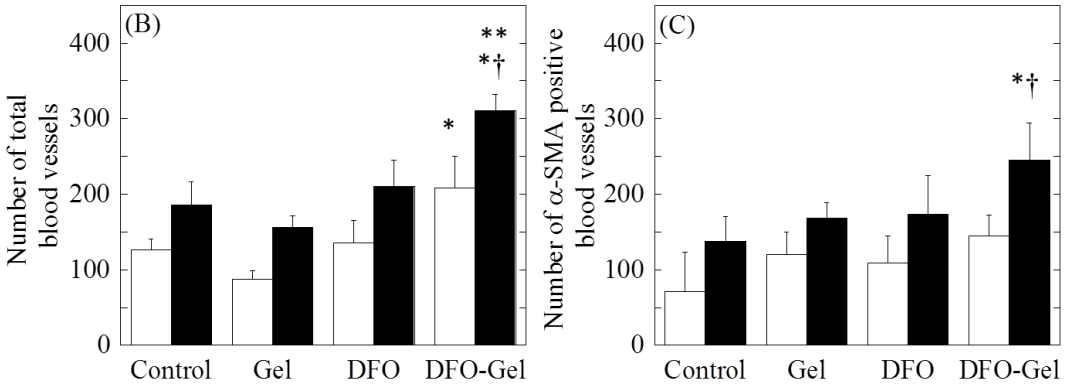
(B)
Number of total blood vessels
400
300
200
100
0
*
**
*†
Control
Gel
DFO
DFO-Gel
(C)
Number of α-SMA positive blood vessels
400
300
200
100
0
*†
Control
Gel
DFO
DFO-Gel

Figure 5. (A) Histological sections of hind limb ischemia tissues 7 days after application with the hydrogel incorporating DFO: control (a and b), DFO-free gelatin (c and d), free DFO (e and f), hydrogels incorporating DFO (g and h), and H&E (a, c, e and g) and anti-α-SMA immunohistochemical stainings (b, d, f and h). The number of total (B) and anti-α-SMA-positive blood vessels (C) of the entire cross-section of the leg tissues 3 days (□) and 7 days (■) after application of DFO-free gelatin hydrogels (Gel), hydrogels incorporating DFO (DFO-gel), and free DFO (DFO). The arrows indicate blood vessels. $*P < 0.05$; significant vs. the value of control group at the corresponding day. †$P < 0.05$; significant vs. the value of same treatment for 3 days. $**P < 0.05$; significant vs. the value of free DFO group at the corresponding day.

DISCUSSION

This study demonstrates that biodegradable gelatin hydrogel can release DFO, resulting in biological activity. From the *in vitro* release test, DFO was released from hydrogel as a result of hydrogel degradation. The initial 60% release is due to the simple diffusion of DFO and does not involve interaction with the gelatin molecules of the hydrogels. In this release system, the DFO molecules physicochemically interacting with gelatin are not released from the hydrogels when these do not degrade. When the hydrogel is degraded to generate water-soluble gelatin fragments, the DFO can be released via interaction with these fragments. Therefore, in the presence of collagenase, the time profile of DFO release was in good accordance with that of hydrogel degradation (**Figure 4**). Since the DFO molecule contains one amino group, it can electrostatistically interact with the carboxyl group of gelatin molecules. In addition, the

desalted form of DFO may interact with gelatin because of its hydrophobicity. It is possible that this interaction enables DFO molecules to interact with gelatin, resulting in hydrogel degradation-related DFO release. It is highly conceivable that the interaction is so weak that a large amount of DFO is initially released. The method used to detect DFO is the conventional Fe(II) chelate activity assay. This method could not always detect the precise DFO concentration in the presence of Fe(II), such as in the medium and the body. Therefore, we demonstrated the DFO release test *in vitro* to check the release profiles. In the collagenase-free PBS, ~61% of the DFO incorporated in the gelatin hydrogel was initially released, but thereafter no release occurred. The DFO incorporated into the hydrogel was released over time, and the time profile was similar to that of hydrogel degradation (**Figure 4**). This indicates that ~61% of DFO may initially release into the body. Thereafter, the hydrogel can be enzymatically degraded to release the remaining DFO into the body. This hydrogel still remained 3 days after application, but was completely degraded 7 days after application (data not shown). In the collagenase-free PBS, the DFO release profiles indicated initial burst release. The DFO initial release results from the simple diffusion of DFO which does not immobilize to the crosslinked gelatin molecules. In the tissue, certain enzymes can degrade gelatin when the gelatin hydrogel incorporating DFO is placed in the body, and these enzymes will degrade the hydrogel to generate water-soluble gelatin fragments. The DFO immobilized to the gelatin is released from the hydrogel as a result of gelatin water-solubilization due to the hydrogel degradation. The DFO release and gelatin degradation studies demonstrated that the time profile of DFO release matched that of hydrogel degradation.

The HIF-1α and VEGF expression levels of HUVECs cultured at 1.0% O_2

were significantly higher than those at 5.0% O_2 (**Figure 1**). This is because of the hypoxic condition. In addition, DFO addition similarly enhanced the levels in a dose-dependent manner. This confirms the ability of DFO to induce an hypoxia-mimicking condition due to Fe(II) removal inside the HUVECs. When the cells were cultured with or without DFO at 1.0% and 5.0% O_2 for 2 and 4 h, the HIF-1α level of cells treated without DFO at 1.0% O_2 was not significantly higher compared with that of 5.0% O_2 (data not shown). This result suggests that a long time period is needed for DFO to induce the hypoxia-mimicking response. When DFO was added to the 1.0% and 5.0% O_2 culture, the HIF-1α level increased with an increase in DFO concentration (**Figure 1A**). However, the level of VEGF expression was gradually decreased for the cells cultured with 1.0% O_2 at higher concentrations of DFO (**Figure 1B**). In addition, the level of VEGF expression was not changed for cells cultured with 20% O_2 for all the DFO concentrations investigated **(Figure 1B**). The active HIF complex (i.e. HIF-1α, β and p300/CBP complex) binds to the HRE which can induce VEGF expression. It is known that HIF-1α recruits the transcriptional coactivator of p300/CBP in the nucleus. In the 1.0% O_2 culture, HIF-1α, β and p300/CBP complex are not generated although the HIF-1α level increased. We cannot explain this finding, but we think that DFO may provide an appropriate condition to suppress the formation of HIF-1α, β and p300/CBP complex or the binding to the HRE.

The WST-8 activity of HUVECs increased with DFO addition, and this increase was observed at 1.0% and 5.0% O_2, in contrast to that at 20% O_2. DFO has the ability to increase the mitochondrial activity at lower O_2 levels although it was cytotoxic at the mitochondrial activity level. Reactive Fe(II) is necessary for cell viability as it serves as a cofactor in DNA, RNA and protein synthesis, for heme and non-heme

enzymes involved in mitochondrial respiration [30]. Fe(II) is a trace element essential for cell survival. However, a high concentration of Fe(II) may cause cell injury, resulting in cellular toxicity, because of the ability to catalyze the production of reactive oxygen species [31], and it is known that Fe(II) deficiency results in cell impairment. The LD50 of DFO in mice is 250 mg/kg [29]. Since the gelatin hydrogel contains 2.5 mg/kg body weight DFO for local release, it should be of low cytotoxicity *in vivo*. No inflammation and necrosis around the hydrogel 3 and 7 days after application were observed visually (data not shown).

DFO promotes angiogenesis via the activation of vascular endothelial cell functions [27]. *In vitro* HIF-1 stabilization contributes to prolonging strongly hypoxic conditions over several hours [32]. The *in vitro* cell culture experiments revealed that 5.0% O_2 is not sufficient to induce HIF-1 production [33]. Considering these findings, the controlled release of DFO from gelatin hydrogels is useful for inducing HIF-1. In addition, the lifetime of DFO is very short [29]. It is conceivable that the maintenance of DFO action for a long time period results in an enhanced hypoxia-mimicking to achieve HIF-1α -induced angiogenesis.

When the DFO was added to the 5.0% O_2 culture, the levels of *ANGPT2*, *EGF* and *PDGF-B* mRNA expressions were increased (**Figure 2**). Expression of the hypoxia-mimicking deriving protein was not observed for cells cultured with 1.0% O_2 with DFO addition. Therefore, we did not evaluate the mRNA expression of *ANGPT2*, *EGF* and *PDGF-B* in the 1.0% and 20% O_2 conditions.

H&E and anti-α-SMA immunohistochemical staining allow counting of the number of total blood vessels and vascular smooth muscle-positive blood vessels, respectively.

In hyperglycemia, hypoxia-induced angiogenesis does not occur naturally [33]. On the contrary, the overexpression of HIF-1 prevents the deterioration of cardiac remodeling in streptozotocin-induced diabetic mice [34]. In addition, human aortic endothelial cells from diabetic patients do not up-regulate hypoxia-induced VEGF expression in 0.5% O_2 culture [28]. On the other hand, the hypoxia-mimicking condition induced by DFO treatment can increase VEGF expression in diabetic tissues [28]. The findings indicate that low pO_2-induced hypoxia is different from the hypoxia-mimicking condition induced by DFO. One of the adverse effects of DFO is retinopathy following systemic administration for diabetes. As one possible way to reduce the effect, controlled and local release of DFO is promising. DFO local release may be effective even in diabetic conditions.

REFERENCES

[1] A. Carreau, B. El Hafny-Rahbi, A. Matejuk, C. Grillon, C. Kieda, Why is the partial oxygen pressure of human tissues a crucial parameter? Small molecules and hypoxia, Journal of cellular and molecular medicine, 15 (2011) 1239-1253.

[2] M. Korsic, D. Jugovic, B. Kremzar, Intracranial pressure and biochemical indicators of brain damage: follow-up study, Croatian medical journal, 47 (2006) 246-252.

[3] Q.T. Le, E. Chen, A. Salim, H. Cao, C.S. Kong, R. Whyte, J. Donington, W. Cannon, H. Wakelee, R. Tibshirani, J.D. Mitchell, D. Richardson, K.J. O'Byrne, A.C. Koong, A.J. Giaccia, An evaluation of tumor oxygenation and gene expression in patients with early stage non-small cell lung cancers, Clinical cancer research : an official journal of the American Association for Cancer Research, 12 (2006) 1507-1514.

[4] A.J. Brooks, J.S. Hammond, K. Girling, I.J. Beckingham, The effect of hepatic vascular inflow occlusion on liver tissue pH, carbon dioxide, and oxygen partial pressures: defining the optimal clamp/release regime for intermittent portal clamping, The Journal of surgical research, 141 (2007) 247-251.

[5] M. Muller, W. Padberg, E. Schindler, J. Sticher, C. Osmer, S. Friemann, G. Hempelmann, Renocortical tissue oxygen pressure measurements in patients undergoing living donor kidney transplantation, Anesthesia and analgesia, 87 (1998) 474-476.

[6] R.S. Richardson, S. Duteil, C. Wary, D.W. Wray, J. Hoff, P.G. Carlier,

Human skeletal muscle intracellular oxygenation: the impact of ambient oxygen availability, The Journal of physiology, 571 (2006) 415-424.

[7] J.S. Harrison, P. Rameshwar, V. Chang, P. Bandari, Oxygen saturation in the bone marrow of healthy volunteers, Blood, 99 (2002) 394.

[8] J.A. Bertout, S.A. Patel, M.C. Simon, The impact of O_2 availability on human cancer, Nature reviews. Cancer, 8 (2008) 967-975.

[9] J.S. Lewis, J.A. Lee, J.C. Underwood, A.L. Harris, C.E. Lewis, Macrophage responses to hypoxia: relevance to disease mechanisms, J Leukoc Biol, 66 (1999) 889-900.

[10] J.E. Shay, M. Celeste Simon, Hypoxia-inducible factors: crosstalk between inflammation and metabolism, Seminars in cell & developmental biology, 23 (2012) 389-394.

[11] Y.Z. Gu, S.M. Moran, J.B. Hogenesch, L. Wartman, C.A. Bradfield, Molecular characterization and chromosomal localization of a third alpha-class hypoxia inducible factor subunit, HIF3alpha, Gene expression, 7 (1998) 205-213.

[12] G.L. Wang, G.L. Semenza, Purification and characterization of hypoxia-inducible factor 1, J Biol Chem, 270 (1995) 1230-1237.

[13] G.L. Semenza, Hypoxia-inducible factors in physiology and medicine, Cell, 148 (2012) 399-408.

[14] B.L. Ebert, J.D. Firth, P.J. Ratcliffe, Hypoxia and mitochondrial inhibitors regulate expression of glucose transporter-1 via distinct Cis-acting sequences, J Biol Chem, 270 (1995) 29083-29089.

[15] J.D. Firth, B.L. Ebert, C.W. Pugh, P.J. Ratcliffe, Oxygen-regulated

control elements in the phosphoglycerate kinase 1 and lactate dehydrogenase A genes: similarities with the erythropoietin 3' enhancer, Proc Natl Acad Sci U S A, 91 (1994) 6496-6500.

[16] J.W. Jeong, M.K. Bae, M.Y. Ahn, S.H. Kim, T.K. Sohn, M.H. Bae, M.A. Yoo, E.J. Song, K.J. Lee, K.W. Kim, Regulation and destabilization of HIF-1alpha by ARD1-mediated acetylation, Cell, 111 (2002) 709-720.

[17] A.P. Levy, N.S. Levy, S. Wegner, M.A. Goldberg, Transcriptional regulation of the rat vascular endothelial growth factor gene by hypoxia, J Biol Chem, 270 (1995) 13333-13340.

[18] D.J. Manalo, A. Rowan, T. Lavoie, L. Natarajan, B.D. Kelly, S.Q. Ye, J.G. Garcia, G.L. Semenza, Transcriptional regulation of vascular endothelial cell responses to hypoxia by HIF-1, Blood, 105 (2005) 659-669.

[19] G.L. Semenza, P.H. Roth, H.M. Fang, G.L. Wang, Transcriptional regulation of genes encoding glycolytic enzymes by hypoxia-inducible factor 1, J Biol Chem, 269 (1994) 23757-23763.

[20] A. Zagorska, J. Dulak, HIF-1: the knowns and unknowns of hypoxia sensing, Acta biochimica Polonica, 51 (2004) 563-585.

[21] L.E. Huang, Z. Arany, D.M. Livingston, H.F. Bunn, Activation of hypoxia-inducible transcription factor depends primarily upon redox-sensitive stabilization of its alpha subunit, J Biol Chem, 271 (1996) 32253-32259.

[22] U. Berchner-Pfannschmidt, S. Tug, M. Kirsch, J. Fandrey, Oxygen-sensing under the influence of nitric oxide, Cell Signal, 22 (2010) 349-356.

[23] C. Brahimi-Horn, N. Mazure, J. Pouyssegur, Signalling via the hypoxia-inducible factor-1alpha requires multiple posttranslational modifications, Cell Signal, 17 (2005) 1-9.

[24] J.M. Gleadle, B.L. Ebert, J.D. Firth, P.J. Ratcliffe, Regulation of angiogenic growth factor expression by hypoxia, transition metals, and chelating agents, Am J Physiol, 268 (1995) C1362-1368.

[25] C.J. Schofield, P.J. Ratcliffe, Oxygen sensing by HIF hydroxylases, Nature reviews. Molecular cell biology, 5 (2004) 343-354.

[26] G.L. Wang, G.L. Semenza, Desferrioxamine induces erythropoietin gene expression and hypoxia-inducible factor 1 DNA-binding activity: implications for models of hypoxia signal transduction, Blood, 82 (1993) 3610-3615.

[27] Y. Ikeda, S. Tajima, S. Yoshida, N. Yamano, Y. Kihira, K. Ishizawa, K. Aihara, S. Tomita, K. Tsuchiya, T. Tamaki, Deferoxamine promotes angiogenesis via the activation of vascular endothelial cell function, Atherosclerosis, 215 (2011) 339-347.

[28] H. Thangarajah, D. Yao, E.I. Chang, Y. Shi, L. Jazayeri, I.N. Vial, R.D. Galiano, X.L. Du, R. Grogan, M.G. Galvez, M. Januszyk, M. Brownlee, G.C. Gurtner, The molecular basis for impaired hypoxia-induced VEGF expression in diabetic tissues, Proc Natl Acad Sci U S A, 106 (2009) 13505-13510.

[29] P.E. Hallaway, J.W. Eaton, S.S. Panter, B.E. Hedlund, Modulation of deferoxamine toxicity and clearance by covalent attachment to biocompatible polymers, Proc Natl Acad Sci U S A, 86 (1989) 10108-10112.

[30] R.J. Ward, D. Dexter, A. Florence, F. Aouad, R. Hider, P. Jenner, R.R. Crichton, Brain iron in the ferrocene-loaded rat: its chelation and influence on dopamine metabolism, Biochemical pharmacology, 49 (1995) 1821-1826.

[31] M. Tanaka, A. Sotomatsu, H. Kanai, S. Hirai, Dopa and dopamine cause cultured neuronal death in the presence of iron, Journal of the neurological sciences, 101 (1991) 198-203.

[32] T. Lofstedt, E. Fredlund, L. Holmquist-Mengelbier, A. Pietras, M. Ovenberger, L. Poellinger, S. Pahlman, Hypoxia inducible factor-2alpha in cancer, Cell Cycle, 6 (2007) 919-926.

[33] S.B. Catrina, K. Okamoto, T. Pereira, K. Brismar, L. Poellinger, Hyperglycemia regulates hypoxia-inducible factor-1alpha protein stability and function, Diabetes, 53 (2004) 3226-3232.

[34] W. Xue, L. Cai, Y. Tan, P. Thistlethwaite, Y.J. Kang, X. Li, W. Feng, Cardiac-specific overexpression of HIF-1{alpha} prevents deterioration of glycolytic pathway and cardiac remodeling in streptozotocin-induced diabetic mice, The American journal of pathology, 177 (2010) 97-105.

Chapter 2

Enhancement of gene suppression by controlled release of small interfering RNA from gelatin hydrogels

INTRODUCTION

RNA interference (RNAi) is a biological phenomenon to turn off gene expression by directing degradation of the targeting mRNA, which was discovered in 1998 [1]. Small interfering RNA (siRNA) is a short double-strand RNA of average only 21–23 base pairs which can induce RNAi [2]. Since siRNA can specifically inhibit the expression of target genes, the applications are widely being expected, for example, experimental tools to suppress gene expression in the sequence-specific manner [3, 4] and molecular-targeted therapy to inhibit the expression of pathogenic proteins related to cancer and viral infections [5, 6]. However, siRNA alone cannot always induce RNAi phenomena because of the low cell interaction and the low stability in the body. To effectively use siRNA-based gene suppression as both experimental and therapeutic tools, some technologies and methodologies should be established. Virus vectors have a high gene transfection efficiency and the long-term maintenance of gene expression [7], but the safety seems to be a major problem [8]. Compared to the viral vectors, the non-viral vectors are relatively safe, however they need more enhancements for efficient introduction of genes into the target cells. Physical stimulation (e.g. electroporation [9], sonoporation [10], and iontophoresis [11]) enhanced the efficacy of gene transfection, although the technology is costly. To effectively use siRNA-based gene silencing as both the experimental and therapeutic tools, the leveland duration of gene silencing need to be optimized.

Chapter 2

The objective of this chapter is to create a gelatin hydrogel system for the controlled release of bioactive siRNA. Cationized gelatin (CG) was prepared to form the polyion complex of siRNA. The complex was mixed with gelatin, followed by chemical crosslinking to prepare gelatin hydrogels incorporating the complex of siRNA and CG. The siRNA release profile from the hydrogel was investigated while the activity of siRNA released was evaluated.

EXPERIMENTAL

Materials

The nucleotide sequences of siRNA targeted at the firefly luciferase gene (Luc siRNA) (Forward) 5'- CUUACGCUGAGUACUUCGATT -3' and (Reverse) 5'- UCGAAGUACUCAGCGUAAGTT -3' was purchased from B-Bridge International (Sunnyvale, CA, USA). All reagents were obtained from Nacalai Tesque, Kyoto, Japan except as indicated otherwise.

Preparation of Luc siRNA and cationized gelatin complexes

The cationized gelatins (CGs) with different cationization extents were prepared. Briefly, various amounts of ethylenediamine (EDA) were added into 25 ml of 0.1 M phosphate-buffered solution (PB, pH = 5.0) containing 1.0 g of pI9 gelatin. The solution pH was adjusted to 5.0 by adding 6 M HCl aqueous solution, and PB was added into the solution to give the final volume of 50 ml. Then, 1-ethyl-3-(3-dimethylaminopropyl) carbodiimide hydrochloride (EDC) was added into

the solution, followed by the agitation at 37 °C for 4 hr and dialysis against double-distilled water (DDW) for 3 days at room temperature. The dialyzed solution was freeze-dried to obtain CGs. The extent of cationized gelatin was determined by the conventional 2,4,6-trinitrobenzene sulfonic acid (TNBS) method. Briefly, pI9 gelatin and cationized gelatins were dissolved into 0.1 M phosphate-buffered saline solution (PBS, pH = 7.4) at 1.0 mg/ml. Then, 4 wt% of sodium hydrogen carbonate aqueous solution (200 μl) and 0.1 wt% of TNBS aqueous solution (200 μl) were added into the gelatin solution (100 μl), and then the mixed solution was allowed to react for 2 hr at 37 °C. After reaction, 10 wt% of SDS aqueous solution (200 μl) and 1 N HCl (100 μl) were added into the mixed solution. The percentage of EDA introduced, the cationization extent was measured from the decrement of amino groups in gelatin by the conventional TNBS method. Next, the complexation of Luc siRNA and CG was performed by simply mixing at various mixing ratios of amino group number of CG per the phosphate group number of Luc siRNA (N/P) in aqueous solution. Briefly, deionized and sterilized water (RNase-free, DSW, 100 μl) containing different amounts of CG was slowly added to the same volume of 100 mM phosphate-buffered saline solution (PBS, pH = 7.4, 100 μl) containing 10 nM of Luc siRNA at N/P mixing ratios of 1, 5, 10, 20, 30, and 50. The mixed solution was gently agitated at 37 °C for 10 min to form Luc siRNA and CG complexes. The CGs were sterilized by ethylene oxide gas (EOG) on a EOGelk SA-360ECO (ELK corporation, Osaka, Japan) before using.

Dynamic light scattering and zeta potential measurements of CG complexes with Luc siRNA

To evaluate the nanocomplex size and zeta potential of CG and the Luc siRNA complexes, dynamic light scattering (DLS) and electrophoretic light scattering (ELS) measurements were carried out. The DLS measurement was carried out on aDLS-DPA-60HD (Otsuka Electronic Co. Ltd., Osaka, Japan) equipped with a He–Ne laser at a detection angle of 90 ° at 37 °C. ELS (ELS-7000, Otsuka Electronic Co. Ltd., Osaka, Japan) was measured at room temperature and an electric field strength of 100 V/cm. The experiment was done three times independently for every sample unless otherwise mentioned.

Cytotoxicity evaluation of CG

A luciferase-expressing cell line derived from colon 26 (Colon26-Luc) was kindly supplied by Dr. Takakura of Graduate School of Pharmaceutical Sciences, Kyoto University, Kyoto, Japan. The Colon26-Luc cells were cultivated in the Dulbecco's modified Eagle medium (DMEM) containing 10 vol% fetal bovine serum (FBS) and 1.0 vol% penicillin and streptomycin (DMEM-FBS) at 37 °C in a 95% air–5% CO_2 atmosphere. The cytotoxicity of CG was evaluated by an in vitro bioassay by WST-8 assay as described chapter 1. The percentage of cell viability was expressed as 100% for cells cultured without gelatin. The experiment was done 5 five times independently for each sample.

Evaluation of gene suppression of Luc siRNA and CG complexes

Gene suppression with Luc siRNA and CG complexes were evaluated according to the method reported previously [12]. Colon26-Luc cells were seeded into each well of 12-well multi-well culture plate (Corning Inc., NY, USA) at a density of 50,000 cells (1.0 ml/well) in the DMEM. After 24 h incubation, the medium was removed, and the well was washed by PBS (1.0 ml) twice. Then, Opti-MEM Reduced-Serum Medium (Opti-MEM, Life Technologies Japan Ltd., Osaka, Japan) of gene transfection medium (450 μl) and the complex solution of Luc siRNA at different concentrations of CG (50 μl) were added into each well, followed by 6 h incubation. After rinsing with PBS, cells were continued to culture in DMEM-FBS further for 0, 18, and 42 h. To evaluate the biological activity of Luc siRNA, cells were washed with PBS twice, lysed in 100 μl of cell-culture lysis reagent (Promega KK, Osaka, Japan). Then, 100 μl luciferase assay reagent (Promega KK, Osaka, Japan) was added to 10 μl of supernatant while the relative light unit (RLU) of the samples was determined by a luminometer (MicroLumatPlus LB 96V, Berthold, Tokyo, Japan). The total protein content in each well was determined by micro bicinchonic acid (BCA) protein assay kit (Pierce, Rockford, IL, USA) according to the manufacturers' instructions to normalize the influence of number variance of cells on the luciferase activity. Each experimental group was carried out three times independently.

Preparation of gelatin hydrogels incorporating Luc siRNA and CG complexes

To prepare the complex of Luc siRNA and CG, Luc siRNA (10 nmole/ml, 100 μl) was mixed with various N/P ratios of CG in DSW (100 μl) at 37 °C. Next, aqueous solution of pI5 gelatin (20 wt%, 200 μl) was added to the complex solution at 37 °C.

Then, the solution was mixed with 25 wt% of glutaraldehyde (2.5 μl) at a concentration of 0.63 vol%, and cast into a polypropylene dish (1.0 mm × 1.0 mm, Sakura Finetek Japan Co., Ltd., Tokyo, Japan), followed by leaving at 4 °C for 8 hr for chemical crosslinking of gelatin. The hydrogels were agitated in 100 mM glycine solution at 37 °C for 1 hr to block the residual aldehyde groups of glutaraldehyde. Following 1 hr washing three times with DSW, the hydrogels were freeze-dried to obtain the gelatin hydrogels incorporating Luc siRNA and CG complex.

Release test of Luc siRNA from gelatin hydrogels incorporating Luc siRNA and CG complexes

Hydrogels of 5.0– to 7.0 mg in dry weight were placed in PBS (500 μl) at 37 °C. The PBS supernatant was exchanged 1, 2, 4, 8, 24, 48, and 96 hr later and subsequently the hydrogels were completely degraded by PBS containing collagenase (5.0 μg/ml, 500 μl). The release test was performed in PBS for the initial 24 hr and after that done in PBS containing collagenase (5.0 μg/ml). The amount of Luc siRNA in solution sampled was determined by the conventional method of ethidium bromide (Et-Br) with fluorescence spectrometry (Le Pecq & Paoletti, 1966). Briefly, Et-Br was dissolved in 0.1 M NaCl and 0.1 M tris (hydroxymethyl) aminomethane aqueous solution (10 μg/ml). The Et-Br solution (150 μl) and sample solution (150 μl) were mixed in each well of 96-well multi-well culture black plate (Corning Inc., NY, USA) A calibration curve was prepared with the determined amounts of Luc siRNA. Fluorescence spectra were measured at room temperature on a SpectraMax Gemini EM (Molecular Device, Osaka, Japan) at the excitation and emission wavelengths of 546 and 596 nm, respectively. The percent introduced was determined based on the

calibration curve and the fluorescence of samples. The experiment was done three times independently for every sample unless otherwise mentioned.

Degradation evaluation of hydrogels incorporating Luc siRNA and CG complexes

Hydrogels of 5.0– to 7.0 mg in dry weight were placed in PBS (500 μl) at 37 °C. The PBS supernatant was exchanged 1, 2, 4, 8, and 24 h later and subsequently PBS containing collagenase (5.0 μg/ml) was added. PBS containing collagenase supernatant was exchanged every 3 hr and fresh one was added. The amount of gelatin solution sampled was determined by micro BCA protein assay described above.

Evaluation of gene suppression experiments of Luc siRNA released from hydrogels

The hydrogel of 5.0– to 7.0 mg in dry weight was placed in Opti-MEM (1.0 ml) at 37 °C. The Opti-MEM supernatant was collected 24 hr later, and then 1.0 ml of Opti-MEM containing collagenase (5.0 μg/ml, Opti-MEM-col) was added. The Opti-MEM-col was exchanged 3, 6, 9, and 12 hr later to collect the supernatant. The hydrogel was gradually degraded in Opti-MEM-col with time to release the Luc siRNA incorporated. The amount of gelatin in the supernatant sampled was determined by the micro BCA protein assay described above. The Luc siRNA concentration of supernatant sampled was determined by the Et-Br fluorescence spectrometry described above. The gene suppression activity of Luc siRNA in the supernatants collected, was performed according to the method previously reported [12]. Briefly, Colon26-Luc cells were cultured in each well of 12-well multi-well culture plate at a density of 50,000 cells (1.0 ml) in the DMEM for 24 hr at 37°C in 5% CO_2–95% air atmosphere. After washing of the well by PBS (1.0 ml) twice, the supernatant of Opti-MEM or Opti-MEM-col (500

μl) was added into each well, followed by 6 hr incubation. The luciferase and micro BCA protein assays were performed described above. As a control, the similar experiment for the complex of Luc siRNA freshly prepared at the same concentration as the supernatant collected at the corresponding N/P ratio and CG type was carried out. The percent suppression activity was calculated using the following formula.

Suppression activity (%) = (100 percent luciferase expression of supernatant) × 100 / (100 percent luciferase expression of control complex)

The experiment was done three times independently for every sample unless otherwise mentioned.

Statistical analysis

All the results were expressed as the mean ± standard deviation (SD). Significant analysis was done based on Fisher's least significant difference test for multiple comparisons, and the difference was considered to be significant at $P < 0.05$.

RESULTS

Characterization of Luc siRNA and CG complexes

Table 1 summarizes the preparation of CG and the complexes with Luc siRNA. **Figure 1** shows the apparent molecular size and zeta potential of CG with different cationization extents and the Luc siRNA complexes. The molecular size of CGs and the Luc siRNA complex tended to reach to a certain value when the N/P ratio was higher than 10. The complexes size ranged from 100 to 300 nm at higher N/P ratios. The zeta potential of CGs and the Luc siRNA complexes tended to increase with the cationization extent of gelatin and N/P mixing ratio.

Figure 2 shows the cytotoxicity of CGs. CGs with lower extents of cationization showed no cytotoxicity. On the contrary, the E-7.0 and E-50 CGs showed cytotoxicity. Overall, the cytotoxicity increased with an increase in the CG amount.

Table 1. Preparation and characterization of CGs and the complexation with LMWH.

Code	Gelatin concentration (g/ml)	EDA concentration (ml)	EDA used molar ratio[a]	Percrntage of EDA introduced[b]	Amount of cationized gelatin used for complexation[c] (mg)
E-0.5	1	0.031	0.5	4.6±3.8	37.5
E-1.0	1	0.063	1.0	16.7±1.8	35.0
E-2.0	1	0.125	2.0	19.8±5.4	35.0
E-3.0	1	0.188	3.0	27.0±2.8	25.0
E-5.0	1	0.314	5.0	31.1±3.9	22.5
E-7.0	1	0.439	7.0	36.0±1.2	22.5
E-10	1	0.627	10	38.3±3.9	17.5
E-50	1	3.14	50	56.5±4.5	7.5

[a] The molar ratio of EDA added to the carboxyl groups of gelatin

[b] The molar percentage of EDA introduced to the carboxyl groups of gelatin

[c] The amount for 2.5 mg of LMWH

Figure 1

(A)

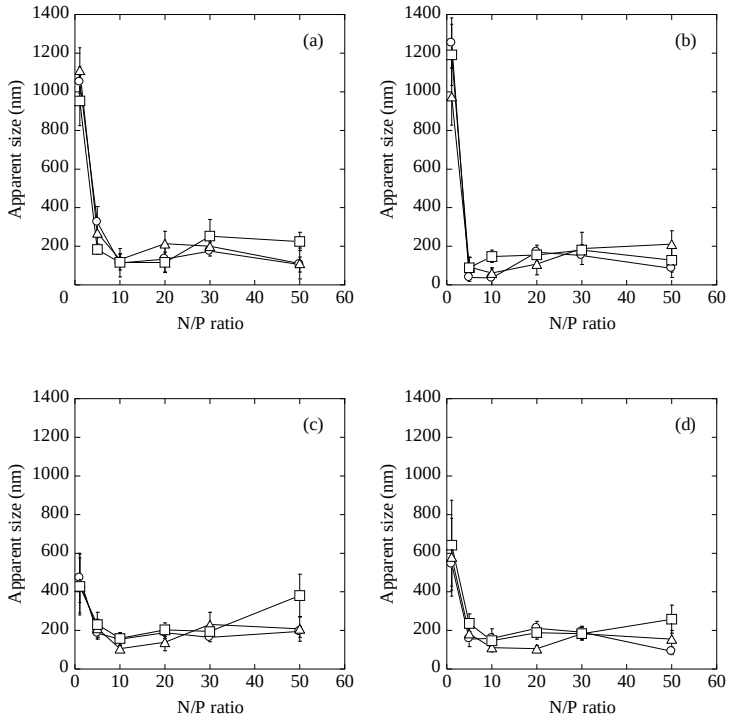

(B)

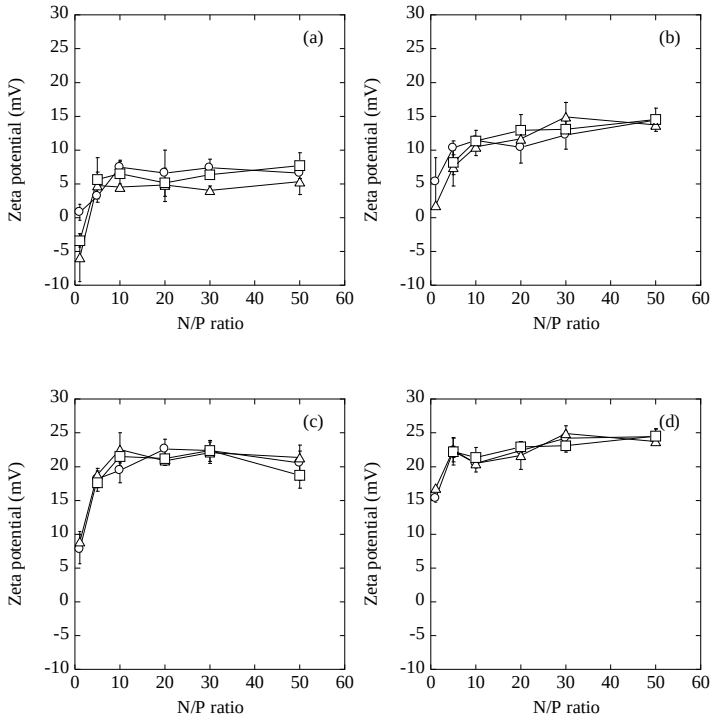

Figure 1. Nanocomplex sizes (A) and zeta potentials (B) of Luc siRNA and CG complexes. The complexes were prepared for 1.0 (○), 10, (△), and 100 nM (□) of Luc siRNA with E-1.0 (a), E-3.0 (b), E-7.0 (c), and E-50 CGs (d) in DDW at 37 °C.

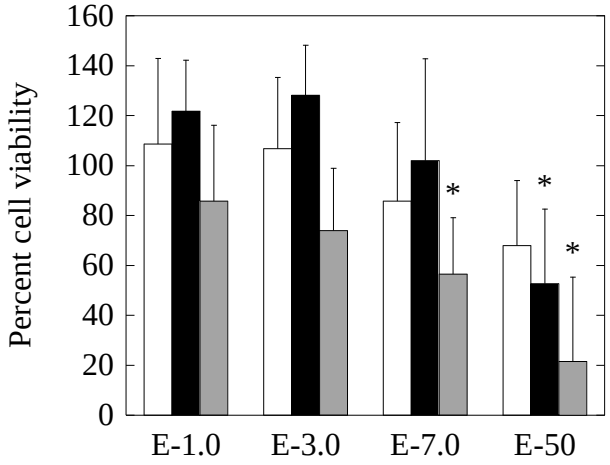

Figure 2. Cytotoxicity of CGs with different cationization extents. Colon26-Luc cells were cultured in the fresh medium containing CG at concentrations of 0.1 (□), 1.0 (■), and 10 nM (■) for 24 hr. The percentage of cell viability was expressed as 100% for cells cultured in fresh medium containing pI9 gelatin. *, $P < 0.05$; significant against the viability of cells cultured in the medium containing pI9 gelatin.

Gene suppression of Luc siRNA and CG complexes

Table 2 summerizes the amount of LUC siRNA released from gelatin hydrogels in Opti-MEM or Opti-MEM-col. **Figure 3** shows the gene expression suppression of Luc siRNA and CG complexes. Higher suppression of gene expression was observed for the Luc siRNA complexes of E-7.0 and E-50 CGs than those of E-1.0 and E-3.0 ones. The E-50 complex showed the strongest and longest gene suppression.

Table 2. The amount of Luc siRNA released in Opti-MEM with or without collagenase.

Code	Luc siRNA released in Opti-MEM (nM)	
	without collagenase	with collagenase
E-7.0, N/P = 10	85.3 ± 10.5	126.9 ± 16.7
E-7.0, N+P = 50	75.0 ± 5.7	120.0 ± 24.5
E-50, N/P = 10	76.3 ± 0.72	117.5 ± 43.8
E-50, N/P = 50	80.6 ± 15.2	132.6 ± 4.7

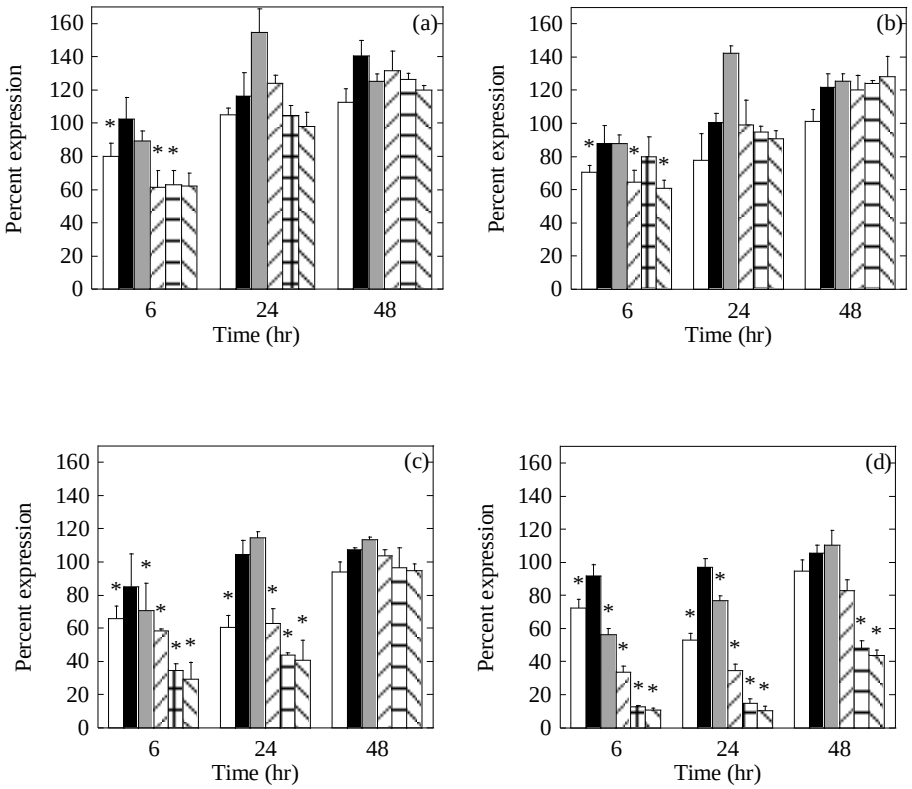

Figure 3. Gene suppression of Luc siRNA and CG complexes. The complexes were prepared for 100 nM of Luc siRNA with E-1.0 (a), E-3.0 (b), E-7.0 (c), and E-50 CGs (d) in DSW at the N/P ratio of 1 (first bar), 5 (second bar), 10 (third bar), 20 (fourth bar), 30 (fifth bar), and 50 (sixth bar).*, $P < 0.05$; significant against the gene expression of colon26-Luc without Luc siRNA.

In vitro time profiles of Luc siRNA release from gelatin hydrogels incorporating Luc siRNA and CG complexes

Figure 4 shows the in vitro time profiles of Luc siRNA release from gelatin hydrogels incorporating Luc siRNA and CG complexes in PBS with or without collagenase. About 35% of Luc siRNA was released initially, but after that no release

was observed. On the other hand, in PBS containing collagenase, the Luc siRNA was released similarly, irrespective of the CG type and N/P ratio.

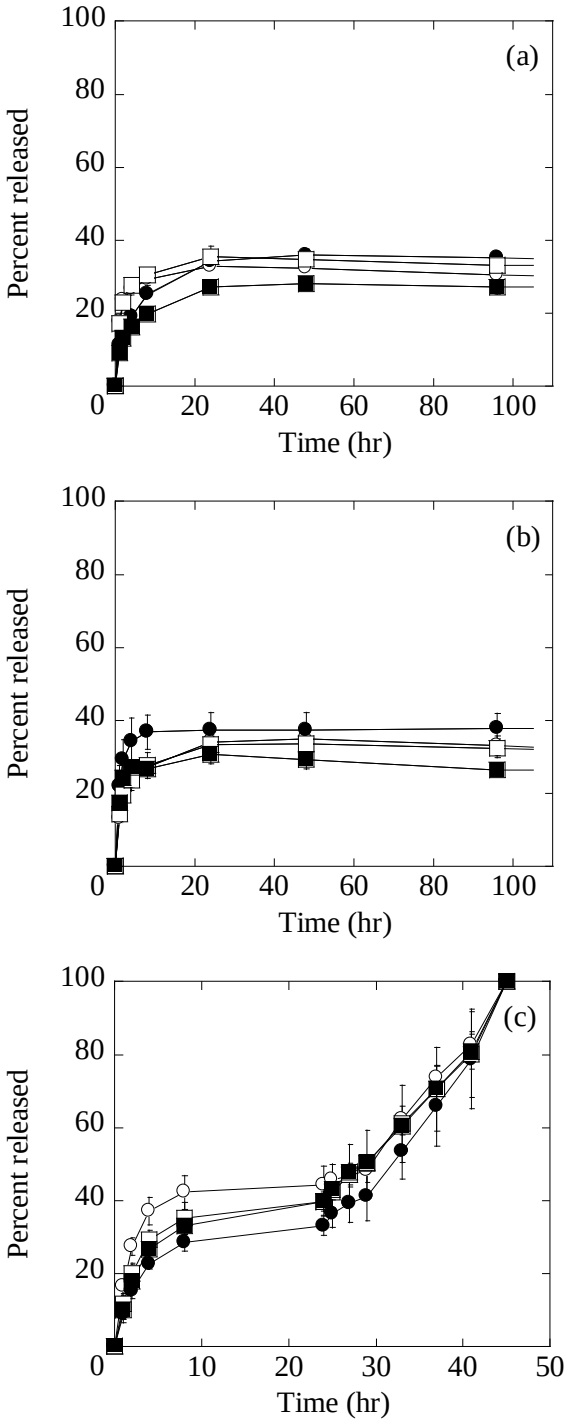

Figure 4. In vitro release profiles of Luc siRNA from gelatin hydrogels incorporating complexes of Luc siRNA and CG without collagenase (a and b). The complexes were prepared for siRNA with E-1.0 (○), E-3.0 (●), E-7.0 (□), and E-50 CGs (■). The N/P ratios are 10 (a) and 50 (b). (c) In vitro release profiles of Luc siRNA from gelatin hydrogels incorporating complexes of Luc siRNA and E-7.0 CG at N/P ratios of 10 (○) and 50 (●) and E-50 CG, at N/P ratios of 10 (□) and 50 (■). The release test was performed in PBS for the initial 24 h, and thereafter in collagenase PBS solution (5 μg/ml) at 37 °C.

In vitro time profiles of hydrogel degradation

Figure 5 shows in vitro time profiles of gelatin hydrogel degradation in PBS with or without collagenase. About 29% of hydrogel was degraded initially, but after that no degradation was observed. On the other hand, in PBS containing collagenase, the hydrogel was degraded similarly, irrespective of the CG type and N/P ratio.

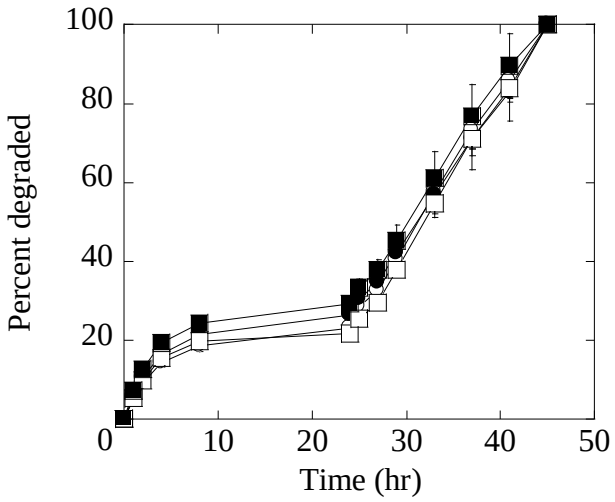

Figure 5. In vitro degradation profiles of gelatin hydrogels incorporating complex of siRNA and E-7.0, at N/P ratios of 10 (○) and 50 (●) and E-50 CG, at N/P ratios of 10 (□) and 50 (■). The degradation test was performed in PBS for the initial 24 hr, and thereafter in collagenase PBS solution (5 μg/ml) at 37 °C.

Gene suppression activity of Luc siRNA released

Figure 6 shows the gene suppression activity of medium supernatants after culture with hydrogels incorporating Luc siRNA and CG complex. The Opti-MEM supernatant did not show the suppression activity of gene expression (b) irrespective of the N/P ratio and CG type. On the contrary, the Opti-MEM-col supernatant had significant suppression activity (a). The suppression activity for gelatin hydrogels incorporating Luc siRNA and CG complexes at the N/P ratio of 50 had significantly higher than that of hydrogels at the N/P ratio of 10 (c). Even after 3, 6, and 9 h

incubation in Opti-MEM-col, the supernatants showed significant gene suppression activity (d). However, after 12 hr incubation in Opti-MEM-col, any supernatant did not show gene suppression activity because the amount of Luc siRNA in the supernatant was very low (data not shown). **Table 3** summarizes the amount of Luc siRNA released from gelatin hydrogels in Opti-MEM-col. Luc siRNA was gradually released from gelatin hydrogel and the released amount of siRNA maintained the suppression activity (d).

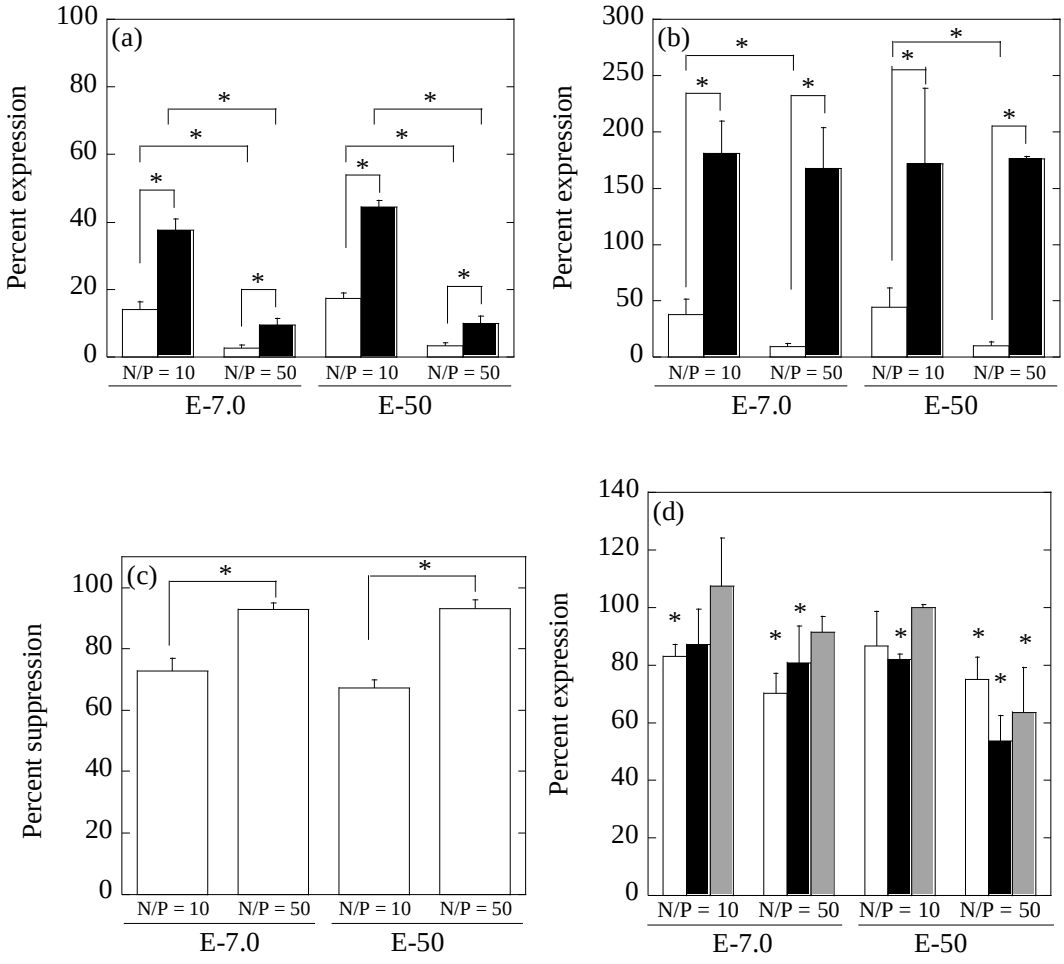

Figure 6. Percent gene expression of Luc siRNA released from gelatin hydrogels incorporating Luc siRNA and CG complexes in Opti-MEM with (a) and without collagenase (b). Gene suppression of fresh Luc siRNA and CG complex (□) and the supernatant (■) 24 h after incubation with hydrogels incorporating complex in Opti-MEM. *,$P < 0.05$; significant between the twogroups. (c) Percent suppression activity calculated by the formulation described above. *,$P < 0.05$; significant between the two groups. (d) Percent gene expression of Luc siRNA released from gelatin hydrogels incorporating Luc siRNA and CG complexes in Opti-MEM with collagenase. The supernatant was collected 3 (□), 6 (■), and 9 h (■) after culturing with the hydrogels incorporating complex to check the gene suppression activity. *,$P < 0.05$; significant against the gene expression of colon26-Luc without Luc siRNA. The percentage of luciferase expression was expressed as 100% for colon26-Luc cultured in Opti-MEM without Luc siRNA.

Table 3. The amount of Luc siRNA released in Opti-MEM contains collagenase.

Time (hr)	E-7.0 (nM)		E-50 (nM)	
	N/P = 10	N/P = 50	N/P = 10	N/P = 50
3	27.3±2.3	27.7±6.7	37.9±1.5	22.4±3.8
6	32.0±3.3	32.4±6.3	35.5±4.7	27.1±7.6
9	13.2±2.9	6.2±4.5	11.6±7.7	15.9±6.3
12	3.7±2.2	1.6±1.2	3.6±1.4	12.9±7.5

DISCUSSION

The present study demonstrates that the biological activity of siRNA was associated with the release rate of siRNA from the hydrogel and to the enzymatic degradation of gelatin hydrogels. When the siRNA was directly incorporated into the hydrogels prepared by the chemical crosslinking of pI5 or pI9 gelatin, an initial burst in siRNA release (about 80%) was observed (data not shown). For hydrogels prepared from pI5 gelatin (5 wt%), an initial burst in siRNA release (34.3 to –53.4%) was observed (data not shown). This is because the siRNA molecules do not always interact with the gelatin molecules, resulting in the burst release by the simple diffusion of siRNA. One of the methods to enhance the interaction of siRNA with gelatin is to use the cationized derivative which can electrostatically interact with negatively charged siRNA. The hydrogel of cationized gelatin worked well to achieve the controlled release of siRNA in vivo [13]. However, the cationized hydrogel sometimes induces severe inflammation reaction compared to the normal gelatin. Therefore, the siRNA of negative charge (phosphate group) was mixed with the CG to form the nanocomplex. Then, the complex was mixed with aqueous gelatin solution at a high concentration (20 wt%) to obtain the hydrogels. The complex of positive charge enabled the immobilization into the hydrogel of pI5 gelatin with a negative charge. In this release system, the siRNA is released in the complex form with the CG hydrogel only when the hydrogel is enzymatically degraded to generate water-soluble gelatin fragments. The siRNA activity to suppress the gene expression is high for the complex form compared with siRNA in the free form [14]. It is possible that the siRNA was released from the hydrogel in the form of complex with CG. CG will accelerate the cellular internalization of siRNA, resulting in the enhanced gene suppression activity.

Several researchers investigate the carrier for the sustained release of gene in vitro [15-17] and in vivo [18, 19]. For example, the hydrogels of photo-crosslinked alginate and collagen achieved the sustained delivery of siRNA [15]. The 3 dimensional hydrogels for sustained delivery of siRNA could suppress gene expression for 6 days in vitro. In addition, the in vivo sustained release of siRNA could be achieved with solid lipid nanoparticles [19]. The present hydrogel system is applicable for the sustained release of siRNA as a result of enzymatic hydrogel degradation. The release profiles of siRNA were in good accordance with the rate of hydrogel degradation. This again supports the release of siRNA in the complex form with the degraded fragment of CG. For the hydrogel system, the time profile of siRNA release can be changed by altering that of hydrogel degradability which can be controlled by the crosslinking extent of hydrogels. This release mechanism is similar to that of growth factors reported previously [20]. Time period of siRNA release can be changed from a few days to several months. These controlled gene silencing technologies have significant potential for use in tissue regeneration applications and experimental tools for suppression of specific gene expression.

The key factor to consider the siRNA action is not only the extent of gene silencing, but also the time period of activity maintenance. Even if the siRNA can be released, the release of inactive siRNA is practically useless. Therefore, in this study, the gene suppression activity of supernatants after the placement of hydrogel in the Opti-MEM-col was assessed (**Figures 6a–d**). When placed in Opti-MEM-col, it is likely that the hydrogel was degraded to release the Luc siRNA complex incorporated in the hydrogel. When compared at the same siRNA concentration, the supernatant containing the complex released exhibited significant gene suppression activity

although the activity was low compared with the fresh complex as a control. siRNA released from gelatin hydrogels incorporating Luc siRNA and CGcomplex (N/P ratio = 50) showed higher transfection efficacy than those of CG at the N/P ratio of 10. It is highly conceivable that during enzymatic degradation, the hydrogel gelatin and CG for the complexation with siRNA were randomly degraded. However, the siRNA activity in the supernatant after hydrogel incubation in the Opti-MEM-col remained. It is highly conceivable that even by enzymatic degradation, the siRNA itself was not degraded because of the complexation. The siRNA would be released in the complex form. In conclusion, the biodegradable hydrogel of gelatin is a promising carrier for the siRNA release which is driven by the hydrogel degradation. The Opti-MEM-col supernatants showed an activity to suppress the expression of the corresponding gene. By using the hydrogel, the biological activity of siRNA can be retained for a long time period.

REFERENCES

[1] A. Fire, S. Xu, M.K. Montgomery, S.A. Kostas, S.E. Driver, C.C. Mello, Potent and specific genetic interference by double-stranded RNA in Caenorhabditis elegans, Nature, 391 (1998) 806-811.

[2] P.D. Zamore, T. Tuschl, P.A. Sharp, D.P. Bartel, RNAi: double-stranded RNA directs the ATP-dependent cleavage of mRNA at 21 to 23 nucleotide intervals, Cell, 101 (2000) 25-33.

[3] D.F. Gilbert, G. Erdmann, X. Zhang, A. Fritzsche, K. Demir, A. Jaedicke, K. Muehlenberg, E.E. Wanker, M. Boutros, A novel multiplex cell viability assay for high-throughput RNAi screening, PloS one, 6 (2011) e28338.

[4] S. Tuzmen, P. Tuzmen, S. Arora, S. Mousses, D. Azorsa, RNAi-based functional pharmacogenomics, Methods Mol Biol, 700 (2011) 271-290.

[5] P.D. Rye, T. Stigbrand, Interfering with cancer: a brief outline of advances in RNA interference in oncology, Tumour biology : the journal of the International Society for Oncodevelopmental Biology and Medicine, 25 (2004) 329-336.

[6] H. Gong, C.M. Liu, D.P. Liu, C.C. Liang, The role of small RNAs in human diseases: potential troublemaker and therapeutic tools, Medicinal research reviews, 25 (2005) 361-381.

[7] H. Xia, Q. Mao, H.L. Paulson, B.L. Davidson, siRNA-mediated gene silencing in vitro and in vivo, Nat Biotechnol, 20 (2002) 1006-1010.

[8] E. Marshall, Gene therapy. What to do when clear success comes with an unclear risk?, Science, 298 (2002) 510-511.

[9] S.D. Reed, S. Li, Electroporation advances in large animals, Curr Gene Ther, 9 (2009) 316-326.

[10] C.M. Newman, T. Bettinger, Gene therapy progress and prospects: ultrasound for gene transfer, Gene therapy, 14 (2007) 465-475.

[11] C. Andrieu-Soler, M. Doat, M. Halhal, N. Keller, L. Jonet, D. BenEzra, F. Behar-Cohen, Enhanced oligonucleotide delivery to mouse retinal cells using iontophoresis, Molecular vision, 12 (2006) 1098-1107.

[12] K. Nagane, M. Kitada, S. Wakao, M. Dezawa, Y. Tabata, Practical induction system for dopamine-producing cells from bone marrow stromal cells using spermine-pullulan-mediated reverse transfection method, Tissue Eng Part A, 15 (2009) 1655-1665.

[13] Y. Obata, T. Nishino, T. Kushibiki, R. Tomoshige, Z. Xia, M. Miyazaki, K. Abe, T. Koji, Y. Tabata, S. Kohno, HSP47 siRNA conjugated with cationized gelatin microspheres suppresses peritoneal fibrosis in mice, Acta biomaterialia, (2012).

[14] H.J. Kim, A. Ishii, K. Miyata, Y. Lee, S. Wu, M. Oba, N. Nishiyama, K. Kataoka, Introduction of stearoyl moieties into a biocompatible cationic polyaspartamide derivative, PAsp(DET), with endosomal escaping function for enhanced siRNA-mediated gene knockdown, J Control Release, 145 (2010) 141-148.

[15] M.D. Krebs, O. Jeon, E. Alsberg, Localized and sustained delivery of silencing RNA from macroscopic biopolymer hydrogels, Journal of the American Chemical Society, 131 (2009) 9204-9206.

[16] D.K. Jensen, L.B. Jensen, S. Koocheki, L. Bengtson, D. Cun, H.M. Nielsen, C. Foged, Design of an inhalable dry powder formulation of DOTAP-modified PLGA nanoparticles loaded with siRNA, J Control Release, 157 (2012) 141-148.

[17] C.E. Nelson, M.K. Gupta, E.J. Adolph, J.M. Shannon, S.A. Guelcher, C.L. Duvall, Sustained local delivery of siRNA from an injectable scaffold, Biomaterials, 33 (2012)

1154-1161.

[18] G.B. Jacobson, E. Gonzalez-Gonzalez, R. Spitler, R. Shinde, D. Leake, R.L. Kaspar, C.H. Contag, R.N. Zare, Biodegradable nanoparticles with sustained release of functional siRNA in skin, Journal of pharmaceutical sciences, 99 (2010) 4261-4266.

[19] T. Lobovkina, G.B. Jacobson, E. Gonzalez-Gonzalez, R.P. Hickerson, D. Leake, R.L. Kaspar, C.H. Contag, R.N. Zare, In vivo sustained release of siRNA from solid lipid nanoparticles, ACS nano, 5 (2011) 9977-9983.

[20] Y. Tabata, A. Nagano, Y. Ikada, Biodegradation of hydrogel carrier incorporating fibroblast growth factor, Tissue Eng, 5 (1999) 127-138.

Chapter 3

Enhancement of in vivo anti-fibrotic effect by controlled release of low-molecular-weight heparin from gelatin hydrogels

INTRODUCTION

Heparin is a negatively charged glycosaminoglycan, which is composed of repeated disaccharide units of alternating glucosamine and glucuronic residues heterogeneously modified by carboxyl groups and N- or O-linked sulfate. It has been clinically used as an anticoagulant agent. In addition, other biological effects have been reported. For example, heparin enables cells to stimulate the production of hepatocyte growth factor HGF [1]. The anti-fibrotic effect of heparin is experimentally confirmed with a mouse model of CCl_4-induced hepatitis and unilateral ureteral obstruction kidney fibrosis [2] and [3]. Heparin has a side-effect of bleeding acceleration [4]. It is reported that compared with normal heparin, low-molecular-weight heparin (LMWH) has the nature to induce less bleeding [5]. The potential to induce the HGF production is similar to that of normal heparin [6]. Based on these findings, the LMWH was chosen as an anti-fibrotic drug in this study.

The objective of this chapter is to design a gelatin hydrogel system for the controlled release of LMWH. CG was prepared to form the water-soluble complex of LMWH. The complex was mixed with gelatin, followed by dehydrothermal cross-linking to prepare gelatin hydrogels incorporating the complex of LMWH and CG. The profile of LMWH release from the hydrogel and the hydrogel degradation was examined while the biological activity of hydrogels was evaluated for a mouse model of peritoneal fibrosis.

EXPERIMENTAL

Materials

LMWH (Mw = 5000, 130 IU/mg) was kindly supplied from Fuso Pharmaceutical Industries Ltd. β-alanine, 1,9-dimethylmethylene blue, sodium dodecyl sulfate (SDS), methanol, formic acid, sodium formic acid, and Cell Count Reagent SF were purchased from Nacalai Tesque, Kyoto, Japan. Testzym® heparin S was purchased from Yashima pure chemicals Co. Ltd. Mild form and chlorhexidine gluconate were purchased from Wako Pure Chemical Industries Ltd., Osaka, Japan. They were all of reagent grade and used without further purification.

Preparation of gelatin hydrogels incorporating LMWH and Cationized Gelatin (CG) complexes

LMWH was mixed with the CG in DDW (1 ml) at 37 °C to prepare the complex of LMWH and CG. Next, aqueous solution of pI5 gelatin (20 wt%, 1 ml) was added to the complexes solution at 37 °C. The mixed solution was poured into a polytetrafluoroethylene mold and frozen in liquid nitrogen, followed by freeze-drying. After that, the hydrogels were placed into the dry oven (AURORA DN-305, Sato Vacuum Inc., Japan) and dehydrothermally cross-linked for 12, 24, 48, 72, and 96 hr at 160 °C.

Release test of LMWH from gelatin hydrogels incorporating LMWH and CG complexes

Hydrogels of 5–7 mg in dry weight were placed in PBS (500 μl) at 37 °C. The PBS supernatant was exchanged 1, 2, 4, 8, 24, 48, and 96 hr later and subsequently

fresh PBS was added. The release test was performed in PBS for the initial 24 hr and after that, newly performed in PBS containing collagenase (1 mg/ml). The amount of LMWH in each solution was determined by the conventional colorimetric method [7]. Briefly, 1,9-dimethylmethylene blue (DMB, 1.6 mg) was dissolved in methanol (0.5 ml). Formic acid (0.2 g) and sodium formic acid (0.2 ml) were added to DDW to give the final volume of 100 ml. Sample solutions (25 μl) were mixed with DMB solution (225 μl). A calibration curve was prepared with the determined amounts of LMWH. The absorbance of solutions at 525 nm was determined by the microplate reader. The percentage introduced was determined based on the calibration curve and the absorbance of samples.

Degradation evaluation of hydrogels incorporating LMWH and CG complexes

Hydrogels of 5–7 mg in dry weight were placed in PBS (500 μl) at 37 °C. The PBS supernatant was exchanged 1, 2, 4, 8, and 24 hr later and subsequently fresh PBS was added. After that, the hydrogels were newly performed in PBS containing collagenase (1 mg/ml). PBS containing collagenase supernatant was exchanged every 3 hr and a fresh one was added. The amount of gelatin in each solution was determined by the colorimetric method [8]. The absorbance of solutions at 280 nm was determined by the microplate reader. A calibration curve was prepared with the determined amounts of pI5 gelatin. The percentage introduced was determined based on the calibration curve and the absorbance of samples.

Evaluation of anti-fibrotic effects

C57B/L6 mice were purchased from Shimizu Laboratory Supplies Co., Kyoto,

Japan. All the animal experimentation was conducted according to the guidance of the Institute for Frontier Medical Sciences, Kyoto University. A peritoneal fibrosis model of mice was prepared [9]. Briefly, mice (9- to 10-week old females weighing 20 g) were intraperitoneally administered with 0.1 vol% chlorhexidine gluconate dissolved in 15 vol% ethanol solution (15 μg/g body weight) every 3 days for 7 times. Gelatin hydrogels of 2.0-2.2 mg incorporating the LMWH and E-7.0 CG complex were implanted 21 days later in the right side of mice peritoneal. The left side of mice peritoneal was not treated. The hydrogel-incorporating complex was applied on the peritoneal wall and sutured for the fixation 3, 7, 10, 14, and 21 days after hydrogel application. The hydrogel-incorporating complex was cross-linked for 12 and 24 h. As controls, the complex-free hydrogel was applied and mice were not treated. The abdominal wall containing the hydrogel was taken and fixed in 4 vol% paraformaldehyde solution. They were embedded in paraffin and histological sections with 4 μm thickness were prepared by the rotary microtome (RM2125RT, Leica Microsystems Inc., Osaka, Japan). The sections were stained with hematoxylin and eosin staining and Masson trichrome without nucleus staining and viewed to evaluate the thickness of fibrotic walls using a microscope (PROVIS AX80, Olympus Co., Japan). Histological sections randomly selected (two sections for each experimental group) were observed and the average thickness was calculated.

Evaluation of LMWH activity of hydrogels incorporating LMWH and CG complexes

Gelatin hydrogels incorporating LMWH and CG complexes were completely dissolved in PBS containing 1 mg/ml of collagenase at 37 °C. The hydrogels were

cross-linked for 12 and 24 hr at 160 °C while non-cross-linked hydrogels were used as a control. The LMWH activity was evaluated by using Testzym® heparin S (Sekisui medical Co. Ltd., Osaka Japan). Briefly, hydrogels were dissolved by collagenase solution and the resulting solution (10 μl) was mixed with a plasma solution (10 μl), 1.0 IU/ml of antithrombin III solution (10 μl) and a 50 mmol/l of 2-amino-2-methyl-1,3-propanediol buffer solution (pH = 8.4, 70 μl) for 6 min at 37 °C. Factor Xa solution (50 μl, 7.1 nkt/ml) was added into the mixed solution for 30 s at 37 °C. N-Benzoyl-l-isoleucyl-l-glutamyl (γ-OR)–glycyl-l-arginyl-p-nitroanilide hydrochloride (100 μl) was added into the mixed solution for 3 min at 37 °C. Immediately after that, 50 vol% of acetic acid was added into this mixture to stop the reaction. A calibration curve was prepared with the determined amounts of LMWH. The absorbance of solutions at 405 nm was determined by the microplate reader.

Statistical analysis

All the results were expressed as the mean ± standard deviation (SD). Significant analysis was done based on the one-way ANOVA, and the difference was considered to be significant at $P < 0.05$.

RESULTS

Characterization of CG and LMWH complexes

Figure 1 shows the apparent molecular size and zeta potential of CG with different cationization extents and the LMWH complexes. The molecular size of CGs and the LMWH complex tended to decrease when the cationization extent of gelatin was higher than 27.0%. The size of complexes was larger than that of the corresponding CG with cationization extent of 27.0% or lower. However, at the higher extents, the complex size became smaller. The zeta potential of CG was higher than that of the corresponding complexes and tended to increase with increasing cationization extent of gelatin. At the cationization extent of 56.5%, the zeta potential of complexes was negatively charged.

Figure 2 shows the cytotoxicity of CGs. CGs at lower extents of cationization showed no cytotoxicity whereas the E-10 and E-50 CG did show cytotoxicity.

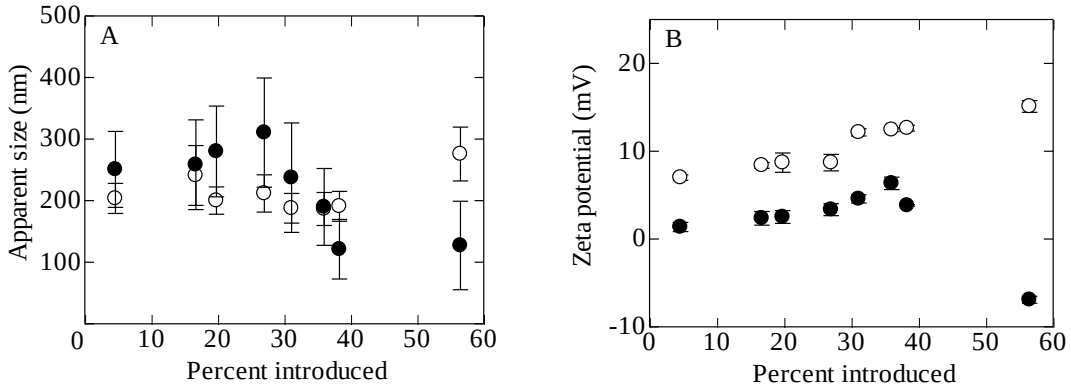

Figure 1. Apparent molecular sizes (A) and zeta potentials (B) of CGs (○) and the LMWH complexes (●) as a function of the cationization extent.

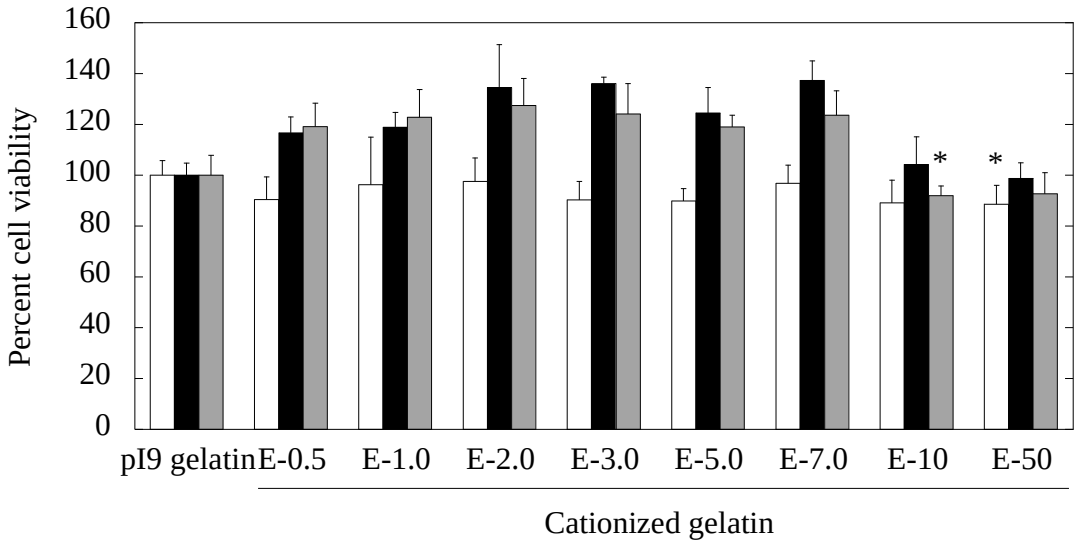

Figure 2. Cytotoxicity of CGs with different cationization extents. L929 cells were cultured in the presence or absence of CGs for 6 (□), 24 (■) and 48 hr (■).The percentage of cell viability was expressed as 100% for cells cultured with pI9 gelatin. *, $P < 0.05$; significant against the viability of cells cultured with pI9 gelatin at the corresponding time period.

In vitro time profiles of LMWH release from gelatin hydrogels incorporating LMWH and CG complexes

Figure 3 shows in vitro time profiles of LMWH release from gelatin hydrogels incorporating LMWH and CG complexes in PBS with or without collagenase. With increasing the cationization extent of gelatin, the initial burst release of LMWH tended to be suppressed. When examined in PBS, the gelatin hydrogels incorporating LMWH and CG complexes showed similar release profile, irrespective of the time period of hydrogel cross-linking. On the contrary, in PBS containing collagenase, the time profile of LMWH release depended on the cross-linking time. The LMWH release became slower as the time of hydrogel cross-linking became longer.

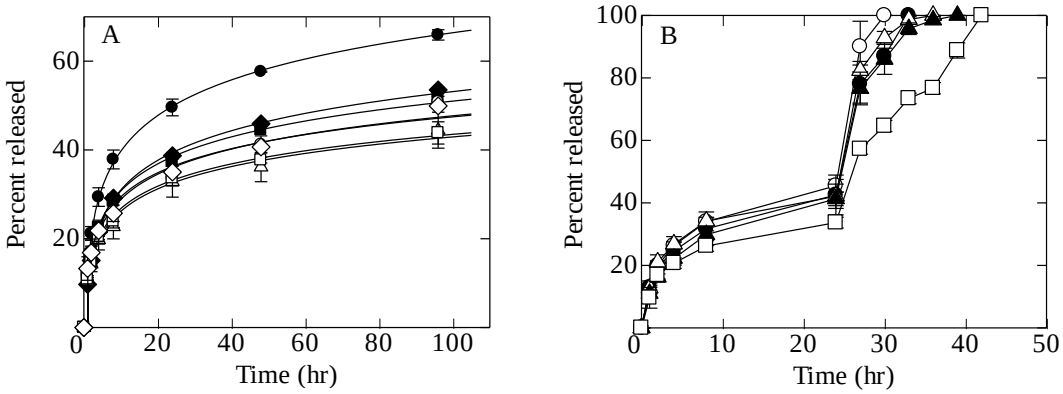

Figure 3. In vitro release profiles of LMWH from gelatin hydrogels incorporating complexes of LMWH and CG (A). The complexes were prepared for LMWH with E-0.5 (●), E-1.0 (▲), E-2.0 (■), E-3.0 (◆), E-5.0 (○), E-7.0 (△), E-10 (□), and E-50 CG (◇) in PBS at 37 °C. The hydrogels incorporating complex were dehydrothermally cross-linked at 160 °C for 24 hr. (B) The hydrogel incorporating complex of LMWH and E-7.0 CG were dehydrothermally cross-linked at 160 °C for 12 (○), 24 (●), 48 (△), 72 (▲), and 96 hr (□). The release test was performed in PBS for the initial 24 hr and thereafter in collagenase solution in PBS at 37 °C.

In vitro time profiles of hydrogel degradation

Figure 4A shows in vitro time profiles of hydrogel degradation in PBS with or without collagenase. With increasing the cross-linking extent of the hydrogels, the initial burst degradation of hydrogels tended to be suppressed. When examined in PBS, the gelatin hydrogels incorporating LMWH and CG complexes showed similar degradation profile, irrespective of the time period of hydrogel cross-linking. On the contrary, in PBS containing collagenase, the time profile of hydrogel degradation depended on the cross-linking time. The hydrogel degradation became slower as the time of hydrogel cross-linking became longer.

Figure 4B shows the relationship of half-life period between the LMWH release and hydrogel degradation. The half-life period was determined from the time profiles of LMWH release and hydrogel degradation in the test with collagenase. A good correlation in the half-life time between the LMWH release and hydrogel was observed.

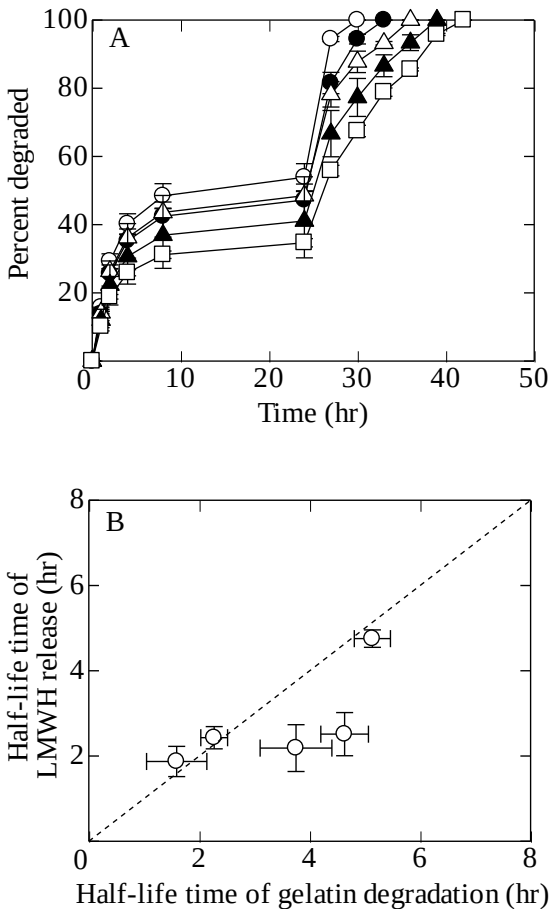

Figure 4. (A) In vitro degradation profiles of gelatin hydrogel-incorporating complex of LMWH and E-7.0 CG. The hydrogels were dehydrothermally cross-linked at 160 °C for 12 (○), 24 (●), 48 (△), 72 (▲), and 96 hr (□). The degradation test was performed in PBS for the initial 24 hr and thereafter in collagenase solution in PBS at 37 °C. (B) The relationship of half-life period between the LMWH release and hydrogel degradation. The half-life period was determined from the time profiles of LMWH release and hydrogel degradation in the test with collagenase.

Anti-fibrotic effects of gelatin hydrogels incorporating LMWH and CG

Figure 5 shows histological sections (H&E and Masson trichrome staining) of peritoneal fibrosis tissues before (**Figures A and B**) and 21 days after application with hydrogel incorporating LMWH and CG (**Figures 5C and D**), which is prepared through

dehydrothermal cross-linking 24 h (**Figure 5C**) and without any treatment (**Figure 5D**). Apparently, the application of hydrogels incorporating LMWH and CG complex decreased the thickness of fibrotic peritoneal walls.

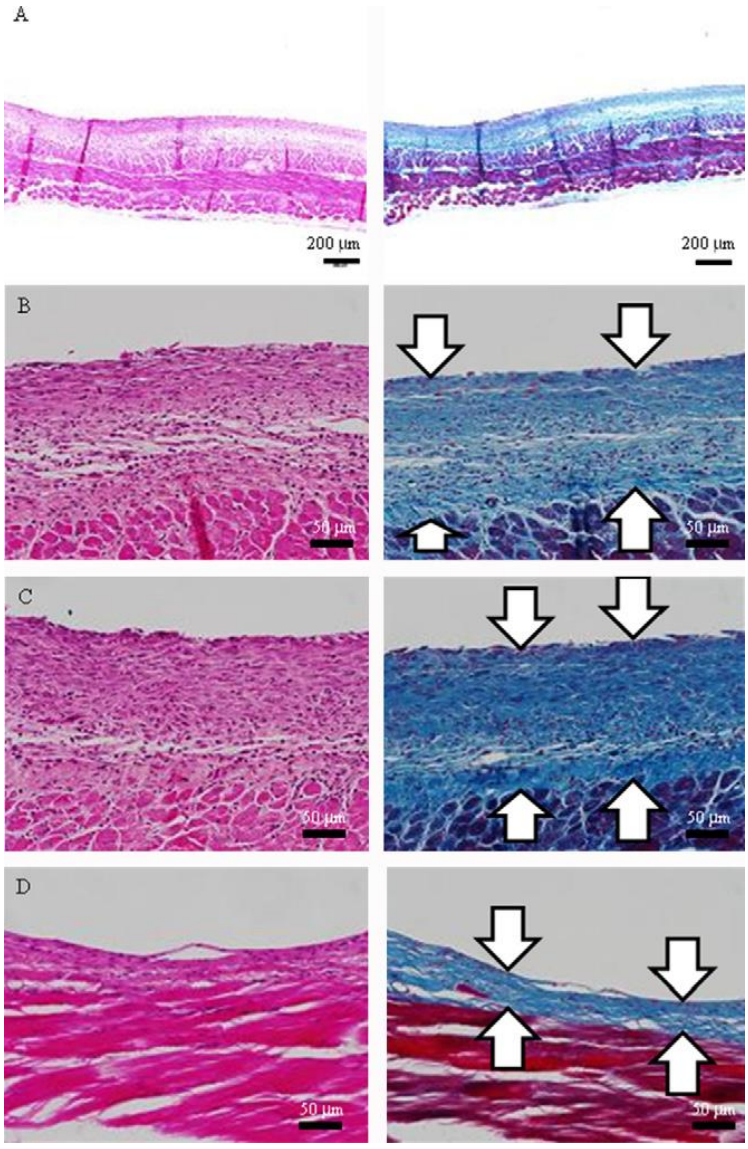

Figure 5. Histological sections (H&E and Masson trichrome staining) of peritoneal fibrosis tissues (A and B) and 21 days after application with hydrogel incorporating LMWH and CG, which is prepared through dehydrothermal cross-linking 24 h (C) and without any treatment (D).

Figure 6A shows the anti-fibrotic effects of gelatin hydrogels implanted for a mouse model of abdominal fibrosis. Significant anti-fibrotic effect was observed for the hydrogel-incorporating complex 10, 14, and 21 days after the application, irrespective of the hydrogel cross-linking time. On the contrary, the complex-free hydrogels did not show any biological activities, which is similar to that of the non-treated control group. On the other hand, no significant anti-fibrotic effect of the non-treated left side was observed (**Figure 6B**). The peritoneal wall thickness at the site applied with the complex-free hydrogel was similar to that of the non-treatment group.

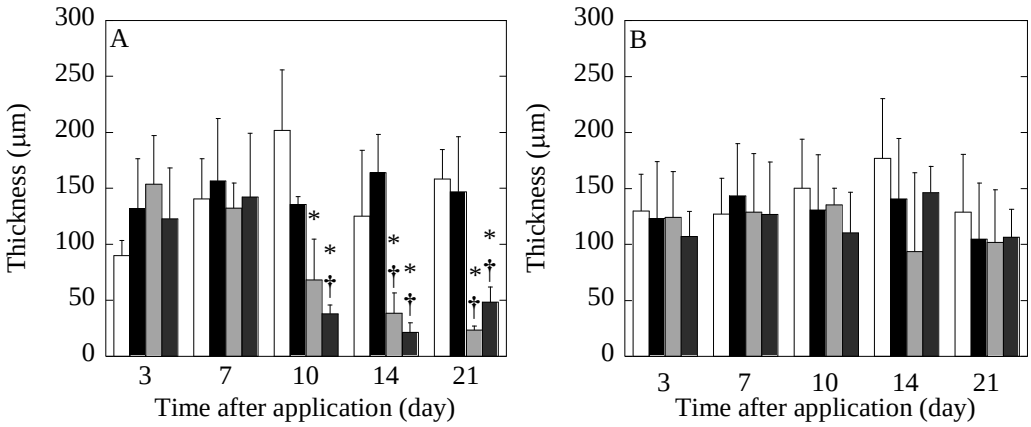

Figure 6. Anti-fibrotic effects of gelatin hydrogel-incorporating complex of LMWH and E-7.0 CG. The peritoneal wall thickness was measured at the site applied with the hydrogel-incorporating complex (■, ■) and the complex-free hydrogel (■) or without any treatments (□). The hydrogels were dehydrothermally cross-linked at 160 °C for 12 (■) and 24 hr (■). ∗$P < 0.05$; significant against the tissue thickness of non-cross-linked hydrogels. †$P < 0.05$; significant against tissue thickness of complex-free hydrogels.

Figure 7 shows the LMWH activity collected from gelatin hydrogels incorporating LMWH and CG complexes. The LMWH activity remaining was detected even though it was dehydrothermally cross-linked.

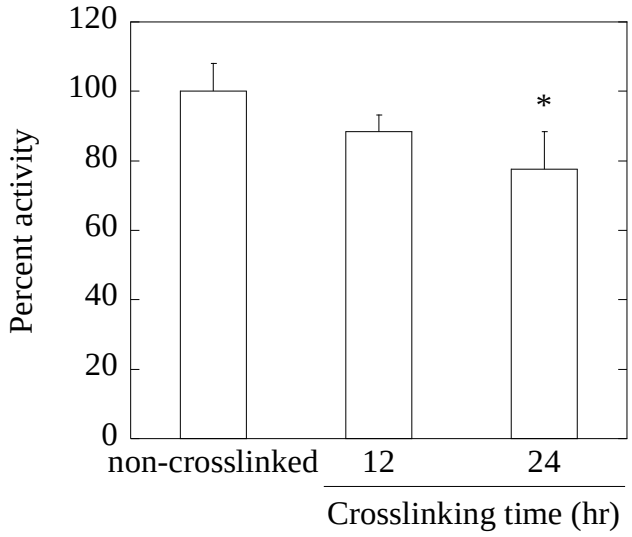

Figure 7. Biological activity of LMWH collected from gelatin hydrogel incorporating the complex of LMWH and E-7.0 CG. $*P < 0.05$; significant against the LMWH activity of non-cross-linked hydrogels.

DISCUSSION

This study demonstrates that the biodegradable gelatin hydrogel could release the LMWH of biological activity in different release profiles when the LMWH complex with CG was incorporated into the hydrogel. Gelatin and the derivatives have been used to prepare the hydrogel of carrier material for the controlled release of various drugs, proteins, and genes, because of the biodegradability and biocompatibility. When the LMWH was directly into the hydrogels prepared by the dehydrothermal cross-linking of pI5 or pI9 gelatin, an initial burst in LMWH release (~80%) was observed (data not shown). This is because the LMWH of small molecules did not interact with the gelatin molecules and the consequent release by the simple diffusion. Therefore, the LMWH of

negative charge was mixed with the CG to form nano-sized complexes. The complex of positive charge was immobilized into the hydrogel of pI5 gelatin with negative charge. The initial burst of LMWH release was effectively suppressed (**Figure 3A**). It is possible that the complex with positive charge (**Figure 1B**) interacted with pI5 gelatin, resulting in the suppressed initial burst. The release test in collagenase solution revealed that the LMWH release became slower as the time period of hydrogel cross-linking (**Figure 3B**). At the cationization extent of 56.5%, the zeta potential of complexes was negatively charged. This is because the complex surface had an excessive positive charge which can be firmly interacted with the LMWH. The strong interaction would make the surface charge negative. This complex system could not be interacted with pI5 gelatin. Therefore, the initial burst release of LMWH from gelatin hydrogels incorporating LMWH and E-50 CG was larger than that of E-7.0 and E-10 CG (**Figure 3A**).

The time period of LMWH release corresponded well with that of hydrogel degradation (**Figure 4B**). The extent of hydrogel cross-linking would increase with an increase in the cross-linking time. It is highly conceivable that the hydrogel was degraded enzymatically to generate water-soluble gelatin fragments, resulting in the release of LMWH in the complexed state. The complex had positive charge although the charge was lower than that of CG. This positive charge is necessary to electrostatistically interact with the pI5 gelatin of negative charge, but sometimes causes cytotoxicity. Cationized materials show the cytotoxicity higher than anionized ones [10]. It is apparent that CG with higher extents of cationization showed cytotoxicity (**Figure 2**). Taken together, the E-7.0 CG was selected to form the complexes with LMWH.

In the in vitro release test with collagenase-free PBS, the factor immobilized is

not released although the small amount of initial release is observed for the factor without interaction with gelatin matrix. However, when the release test is performed in collagenase solution, the hydrogel is enzymatically degraded with time and consequently the factor immobilized is released from the hydrogel. The present LMWH release is based on this mechanism of carrier matrix degradation. The LMWH complexes are immobilized in the gelatin hydrogel matrix. When degraded by collagenase, the hydrogel can release the LMWH complexes, as shown in **Figure 3B**. The time profile of LMWH is regulated by that of hydrogel degradation.

The hydrogels incorporating LMWH and CG showed significant anti-fibrotic effects (**Figure 5 and Figure 6**). It is reported that the LMWH promotes the production of HGF, which has an anti-fibrotic activity [2, 3]. Several researches have been reported on the HGF-based anti-fibrotic activity [11-13]. There are some mechanisms about that. HGF has an ability to induce the Matrix Metalloproteinase (MMP)-1 production, which can digest the fibrosis of collagen, resulting in reduced fibrosis [14]. It is well known that transforming growth factor (TGF) β1 has been implicated as a major inducer of fibrosis in many tissues [15]. On the other hand, HGF has an ability to suppress the TGF-β1 production [16]. It is possible that HGF suppresses the TGF-β1 production, resulting in the reduced progression of fibrosis. We can say with certainty that the local release of LMWH functioned the surrounding cells to induce the HGF production, resulting in the HGF-induced anti-fibrotic effect. The peritoneal wall thickness at the site applied with the complex-free hydrogel and without any treatments had no significant effects. This indicates that the hydrogels incorporating E-7.0 CG are of non- or low-inflammation induction.

REFERENCES

[1] K. Matsumoto, H. Tajima, H. Okazaki, T. Nakamura, Heparin as an inducer of hepatocyte growth factor, J Biochem, 114 (1993) 820-826.

[2] W. Abe, K. Ikejima, T. Lang, K. Okumura, N. Enomoto, T. Kitamura, Y. Takei, N. Sato, Low molecular weight heparin prevents hepatic fibrogenesis caused by carbon tetrachloride in the rat, J Hepatol, 46 (2007) 286-294.

[3] I.M. Pecly, R.G. Goncalves, E.P. Rangel, C.M. Takiya, F.S. Taboada, C.A. Martinusso, M.S. Pavao, M. Leite, Jr., Effects of low molecular weight heparin in obstructed kidneys: decrease of collagen, fibronectin and TGF-beta, and increase of chondroitin/dermatan sulfate proteoglycans and macrophage infiltration, Nephrol Dial Transplant, 21 (2006) 1212-1222.

[4] A.G. Turpie, A.S. Gallus, J.A. Hoek, A synthetic pentasaccharide for the prevention of deep-vein thrombosis after total hip replacement, N Engl J Med, 344 (2001) 619-625.

[5] E. Gray, B. Mulloy, T.W. Barrowcliffe, Heparin and low-molecular-weight heparin, Thromb Haemost, 99 (2008) 807-818.

[6] R. Sakiyama, K. Fukuta, K. Matsumoto, M. Furukawa, Y. Takahashi, T. Nakamura, Stimulation of hepatocyte growth factor production by heparin-derived oligosaccharides, J Biochem, 141 (2007) 653-660.

[7] J.G. de Jong, R.A. Wevers, C. Laarakkers, B.J. Poorthuis, Dimethylmethylene blue-based spectrophotometry of glycosaminoglycans in untreated urine: a rapid screening procedure for mucopolysaccharidoses, Clin Chem, 35 (1989) 1472-1477.

[8] T. Tanigo, R. Takaoka, Y. Tabata, Sustained release of water-insoluble simvastatin from biodegradable hydrogel augments bone regeneration, J Control Release, 143 (2010) 201-206.

[9] Y. Yoshio, M. Miyazaki, K. Abe, T. Nishino, A. Furusu, Y. Mizuta, T. Harada, Y. Ozono, T. Koji, S. Kohno, TNP-470, an angiogenesis inhibitor, suppresses the progression of peritoneal fibrosis in mouse experimental model, Kidney Int, 66 (2004) 1677-1685.

[10] D.M. Morgan, V.L. Larvin, J.D. Pearson, Biochemical characterisation of polycation-induced cytotoxicity to human vascular endothelial cells, J Cell Sci, 94 (Pt 3) (1989) 553-559.

[11] S. Mizuno, K. Matsumoto, T. Nakamura, HGF as a renotrophic and anti-fibrotic regulator in chronic renal disease, Front Biosci, 13 (2008) 7072-7086.

[12] R.A. Panganiban, R.M. Day, Hepatocyte growth factor in lung repair and pulmonary fibrosis, Acta Pharmacol Sin, 32 (2011) 12-20.

[13] S. Schievenbusch, I. Strack, M. Scheffler, K. Wennhold, J. Maurer, R. Nischt, H.P. Dienes, M. Odenthal, Profiling of anti-fibrotic signaling by hepatocyte growth factor in renal fibroblasts, Biochem Biophys Res Commun, 385 (2009) 55-61.

[14] M. Jinnin, H. Ihn, Y. Mimura, Y. Asano, K. Yamane, K. Tamaki, Effects of hepatocyte growth factor on the expression of type I collagen and matrix metalloproteinase-1 in normal and scleroderma dermal fibroblasts, J Invest Dermatol, 124 (2005) 324-330.

[15] M.H. Branton, J.B. Kopp, TGF-beta and fibrosis, Microbes Infect, 1 (1999) 1349-1365.

[16] J. Yang, C. Dai, Y. Liu, Hepatocyte growth factor suppresses renal interstitial myofibroblast activation and intercepts Smad signal transduction, Am J Pathol, 163 (2003) 621-632.

PART II

DESIGN OF GELATIN HYDROGELS INCORPORATING WATER-INSOLUBLE LOW MOLECULAR WEIGHT DRUGS

Chapter 4

Enhancement of in vivo macrophage recruitment by Controlled release of sphingosine-1-phosphate agonist from gelatin hydrogels

INTRODUCTION

Macrophage plays a critical role in the inflammation process. If macrophage is depleted, wound repair is often delayed [1, 2]. Macrophage deteriorates during severe inflammation, while it efficiently suppresses inflammation, inducing tissue regeneration [3, 4]. It is thus recognized that the inflammatory condition is greatly influenced by the existence and phenotype of macrophage. The findings suggest that the existence and phenotype of macrophage modify the extent of inflammation, which can regulate the process of tissue regeneration. It is conceivable that enhanced recruitment of macrophage physiologically induces inflammation, thus initiating the regeneration and repair process of injured or damaged tissues, although the quality of inflammation greatly affects the healing process. However, the healing process will not start without suitable induction of inflammation. As the first trial to induce inflammation, it is essential to design a technology to enhance in vivo macrophage recruitment. The objective of this study is to develop such a technology for macrophage recruitment and evaluate the extent of recruitment enhancement.

A “find me” signal is known to function as the chemoattractant for macrophage [5]. Apoptotic cells secrete the “find me” signal by which macrophage is recruited to the cells, leading to phagocytic exclusion. Sphingosin-1-phosphate (S1P) is one of the “find me” signals [6]. However, mouse macrophage has three types of S1P receptors: S1PR1, S1PR2 and S1PR3 [7-9]. When S1P binds to the S1PR1, macrophage migration is

enhanced [8, 10]. Conversely, when S1P binds to S1PR2, macrophage migration is suppressed. SEW2871 (5-[4-phenyl-5-(trifluoromethyl) thiophen-2-yl]-3-[3-(trifluoromethyl) phenyl] 1,2,4-oxadiazole, SEW) is a S1PR1-specific agonist that does not act on S1PR2 [11]. SEW is an effective drug for inducing the recruitment of macrophage [12, 13]. Moreover, it has weaker potential for S1PR1 down-regulation than another agonist of FTY720-P [14]. However, in order to achieve efficient in vivo usage of water-insoluble and low-molecular-weight SEW, it is necessary to develop a pharmaceutical form of administration.

In this chapter, the biodegradable gelatin hydrogel was designed for the controlled release of water-insoluble SEW. A hydrophobic derivative of gelatin was prepared by grafting an L-lactic acid oligomer (LLAo) to gelatin. SEW was water-solubilized by micelle formation with the gelatin grafted by LLAo (LA-Gelatin). The SEW micelles were mixed with gelatin, followed by dehydrothermal crosslinking under different conditions to obtain gelatin hydrogels incorporating SEW micelles. We examine the in vitro and in vivo release of SEW from the hydrogels incorporating SEW micelles. When the hydrogels incorporating SEW micelles were implanted into the back subcutis of mice, macrophage recruitment into the implanted site was evaluated, and compared with that of free SEW micelles.

EXPERIMENTAL

Materials

Disuccimidyl carbonate (DSC), 4-dimethylaminopyridine (DMAP) and other chemicals were purchased from Nacalai Tesque Inc., Kyoto, Japan. SEW was purchased from Cayman Chemical Co., Michigan.

Synthesis of L-lactic acid oligomers

L-lactic acid oligomer (LLAo) with different molecular weights were synthesized from l-lactide monomers by ring-opening polymerization with a stannous octate catalyst and 1-dodecanol as an initiator [15]. Briefly, L-lactide (20 g, 138.8 mmol, Purac Biochemical BV, Gorinchem, Netherlands) was melted at 130 °C in a nitrogen atmosphere, followed by the addition of toluene (5.6 ml) containing 1-dodecanol (4.67 g, 24.6 mmol, 2.10 g, 11.0 mmol or 1.35 g, 7.1 mmol) and stannous octate (0.56 g, 1.38 mmol). After mixing for 4 h at 130 °C, the reaction product was dissolved in chloroform and the solution was poured into ethanol for precipitation three times. After precipitation, the solution was freeze-dried. The number-averaged molecular weight of LLAo prepared was determined by proton nuclear magnetic resonance spectroscopy (JNM-EX, JEOL, Ltd, Tokyo, Japan).

Synthesis of gelatin grafted with LLAo

The pI5 gelatin was dissolved in anhydrous dimethyl sulfoxide (DMSO, 30 ml) at room temperature. Various amounts of LAo with number-averaged molecular weights of 950, 2200 and 3200 (1.0, 3.0 and 5.0 × 10^{-5} mol) were dissolved in 10 ml DMSO, and then DSC and DMAP (1.0, 3.0 and 5.0 × 10^{-5} mol) were dissolved in 2.5 ml of DMSO. The solution was mixed for 3 hr under stirring at room temperature to activate

the hydroxyl groups of LAo. The solution of activated LAo was slowly added to the gelatin solution, while the mixture was stirred overnight at room temperature for LAo grafting to gelatin. The product solution was dialyzed against double distilled water (DDW) with a dialysis tube with the cut-off molecular weight of 12,000–14,000 (UC 30-32-100, EIDIA Co., Ltd, Tokyo, Japan) for 72 hr at room temperature, followed by freeze-drying to obtain the LA-Gelatin.

Measurement of critical micellar concentration of LA-Gelatin

The critical micellar concentration (CMC) of LA-Gelatin was determined by the conventional fluorescence technique with pyrene [15]. LAo-grafted gelatin (LA-Gelatin) was dissolved in 10 mM of phosphate-buffered solution (PBS, pH 7.4) at concentrations from 0.001 to 1 mg/ml. Pyrene was dissolved in acetone at 6 mM. After mixing with the pyrene solution, the change in the emission intensity ratio (I339/I333) of mixed pyrene and polymer solution was measured at excitation wavelengths of 333 and 339 nm and the emission wavelength of 390 nm. The CMC was determined as the concentration at which the intensity ratio was sharply changed on the ratio–polymer concentration plot. Experiments were done independently three times for each sample unless otherwise mentioned.

Dynamic light scattering measurement of LA-Gelatin micelle and SEW micelle

To measure the apparent molecular size of LA-Gelatin micelle, dynamic light scattering (DLS) measurement was carried out on a DLS-DPA-60HD (Otsuka Electronic Co., Ltd, Osaka, Japan) equipped with a He–Ne laser at a detection angle of 90° at room temperature. Each sample was dissolved in DDW (1.0 mg/ml).

Water-solubilization of SEW by LA-Gelatin

LA-Gelatin solution (1.0 mg/ml) in DDW and SEW solution (1.0 mg/ml) in ethanol were prepared. The SEW solution (474 μl) was added to the LA-Gelatin solution (9.0 ml), followed by stirring for 24 hr at room temperature. The reaction mixture was centrifuged (8000 rpm, 5 min, 4 °C) to separate water-insoluble SEW, and freeze-dried to obtain the SEW water-solubilized by LA-Gelatin micelles (SEW micelles). To measure the amount of SEW incorporated into the SEW micelles, acetonitrile was added to the freeze-dried SEW micelles, followed by ultra-sonication for 10 s on ice to allow SEW to be extracted in acetonitrile. After centrifugation (10,000 rpm, 5 min, 4 °C), the amount of SEW in the supernatant was detected by high-performance liquid chromatography (HPLC, LC-20AT (Shimadzu Corp., Kyoto, Japan) and TSKgel® ODS-100 V 5 μm (15 cm × 4.6 mm) column (TOSOH Corp., Tokyo, Japan). The mobile solution was a mixture of water and acetonitrile (10:90, v/v) solution and the flow rate was 1.0 ml/min, while the absorbance of SEW was measured at a wavelength of 242 nm.

Preparation of gelatin hydrogels incorporating SEW micelle

Hydrogels were prepared through the dehydrothermal crosslinking of gelatin, together with SEW micelles at 160 °C for 24 h [16]. Briefly, pI9 gelatin in DDW (100 mg/ml, 1.0 ml) and SEW micelles containing 7.5 or 75 μg/ml of SEW in DDW (1.0 ml) were mixed. Then, the solution (2.0 ml) was cast into a polypropylene dish (20 mm × 20 mm, Sakura Finetek Japan Co., Ltd, Tokyo, Japan), followed by freezing in liquid nitrogen and freeze-drying. The freeze-dried hydrogels were treated under vacuum, followed by heating at 160 °C for 24 hr.

In vitro test of SEW release from gelatin hydrogels incorporating SEW micelles and hydrogel degradation

An in vitro test was performed in PBS at 37 °C for the initial 24 hr, and thereafter in PBS containing collagenase for up to 40 h. The sampling times were 1, 2, 4, 8, 24, 25, 26, 28, 32, 36 and 40 hr. The gelatin hydrogel (5.0–5.5 mg) incorporating SEW micelles containing ~3.8 μg/ml of SEW was placed in 500 μl PBS for the initial 24 hr, followed by sampling to collect the supernatant at different time intervals, and fresh 500 μl PBS was added. PBS (500 μl) was replaced with 500 μl PBS containing 50 μg/ml collagenase, and then a similar release test was continued. The amount of SEW was measured by HPLC, described above. For the in vitro degradation test, the PBS with or without collagenase was used in the same way, and the sampling time was also the same. The amount of protein in the supernatant sampled was determined by the micro bicinchonic acid (BCA) protein assay kit (Pierce, Rockford, IL, USA) to evaluate the time course of hydrogel degradation.

In vivo test of SEW release from gelatin hydrogels incorporating SEW micelles

C57BL/6CrSlc male mice (8–12 weeks old) were purchased from the Shimizu Laboratory Supplies Co., Kyoto, Japan. All the animal experimentation was conducted in accordance with the guidance of the Institute for Frontier Medical Sciences, Kyoto University. For the in vivo release study, the hydrogel was implanted into the back subcutis of mice according to the method reported previously [17]. Briefly, the back skin hair of mice was shaved using a razor under pentobarbital anesthesia (50 mg/kg). Then, the back skin was cut using scissors and from the cut, the hydrogel (8 × 8 × 2

mm^3, 15–16 mg) incorporating SEW micelles containing 12 μg of SEW was implanted into the back subcutis, and then the back skin was sutured. At 1, 3, 7, 10, 14 and 21 days after hydrogel application, the mice were sacrificed with an overdose injection of anesthetic, and then the hydrogels were removed to measure the SEW remaining, using the HPLC technique described above. The experiment was independently performed for three samples per experimental group at each sampling point.

In vitro migration assay

To evaluate the bioactivity of SEW for macrophage migration, mouse-bone-marrow-derived macrophage was used [18]. Briefly, the mouse bone marrow was collected from the femurs and tibias of mice by the conventional syringe aspiration method. The cells collected were resuspended in 10 ml of Iscove's modified Dulbecco's medium (IMDM) containing 20 vol.% fetal calf serum (FCS) and 50 ng/ml recombinant human macrophage-colony stimulating factor (M-CSF), and cultured on 10 cm diameter dishes in 37 °C, 5% CO_2–95% air atmosphere for 6 days. The cultured cells were used as mouse-bone-marrow-derived macrophage. The migration of macrophage was evaluated by the conventional method with a modified Boyden chamber equipped with a polycarbonate filter (5 μm pores; Corning, NY, USA) [6]. Briefly, cells (5×10^4 cells/well) were added to the upper compartment, while the lower chamber was filled with FCS-free culture medium containing different amounts of free SEW and different amounts of SEW micelles released from the hydrogels. For free SEW, SEW solution (1.0 mg/ml) in ethanol was added to the medium to give different amounts. Cells were allowed to migrate for 3 hr, at 37 °C, and then the non-migrating cells present on the top of the filter were removed mechanically. The migrated cells on

the bottom of the filter were fixed, and stained with Hemacolor® (Merck Millipore, Darmstadt, Germany), to count the number of cells that migrated in 12 randomly selected areas of the filter.

Evaluation of macrophage recruitment by hydrogels incorporating SEW micelles in the subcutis of mice

Mice were anesthetized by the intraperitoneal administration of pentobarbital (50 mg/kg). The hydrogels incorporating SEW micelles containing 1 (SEW1Gel) and 10 μg (SEW10Gel) of SEW were implanted into the back subcutis of the mice. The control samples used were SEW-free gelatin hydrogels, ethanol solution of 10 μg SEW, SEW micelles containing 10 μg of SEW (SEW10 μg micelles solution) and PBS alone. At different time intervals, the tissues around the implanted hydrogel and the hydrogel were collected and digested in 2 mg/ml of collagenase D at 37 °C for 1.5 hr, followed by the collection of cell fractions through 40 μm aperture strainers (BD Biosciences, San Jose, California). The tissues and hydrogels were separated manually before collection through the 40 μm aperture strainers. The cell suspensions obtained were lysed in 500 μl of lysis buffer (555899, BD Biosciences, San Jose, California) for 15 min at 37 °C. After washing twice with 500 μl of PBS, the cells were treated with fluorescent-labeled FITC 7-AAD (BD Biosciences, San Jose, California), CD45 (eBioscience, Inc., San Diego, California), Ly6G (eBioscience, Inc., San Diego, California) CD11b (BD Biosciences, San Jose, California) and F4/80 antibodies (Biolegend, Inc., San Diego, California). The cells labeled were analyzed by flow cytometry (FACSCanto II flow cytometer, BD Biosciences, San Jose, California). The cells with CD45+, Ly6G−, CD11b+ and F4/80+ were defined as macrophage. The

number of animals used for each experimental time point was 3.

Evaluation of macrophage recruitment with a mouse model of skin wound

To evaluate macrophage recruitment to the inflammatory site, a mouse model of the skin wound was prepared [19]. Mice were anesthetized by the intraperitoneal administration of pentobarbital (50 mg/kg). The back hair of the mice was shaved. A skin defect was made on the back subcutis using an 8 mm-size biopsy punch. The gelatin hydrogel (8 × 8 × 2 mm^3, 15–16 mg) alone (Gel) and SEW10Gel were applied and sutured to the surrounding skin. SEW 10 mg micelle solution was applied to the defect, while the defect was not covered by Gel. At different time intervals, the tissue around the wound area and the implanted hydrogel was collected and digested in 2 mg/ml of collagenase D at 37 °C for 1.5 h, followed by the collection of cell fractions through 40 μm strainers (BD Biosciences, San Jose, California). The cells were treated with FITC-labeled antibodies and analyzed by the flow cytometry procedure described above.

Statistical analysis

All the results were expressed as the mean ± standard deviation (SD). Significant analysis was carried out based on the one-way analysis of variance, and the difference was considered to be significant at $P < 0.05$.

RESULTS

Characterization of LA-Gelatin

Table 1 summarizes the physicochemical properties of LA-Gelatin prepared in different conditions. Every LA-Gelatin showed a CMC value, which indicates the nature of micelle formation. The apparent molecular size of LA-Gelatin micelles ranged from 142 to 379 nm. The water solubility of LA-Gelatin tended to decrease with an increase in the molecular weight of LA-Gelatin and the grafted ratio (data not shown).

Table 1. Preparation and characterization of LA-Gelatin

Code	LAo used for grafting		CMC	Apparent moleclar size
	Mn	The ratio of LLAo grafted (mole/mole gelatin)	(μg/ml)	(nm)
LAo1-1	950	1	39.9	142.4±40.6[a)]
LAo1-3	950	3	18.0	189.2±41.4
LAo1-5	950	5	99.2	360.2±83.8
LAo2-1	2200	1	21.4	245.7±127.8
LAo2-3	2200	3	61.3	319.9±157.6
LAo2-5	2200	5	31.6	215.2±128.9
LAo3-1	3200	1	85.8	215.5±43.4
LAo3-3	3200	3	40.8	230.6±44.8
LAo3-5	3200	5	32.7	378.9±85.5

[a)] mean±SD

Water-solubilization of SEW by LA-Gelatin

Figure 1 shows the percentage of SEW water-solubilized by LA-Gelatin. The amount of water-solubilized SEW depended on the molecular weight of LA-Gelatin and the grafted ratio. Based on the results, the LAo2-1 of LA-Gelatin was used in the following experiments.

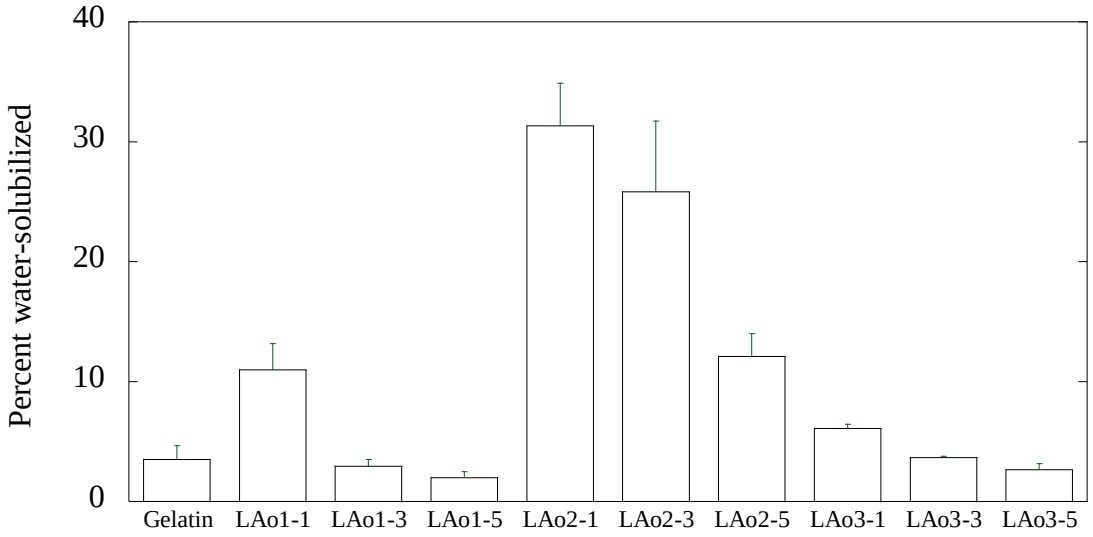

Figure 1. Percentage of SEW water-solubilized by various LAo-gelatin samples.

SEW release from gelatin hydrogels incorporating SEW micelles and hydrogel degradation

Figure 2 shows the time profiles of hydrogel degradation and SEW release from gelatin hydrogels incorporating SEW micelles in PBS with or without collagenase. In the presence of collagenase, SEW was released with time from the gelatin hydrogels. On the contrary, only 4.0% of SEW release was observed in collagenase-free PBS (**Figure 2A**). In PBS containing collagenase, the hydrogels were degraded with time, whereas little hydrogel degradation was observed in PBS (**Figure 2B**). A good correlation in the time profiles was observed between the SEW release and hydrogel degradation. **Figure 3** shows that the SEW was released gradually from the hydrogels incorporating SEW micelles in vivo.

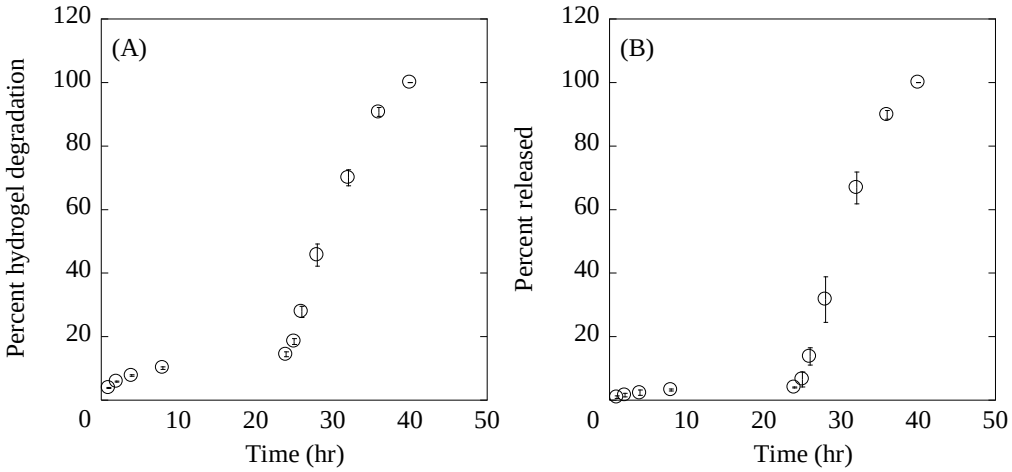

Figure 2. The time profiles of gelatin hydrogels incorporating SEW micelle degradation (A) and SEW release from the hydrogels incorporating SEW micelles (B). The release test was performed at 37 °C in PBS for the initial 24 hr, and thereafter in PBS containing collagenase.

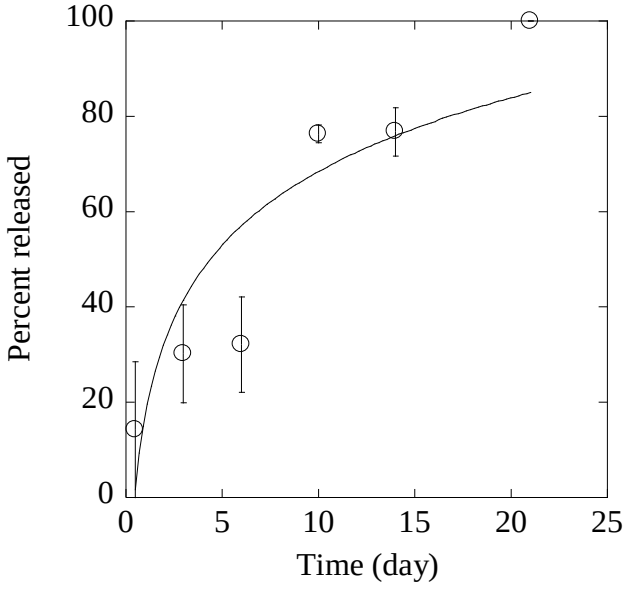

Figure 3. The time profile of in vivo SEW release from gelatin hydrogels incorporating SEW micelles in the back subcutis of mice.

Biological activity of SEW and SEW micelles released from gelatin hydrogels in vitro

Figures 4A and B show macrophage migration by different amounts of free SEW and different amounts of SEW released from hydrogels incorporating SEW micelles for 2 and 16 h incubation in PBS containing collagenase. The percentage of migrated cells in the FCS-free culture medium without SEW was 2.0%. On the contrary, significantly enhanced macrophage migration was observed at 0.1 or higher concentrations of SEW. The SEW released from the hydrogels also enhanced the macrophage migration, irrespective of the SEW amount incorporated and the time period released.

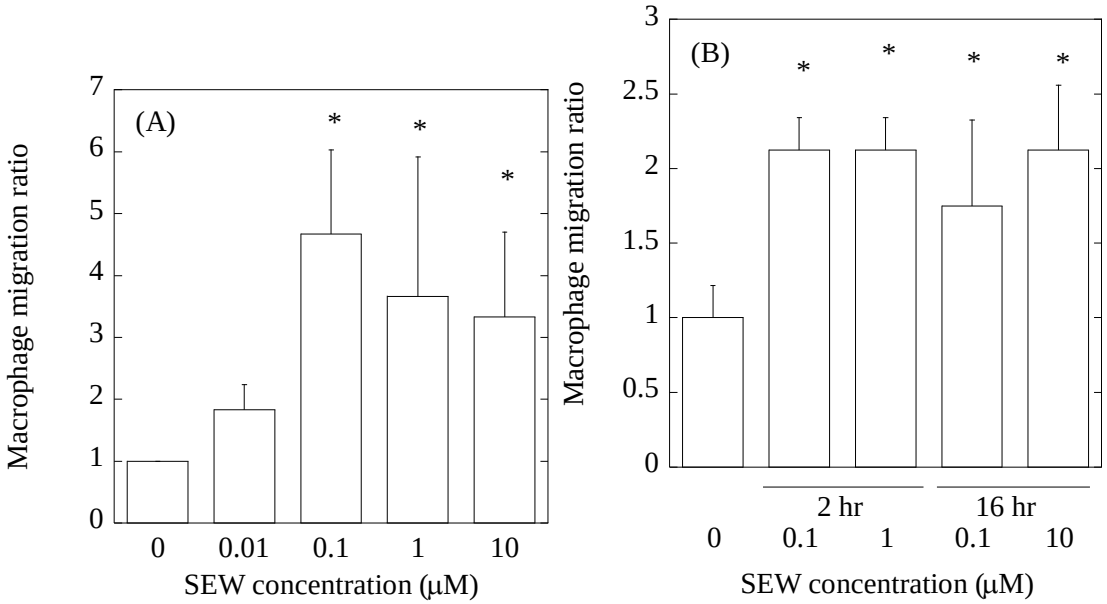

Figure 4. Macrophage migration of SEW and that released from hydrogels incorporating SEW micelles. (A) The effect of SEW concentration on the number of macrophages migrated. (B) SEW released from hydrogels incorporating SEW micelles for 2 and 16 hr in PBS containing collagenase. The concentration of SEW released was adjusted at 0.1 and 1 μM based on the HPLC measurement. The number of macrophages migrated is defined as 1 to calculate the migration ratio of samples. $*p < 0.05$; significant against the value at the SEW concentration of 0.

Biological activity of SEW and gelatin hydrogels incorporating SEW micelles

Figure 5A shows the macrophage recruitment 12 and 24 hr after the implantation of gelatin hydrogels incorporating SEW micelles. The total number of cells migrating into the sponges was ~1.4 and 2.1 × 10^4 cells 12 and 24 hr after treatment, respectively. Significant enhancement of macrophage recruitment was detected for both the SEW1Gel and the SEW10Gel. On the contrary, no recruitment enhancement was observed for the SEW-free gelatin hydrogels.

Figure 5B shows the macrophage recruitment 12 and 24 hr after implantation of gelatin hydrogels incorporating SEW micelles. The total number of cells collected was 5.4 and 5.8 × 103 12 and 24 h after treatment, respectively. An enhanced recruitment was observed for hydrogels incorporating SEW micelles. Macrophage recruitment was not enhanced for the Gel, SEW10 μg solution and SEW10 μg micelle solution.

Figure 6 and **Figure 7** show the time courses of the number ratio of macrophage/total cells infiltrated into the tissue around hydrogels at the normal tissues and the skin wound. For the normal tissue, significant enhancement of macrophage recruitment was observed at the tissue around the SEW10Gel implanted 12 h later. On the other hand, when the SEW10Gel was implanted into the skin wound, macrophage was recruited into the tissue around the hydrogels 1 day after implantation to a significantly great extent compared with Gel + 10 mg SEW micelle solution and gelatin hydrogels alone.

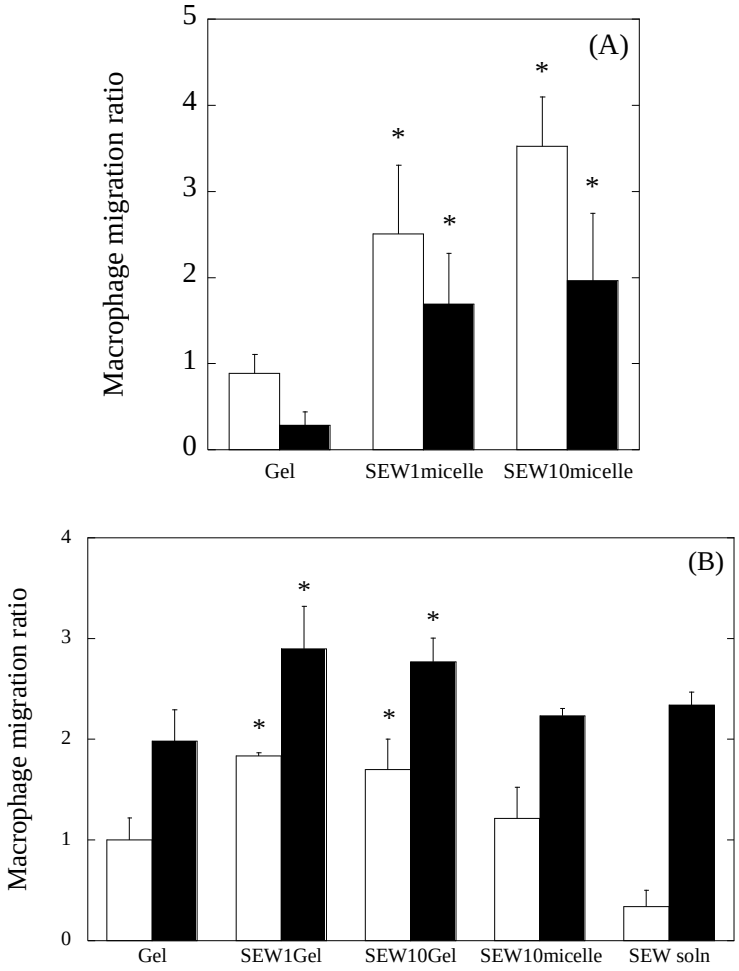

Figure 5. (A) The number ratio of macrophage/total cells recruited into the hydrogels incorporating 1 and 10 μg of SEW or SEW-free hydrogels 12 (□) and 24 hr after implantation (■): SEW-free hydrogels (Gel), hydrogels incorporating SEW micelles containing ~1.0 μg/ml of SEW (SEW1micelle) or SEW-micelles containing about 10 μg/ml of SEW (SEW10micelle). (B) The number ratio of macrophages/total cells recruited at the tissue treated by gelatin hydrogels incorporating SEW micelle, SEW micelle or SEW solution 12 (□) and 24 hr after implantation (■): SEW-free hydrogels (Gel), hydrogels incorporating 1 μg (SEW1Gel) or 10 μg of SEW (SEW10Gel), 10 μg of SEW-micelle (SEW10micelle) and 10 μg of SEW solution (SEW solun). The number of macrophages migrated at the tissue 12 h after Gel implantation is defined as 1 to calculate the migration ratio of samples. The number of animals used for each experimental time point was 3. $*p < 0.05$; significant against the value of Gel group at the corresponding implantation period.

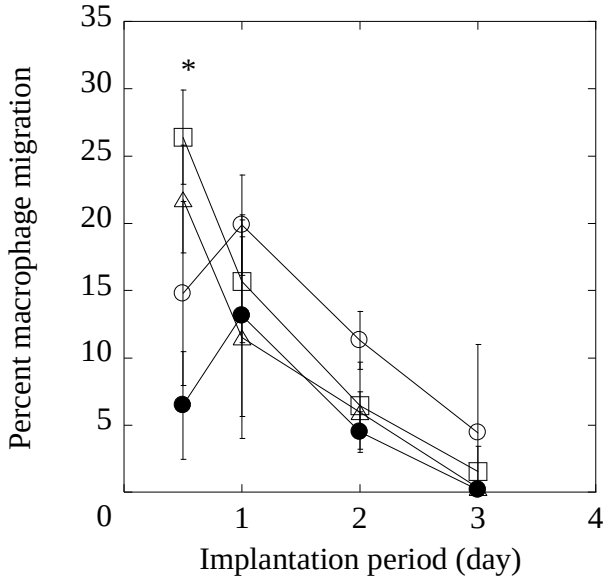

Figure 6. Time courses of the per cent of macrophage/total cells infiltrated at the tissue around hydrogels incorporating 1 and 10 μg of SEW or SEW-free hydrogels after implantation of Gel (○), SEW1Gel (Δ), SEW10Gel (□) and Gel + 10 mg SEW-micelles (●) on the subcutis of mice. ∗p < 0.05; significant against the value of Gel group at the corresponding time.

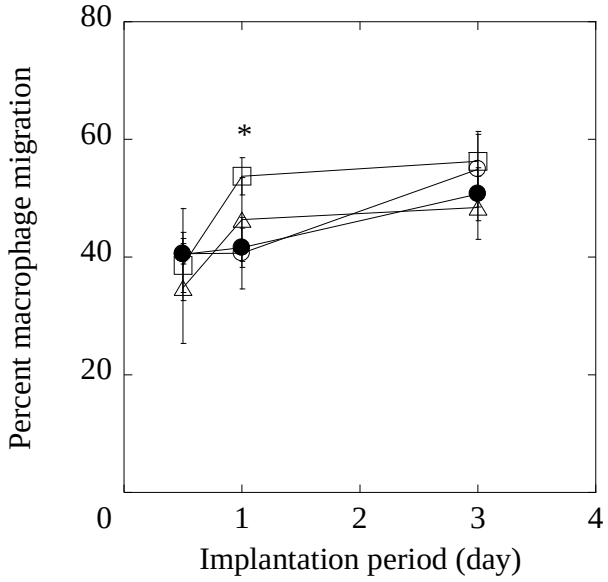

Figure 7. Time courses of the per cent of macrophage/total cells ratio infiltrated into the inflammatory tissue after implantation of Gel (○), SEW1Gel (Δ), SEW10Gel (□) and Gel + 10 mg SEW-micelles (●) into the skin wound. ∗p < 0.05; significant against the value of Gel group at the corresponding time.

DISCUSSION

The present study demonstrates that the biodegradable hydrogel can release the water-insoluble SEW of biological activity. SEW was water-solubilized by the micelle formation with LA-Gelatin with a CMC value. The percentage of water-solubilized SEW was changed by altering the molecular weight of LA-Gelatin and the grafted ratio. It is likely that the difference in the molecular weight of LAo and the grafted ratio causes the different interaction of LAo components and SEW, resulting in the incorporation of varied SEW into the micelles. The micelle stabilization and the amount of SEW solubilized in water are influenced by the hydrophilic–hydrophobic balance of LAo gelatin and the interaction between the SEW and LAo hydrophobic core. LAo2-1 may form the micelle with an inner environment of an appropriate hydrophobicity, and this can entrap SEW. Since gelatin hydrogels are not degraded in collagenase-free PBS, SEW is not released from the hydrogels (**Figure 2**). Gelatin is normally degraded by enzymes, but not by a simple hydrolysis. In the presence of collagenase, the hydrogels would be degraded enzymatically to generate water-soluble gelatin fragments, resulting in SEW release due to the water solubilization of SEW associated with the gelatin fragment. A good correlation in the time profile between the SEW release and the hydrogel degradation was observed. In the hydrogel system, the SEW is released from the hydrogel only if the hydrogel is degraded to generate water-soluble gelatin fragments. However, a certain amount of SEW is initially released because SEW micelles immobilized with non-crosslinked, free gelatin molecules are released by simple diffusion. Most of the SEW micelles immobilized with crosslinked gelatin molecules are released from the hydrogel as a result of gelatin water-solubilization due to hydrogel degradation. This is the mechanism of SEW micelle release from the

hydrogel. In the collagenase-free PBS, the gelatin hydrogel is not enzymatically degraded. In the release test in collagenase-containing PBS the gelatin hydrogel is degraded with time while the SEW micelles are released, accompanied with degradation. The rates of SEW release evaluated from the in vitro release study were in good agreement with those of hydrogel degradation. This finding indicates that the SEW release is governed only by the degradation of hydrogels as the release carrier. The hydrogels achieved the controlled release of SEW even in vivo (**Figure 3**). It is likely that the SEW release in vivo was achieved through the enzymatic degradation of gelatin hydrogels, in a similar manner to the in vitro condition of collagenase-containing PBS.

SEW and the SEW released from the hydrogels enhanced the in vitro macrophage migration (**Figure 4A and B**). This indicates that the activity of SEW remains, even after the dehydrothermal treatment for hydrogel preparation, and the SEW released in the SEW micelle form was also bioactive. The HPLC study revealed that the SEW released showed a peak similar to that of the original SEW in terms of the peak position and shape (data not shown).

The hydrogels incorporating SEW micelles showed significant enhancement of macrophage recruitment in vivo, whereas the SEW-free hydrogels and SEW micelle solution did not (**Figure 5A and B**). Considering the in vivo profile of SEW release, it is conceivable that the concentration gradient of SEW in the tissue formed by the release plays an important role in the enhancement of macrophage recruitment. The significant enhancement of macrophage recruitment was observed for both the normal and wound skins, although the time profiles of macrophage recruitment were different (**Figure 6 and Figure 7**). The macrophage recruitment would be influenced by the tissue inflammation other than the SEW released. This is because macrophage is

generally recruited and plays a critical role in the early stage of inflammation [2].

To evaluate the effect of SEW release profile on the in vivo macrophage recruitment, different types of gelatin hydrogels with different time periods of SEW release for 3, 9 or 21 days were prepared, and the effect on macrophage recruitment was assessed (data not shown). As a result, the enhancement of macrophage recruitment was observed only for the hydrogels incorporating SEW micelles for a 21 day release. This may be explained in terms of the difference in the SEW release profiles. An initial burst in SEW release from hydrogels releasing SEW for 3 and 9 days was large compared with those releasing SEW for 21 days. If the initial burst is too large and the drug is localized around the hydrogel only for a short time period, the concentration of SEW near the hydrogel will fall rapidly. It is possible that the rapid lowering of SEW concentration results in reduced microphage recruitment. Histological evaluation was performed by the hematoxylin and eosin and immunohistochemical staining methods. Unfortunately, however, the difference in the macrophage recruitment among the groups was not always demonstrated by the histological evaluation (data not shown). As the crosslinking extent of hydrogels increases, the time period of SEW release tends to be longer in the back subcutis of mic. It is highly conceivable that the longer in vivo release of SEW generates the large gradient of SEW concentration around the hydrogel, resulting in the enhanced macrophage recruitment in vivo.

REFERENCES

[1] S.J. Leibovich, R. Ross, The role of the macrophage in wound repair. A study with hydrocortisone and antimacrophage serum, The American journal of pathology, 78 (1975) 71-100.

[2] T. Lucas, A. Waisman, R. Ranjan, J. Roes, T. Krieg, W. Muller, A. Roers, S.A. Eming, Differential roles of macrophages in diverse phases of skin repair, J Immunol, 184 (2010) 3964-3977.

[3] B. Mahdavian Delavary, W.M. van der Veer, M. van Egmond, F.B. Niessen, R.H. Beelen, Macrophages in skin injury and repair, Immunobiology, 216 (2011) 753-762.

[4] D.M. Mosser, J.P. Edwards, Exploring the full spectrum of macrophage activation, Nature reviews. Immunology, 8 (2008) 958-969.

[5] S. Nagata, R. Hanayama, K. Kawane, Autoimmunity and the clearance of dead cells, Cell, 140 (2010) 619-630.

[6] D.R. Gude, S.E. Alvarez, S.W. Paugh, P. Mitra, J. Yu, R. Griffiths, S.E. Barbour, S. Milstien, S. Spiegel, Apoptosis induces expression of sphingosine kinase 1 to release sphingosine-1-phosphate as a "come-and-get-me" signal, FASEB journal : official publication of the Federation of American Societies for Experimental Biology, 22 (2008) 2629-2638.

[7] P. Keul, S. Lucke, K. von Wnuck Lipinski, C. Bode, M. Graler, G. Heusch, B. Levkau, Sphingosine-1-phosphate receptor 3 promotes recruitment of monocyte/macrophages in inflammation and atherosclerosis, Circulation research, 108 (2011) 314-323.

[8] C. Li, G. Yang, J. Ruan, Sphingosine kinase-1/sphingosine-1-phosphate receptor type 1 signalling axis is induced by transforming growth factor-beta1 and stimulates cell

migration in RAW264.7 macrophages, Biochemical and biophysical research communications, 426 (2012) 415-420.

[9] J. Michaud, D.S. Im, T. Hla, Inhibitory role of sphingosine 1-phosphate receptor 2 in macrophage recruitment during inflammation, J Immunol, 184 (2010) 1475-1483.

[10] B. Weichand, N. Weis, A. Weigert, N. Grossmann, B. Levkau, B. Brune, Apoptotic cells enhance sphingosine-1-phosphate receptor 1 dependent macrophage migration, European journal of immunology, (2013).

[11] M.G. Sanna, J. Liao, E. Jo, C. Alfonso, M.Y. Ahn, M.S. Peterson, B. Webb, S. Lefebvre, J. Chun, N. Gray, H. Rosen, Sphingosine 1-phosphate (S1P) receptor subtypes S1P1 and S1P3, respectively, regulate lymphocyte recirculation and heart rate, The Journal of biological chemistry, 279 (2004) 13839-13848.

[12] Y.H. Lien, K.C. Yong, C. Cho, S. Igarashi, L.W. Lai, S1P(1)-selective agonist, SEW2871, ameliorates ischemic acute renal failure, Kidney international, 69 (2006) 1601-1608.

[13] K. Takabe, S.W. Paugh, S. Milstien, S. Spiegel, "Inside-out" signaling of sphingosine-1-phosphate: therapeutic targets, Pharmacological reviews, 60 (2008) 181-195.

[14] Y. Maeda, H. Matsuyuki, K. Shimano, H. Kataoka, K. Sugahara, K. Chiba, Migration of CD4 T cells and dendritic cells toward sphingosine 1-phosphate (S1P) is mediated by different receptor subtypes: S1P regulates the functions of murine mature dendritic cells via S1P receptor type 3, J Immunol, 178 (2007) 3437-3446.

[15] T. Okamoto, T. Saito, Y. Tabata, S. Uemoto, Immunological tolerance in a mouse model of immune-mediated liver injury induced by 16,16 dimethyl PGE2 and PGE2-containing nanoscale hydrogels, Biomaterials, 32 (2011) 4925-4935.

[16] T. Saito, Y. Tabata, Preparation of gelatin hydrogels incorporating low-molecular-weight heparin for anti-fibrotic therapy, Acta biomaterialia, 8 (2012) 646-652.

[17] Y. Tabata, A. Nagano, Y. Ikada, Biodegradation of hydrogel carrier incorporating fibroblast growth factor, Tissue engineering, 5 (1999) 127-138.

[18] A. Yamauchi, C. Kim, S. Li, C.C. Marchal, J. Towe, S.J. Atkinson, M.C. Dinauer, Rac2-deficient murine macrophages have selective defects in superoxide production and phagocytosis of opsonized particles, J Immunol, 173 (2004) 5971-5979.

[19] Y. Fang, J. Shen, M. Yao, K.W. Beagley, B.D. Hambly, S. Bao, Granulocyte-macrophage colony-stimulating factor enhances wound healing in diabetes via upregulation of proinflammatory cytokines, The British journal of dermatology, 162 (2010) 478-486.

Chapter 5

Enhancement of osteogenic differentiation of human mesenchymal stem cells by controlled release of dexamethasone and active vitamin D_3 from gelatin hydrogel sponges

INTRODUCTION

Mesenchymal stromal/stem cells (MSC) have been isolated not only from the bone marrow, but also from many other tissues, including adipose tissue, umbilical cord blood, pancreas, and periosteum [1-5]. The MSC can be expanded in the in vitro conventional culture and differentiated into various mesoderm-type lineages, such as bone, cartilage, fat, muscle, tendon, hematopoiesis-supporting stroma, and vasculature [6-10]. When being differentiated into osteoblasts, MSC transform from a fibroblastic to a cuboidal shape, and produce extracellular matrix (ECM), mainly composed of collagen type I (Col1). In addition, the cells form small swelling or aggregation of cells. Finally, calcium (Ca) accumulation (i.e. mineralization) is observed in MSC during the osteogenic differentiation in a later stage [7, 11].

The classical method for osteogenic differentiation of MSC in vitro involves the incubation of MSC monolayer with combinations of dexamethasone (Dex), β-glycerophosphate (β-GP), and ascorbic acid 2-phosphate (Asc2P) for several weeks [9]. In addition, the combination of active vitamin D_3 (calcitriol, 1,25-Dihydroxyvitamin D_3, 1,25-D_3), transforming growth factor-β, and bone morphogenetic proteins is used to promote the osteogenic differentiation [12-15]. Dex is a synthetic glucocorticoid and has been reported to be an essential requirement for osteogenic differentiation in MSC [16]. Dex is generally dissolved in ethanol (EtOH) to

add in the medium, because of the water insolubility. When cultured in a basal medium without osteogenic supplements, MSC show the increased levels of alkaline phosphatase (ALP). However, they fail to express mineralized ECM as well as other osteogenic markers, such as Col1 protein [13]. Although the precise mechanisms of Dex action on the stem cells differentiation and skeletal function are not known, it is supposed that Dex induces transcriptional effects [17]. The presence of both Ca and phosphate ions is essential for matrix mineralization. ALP can enzymatically hydrolyze β-GP to serve as a crucial source of inorganic phosphate [18]. Cultivation of MSC in the culture medium containing β-GP leads to mineral formation. Ascorbic acid (Asc) plays an important role as a cofactor for the hydroxylation of proline and lysine residues in collagens, which are the most abundant group of ECM proteins in the body [19]. However, one difficulty concerning the handling of Asc is its instability at the conventional culture condition (pH 7.5, 37 °C). Thus, it is chosen to use a long-acting derivative of Asc (i.e. Asc2P) is normally used because it is found to be stable under culture conditions [20]. Vitamin D_3 is a secosteroid hormone which is essential for the biological function of osteoblasts. The 1,25-D_3 demonstrates potent antiproliferative effects by blocking the transition from the G1- to the S-phase during the cell cycle. Through interaction with a nuclear vitamin D receptor, 1,25-D_3 has been shown to stimulate the expression of bone-related transcription factors, i.e. runt-related transcription factor 2 and osterix, in addition to osteoblast differentiation markers, e.g. ALP, Col1, osteocalcin, and osteopontin [21]. Although synergized effect between 1,25-D_3 and Dex is observed, the 1,25-D_3 alone is unable to induce matrix mineralization [12, 22].

Three dimensional (3D) cell culture systems have allowed the development of

useful models for investigating stem cell biology and physiology [23]. The 3D scaffolds have a potential to enhance cell transplant into the body. In addition, the efficacy, side effects, toxicity, and screening of drugs are possible with ease by using the 3D scaffolds without animal experiments. There are many material shapes and types of 3D scaffolds to fabricate cell constructs, such as porous sponges [24, 25], particles [26-28], and fibers [29, 30]. However, immense complexity can be found in various tissues and organs [31]. Irrespective of the complexity of target to be repaired, tissue engineering strategies generally involve the application of biomaterials combinations, cells, and biologically active factors to effect tissue formation in vitro.

The objective of this chapter is to design gelatin sponges for the controlled release of Dex and 1,25-D_3. An amphiphilic derivative of gelatin was prepared by grafting L-lactic acid oligomer (LLAo) to gelatin. Dex and 1,25-D_3 were water-solubilized by the micelles formation with the gelatin grafted by LLAo (LA-Gelatin). The Dex and/or 1,25-D_3-loaded micelles were incorporated in the gelatin sponges, followed by the chemical crosslinking to obtain gelatin sponges incorporating the Dex and 1,25-D_3-loaded micelles. The time profile of Dex and 1,25-D_3 release from the gelatin sponges was examined. To improve the osteogenic differentiation efficiency of human MSC in the sponge scaffolds, the way to combine the Dex and 1,25-D_3 with the scaffolds was designed. The ALP activity, the amount of Ca deposition, and histological observation were performed to evaluate the ability of gelatin sponges for osteogenic differentiation enhancement.

EXPERIMENTAL

Materials

Immortalized human MSC (hMSC-hTERT-E6/E7, hMSC) were kindly supplied from Dr. Toguchida at the Institute for Frontier Medical Sciences, Kyoto University, Kyoto, Japan [32]. A dialysis tube with the cut-off molecular weight of 12,000–14,000 (UC 30-32-100) was purchased from EIDIA Co., Ltd, Tokyo, Japan. Low-glucose Dulbecco's Modified Eagle Medium (low-DMEM) was purchased from Life Technologies Corporation, Tokyo, Japan.

Water-solubilization of Dex and 1,25-D_3 by LA-Gelatin micelles

LA-Gelatin micelles incorporating Dex (Dex-micelle) and 1,25-D_3 (D_3-micelle) were prepared. LA-Gelatin solution (1.0 mg/ml) in DDW and Dex solution (1.0 mg/ml) in EtOH or 1,25-D_3 solution (1.0 mg/ml) in EtOH were mixed at 37 °C. The mixed solution was centrifuged (8,000 rpm, 5 min, 4 °C) to separate water-insoluble Dex or 1,25-D_3, and the supernatant was freeze-dried to obtain the Dex or 1,25-D_3 water-solubilized by LA-Gelatin micelles. **Table 1** summarizes Dex- and D_3-micelle prepared. To measure the amount of Dex incorporated into the High or low-Dex-micelle and 1,25-D_3 into the High or low-D_3-micelle, the freeze-dried samples were dissolved in EtOH and sonicated by an ultrasonic generator (handy sonic UR-21P, TOMY SEIKO Co., Ltd, Tokyo, Japan) in 30 sec. The amount of Dex or 1,25-D_3 was measured by high performance liquid chromatography (HPLC), while the Dex or 1,25-D_3 concentration was determined from the standard curve prepared with the EtOH containing various amounts of Dex or 1,25-D_3. The Dex sample solution (10 μl) was injected into the Prominence LC-20AT HPLC analysis system (Shimadzu Corporation, Kyoto, Japan)

equipped with COSMOSIL 5C_{18}-AR-II column (25 cm x 4.6 cm i.d., particle size: 5 mm, Nacalai Tesque Inc., Kyoto, Japan) after it was dissolved in ethanol. The mobile phase for separation was a mixture of DDW and methanol (20:30, vol/vol%). The solvent was maintained at a flow rate of 0.5 ml/min. UV detection was performed simultaneously at wavelengths of 242 nm. The 1,25-D_3 sample solution (10 μl) was injected into the HPLC equipped with COSMOSIL 5C_{18}-AR-II column (25 cm x 4.6 cm i.d., particle size: 5 mm) after it was dissolved in EtOH. The mobile phase for separation was 100% of acetonitrile. The solvent was maintained at a flow rate of 1.0 ml/min. UV detection was performed simultaneously at wavelengths of 265 nm.

Table 1. Preparation of Dex- and D_3-micelle

		Drug	
Code	LA-Gelatin [a)]	Dex [b)]	1,25-D_3 [c)]
High-Dex-micelle	900	100	
Low-Dex-micelle	990	10	
High-D_3-micelle	900		100
Low-D_3-micelle	990		10

[a)] The amount of LA-Gelatin mixed (μg)

[b)] The amount of Dex mixed (μg)

[c)] The amount of 1,25-D_3 mixed (μg)

Preparation of sponge scaffolds of gelatin hydrogels with or without Dex-micelle and/or D_3-micelle

Gelatin sponge and gelatin sponge incorporating Dex-micelle and/or 1,25-D_3-micelle were prepared as previously reported with minor modification [33]. Briefly, 3 wt% aqueous solution of gelatin containing with or without Dex-micelle and/or D_3-micelle was mixed at 5,000 rpm at 37 °C for 3 min by using a homogenizer

(ED-12, Nihonseiki Co., Tokyo, Japan). After aqueous solution of glutaraldehyde (25 wt.%, 676 μl) was added to the mixed solution, the mixed solution was further agitated for 10 sec by the homogenizer at 5,000 rpm. The resulting solution was cast into a polypropylene dish, followed by leaving at 4 °C for 12 hr for gelatin crosslinking. Then, the crosslinked gelatin scaffold of sponges was freeze-dried, and then placed in 100 mM aqueous glycine solution at 37 °C for 1 hr to block the residual aldehyde groups of glutaraldehyde, thoroughly washed with DDW, and freeze-dried, followed by cut into discs with 5 x 5 x 2 mm^3. The amount of Dex or 1,25-D_3 in the sponges was measured by the HPLC as described above.

The gelatin sponges were performed sputter coating with gold/palladium, the samples were viewed on a scanning electron microscope (SEM, S2380N, HITACHI, Japan). The average pore size of sponges was measured for about 30 pores; a, the longest length of pore; b. the shortest length of pore, and pore size is(a + b)/2.

Evaluation of Dex and 1,25-D_3 release from gelatin sponges

Gelatin sponges (5 x 5 x 2 mm^3) were placed in PBS or low-DMEM containing 10 vol% fetal bovine serum (FBS, 500 μl) at 37 °C. The supernatant was collected, while the same volume of free PBS or the DMEM was added to continue. The amount of Dex or 1,25-D_3 in the sponges was measured by the HPLC as described above.

Cell seeding in the gelatin sponge scaffolds and the osteogenic differentiation

The hMSC were seeded into the sponges by an agitated seeding method reported previously [33]. Briefly, 700 μl of cells suspension in low-DMEM containing vol% FBS and 1.0 vol% penicillin/streptomycin (2 x 10^6 cells) and one sponge were

placed into 15 ml tube (IWAKI Glass Co. Ltd., Chiba, Japan) and agitated on an orbital shaker (Bellco Glass, Inc., Vineland, NJ) at 300 rpm for 6 hr. The cell-seeded sponges were taken out with a pair of tweezers and put on the 24-well multi-well culture plate (#3526, Corning Inc., NY, USA). Each well of 24-well multi-well culture plate was coated with 1.0% of polyvinyl alcohol, followed by the sponge addition into the well. One ml of the medium was added and the cells-seeded sponges were cultured by low-DMEM containing 10 vol% FBS and 1.0 vol% penicillin/streptomycin for 2 days. Next, the medium was changed by osteogenic differentiation medium, and changed 3 times/week. The low-DMEM containing 10 vol% FBS and 1.0 vol% penicillin/streptomycin supplemented with or without Asc2P (300 μM), β-GP (10 mM), Dex (100 nM), and 1,25-D3 (100 nM) to prepare the osteogenic differentiation medium. **Table 2** summarizes the component of osteogenic differentiation medium. At different time intervals, the sponges with cells were washed with PBS once, and stored at -80 °C for further experiments.

Table 2. Component of osteogenic differentiation medium.

	Supplement			
Code	Asc2P	β-GP	Dex	1,25-D_3
NM [a)]	-	-	-	-
OM-Dex$^-$ [b)]	+	+	-	-
OM [(c)]	+	+	+	-
OM-D_3^+ [d)]	+	+	+	+

[a)] The low-DMEM containing 10 vol% FBS and 1.0 vol% penicillin/streptomycin

[b)] The osteogenic differentiation medium without Dex

[c)] The conventional osteogenic differentiation medium

[d)] The osteogenic differentiation medium with 1,25-D_3

Biological activity evaluation of cells-seeded gelatin sponges

The cells-seeded gelatin sponges stored were thawed and minced by scissors, and the samples were lysed in 30 mM sodium citrate-buffered saline solution (SSC, pH 7.4) containing 0.2 mg/ml sodium dodecylsulfate (SDS) at 37 °C for 12 hr with occasional mixing. The ALP activity of the cell lysate was determined by LabAssay^{TM} ALP (Wako Pure Chemical Industries Ltd., Osaka, Japan). Briefly, dilute p-nitrophenol solution with DDW as a standard. Sodium p-nitrophenylphosphate was dissolved in 2.0 mmole/l $MgCl_2$, 0.1 mole/l carbonate buffer (pH = 9.8) at 37 °C. After that, the solution was kept in dark. Then, the cell lysate (20 μl) was added into the well of 96-well multi-well culture plate (Corning Inc., NY, USA), and added 100 μl of the buffer to each well. The plate was incubated at 37 °C for 15 min. After incubation, 0.02 N NaOH solution (80μl) was added into each well to stop the reaction. The absorbance was measured at 405 nm by a VERSAmax microplate reader (Molecular Devices, Sunnyvale, CA). Next, the cell lysate solution (100 μl) was mixed with 1N HCl (100 μl) overnight at 4 °C for the Ca measurement. The Ca deposition amounts were determined by Ca E-HA test (Wako Pure Chemical Industries Ltd., Osaka, Japan). Briefly, the solution (2.0 μl) and monoethanolamin (pH = 12, 100 μl) were added into each well of 96-well multi-well culture plate for 5 min at room temperature. And methylxylenol blue and 8-quinolinol solution (50 μl) was added. The absorbance was measured at 600 nm by a VERSAmax microplate reader. All the data were normalized by the cell number counted by DNA assay using Hoechst 33258 (Nacalai Tesque, Kyoto, Japan). Briefly, cell lysate solution (100 μl) and Hoechst solution (100 μl) were added into the well of 96-well multi-well culture plate with black bottom (Corning Inc., NY, USA). The fluorescence of the solution was measured at room temperature on a SpectraMax

Gemini EM (Molecular Device, Osaka, Japan) at excitation and emission wavelengths of 355 and 460 nm.

Histological evaluation of cells-seeded gelatin sponges

The cells-seeded gelatin sponges were embedded in an optimal cutting compound (OCT, Sakura Finetek Japan Co., Ltd, Tokyo, Japan). About 1 mm thickness of the sponges was cut by the freezing microtome (CM 3050 S, Leica Microsystems Inc., Osaka, Japan). And then, histological sections with 10 μm thickness were prepared. The sections were stained with hematoxylin and eosin (H&E). The sections (10 μm thick) were also stained with an alizarin red S (ARS, Sigma–Aldrich Japan KK, Tokyo, Japan). Briefly, 1.0% alizarin red S solution was prepared in DDW and then, pH was adjusted at 6.4 by 1N NaOH. The sections were washed by DDW to remove the OCT compound at room temperature. They were stained the ARS solution for 5 min, followed by DDW washing. The sections were mounted with a super cryomounting medium type R2 (Leica Microsystems Inc., Osaka, Japan) for microscopic observation by fluorescence microscope (BZ-X710, KEYENCE CORPORATION., Osaka, Japan). The sections were randomly selected (three sections for each experimental group) and the staining area of ARS was calculated by BZ-X Analyzer software.

Statistical analysis

All the results were expressed as the mean ± standard deviation (SD). Significant analysis was performed based on the one-way ANOVA, and the difference was considered to be significant at $P < 0.05$.

RESULTS

Water-solubilization of Dex and 1,25-D_3 by LAo-grafted gelatin

Figure 1 shows the percentage of Dex and 1,25-D_3 water-solubilized by LA-Gelatin. The amount of Dex or 1,25-D_3 water-solubilized depended on the molecular weight of LAo grafted and the grafted ratio. Considering the highest percentage, the Dex-micelle using LAo1-3 of LAo-grafted gelatin or D_3-micelle using LAo1-5 was used for the following experiments.

Preparation of gelatin sponges incorporating with or without Dex-micelle and/or D_3-micelle

Gelatin sponges incorporating High-Dex-micelle or High-D_3-micelle were prepared for controlled release test. Gelatin sponges incorporating with or without Low-Dex-micelle and Low-D_3-micelle were prepared for in vitro cell culture experiments. **Figures 2A and B** show scanning electron micrographs of Gelatin-sponge. **Table 3** summarizes the conditions of gelatin sponges prepared. The pore size of sponges ranged from 170 to 190 mm, irrespective of the type of drugs incorporated.

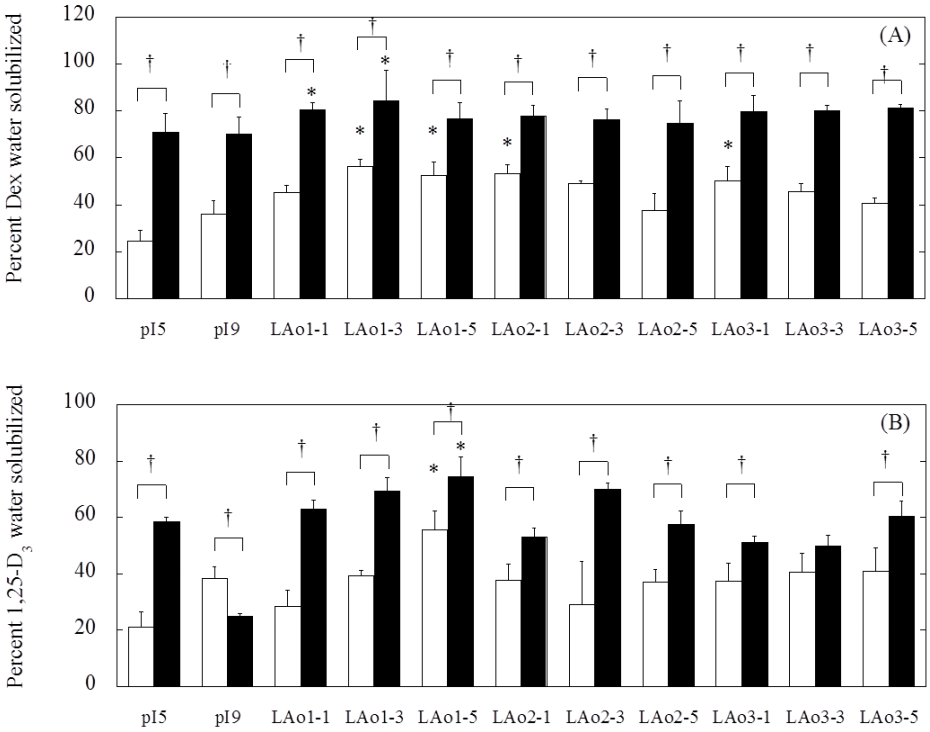

Figure 1. Percentage of Dex (A) and 1,25-D_3 (B) solubilized in water. High- (□) and Low-Dex-micelles (■), or High- (□), and Low-D_3-micelles (■) were prepared by various LAo-gelatin samples.

*, $P<0.05$; significant against the value of the pI9.

†, $P<0.05$; significant between the two groups

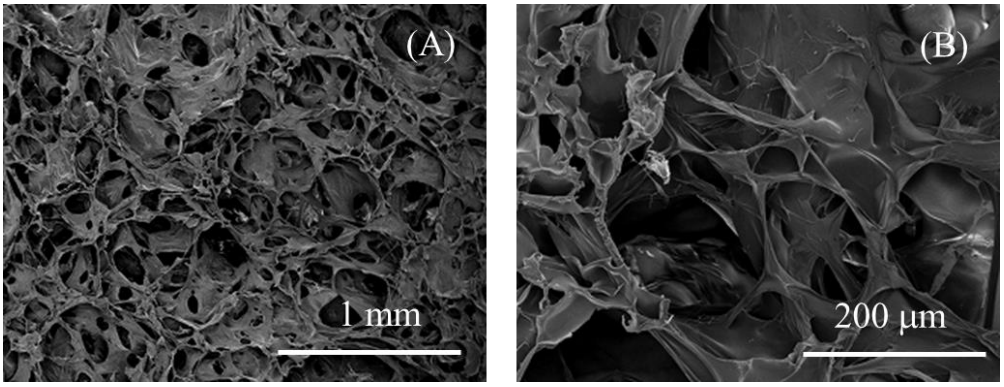

Figure 2. Scanning electron micrographs of Gelatin-sponge at different magnifications (A and B).

Table 3. Preparation and characterization of gelatin sponges incorporating Dex- and D_3-micelle.

	The amount of drugs incorporated (pmole/sponge)		
Code	Dex	1,25-D_3	Pore size (μm)
High-Dex-sponge [a)]	87±3.6 x 10^3		-
High-D3-sponge [a)]		78.3±2.1 x 10^3	-
Gelatin-sponge [b)]			168±29.8
Dex-sponge [b)]	872±104		183±59.4
D3-sponge [b)]		882±78.3	172±41.2
Dex-D3-sponge [b)]	855±38.7	849±115	190±32.7

[a)] Samples for controlled release test

[b)] Samples for in vitro cell culture experiments

Dex or 1,25-D_3 release from High-Dex-sponge or High-D_3 sponge

Figure 3 shows the in vitro time profiles of Dex (A) and 1,25-D_3 release (B) from High-Dex-sponge or High-D_3 sponge in PBS or low-DMEM containing 10 vol% FBS. For both the drugs, the release amount of drugs in PBS was lower than that of the DMEM. In the PBS and DMEM, 46.1 and 51.6% of Dex was initially released for 1 day, respectively. In the PBS and DMEM, 24.8 and 29.8% of 1,25-D_3 was initially released for 1 day, respectively.

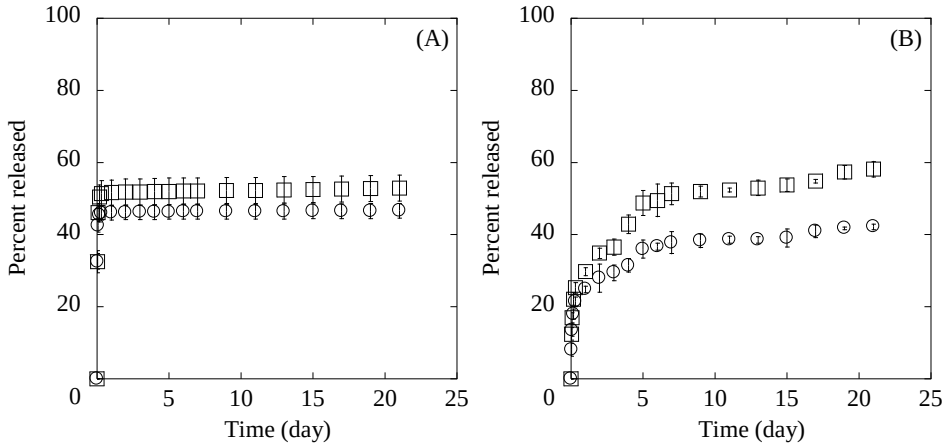

Figure 3. The time profiles of gelatin sponges incorporating High-Dex-micelles (A) and High-D3-micelles (B). The release test was performed at 37 °C in PBS (○) and DMEM (□)

Osteogenic differentiation of hMSC cultured in gelatin sponges

Figure 4A shows the ALP activity of hMSC cultured in different gelatin sponges. **Figure 4B** shows the ALP activity of hMSC cultured in Gelatin-sponge with different culture media. The ALP activity of hMSC cultured with OM was significantly large compared with that with NM for 7 and 14 days. However, the ALP activity was decreased for 21 days. The ALP activity of hMSC cultured with OM-D_3^+ was significantly large compared with that with NM for 7, 14, and 21 days, and OM for 14 and 21 days. **Figure 4C** shows the ALP activity of hMSC cultured in Gelatin-sponge with OM, and Dex-sponge with OM-Dex^-. There was no significant difference in the ALP activity during 21 days culture. **Figure 4D** shows the ALP activity of hMSC cultured in Gelatin-sponge with OM-D_3^+, and D_3-sponge with OM. There was no significant difference in the ALP activity during 21 days culture. Upon culturing in the Dex-D_3-sponge with OM-D_3^+, the ALP activity of hMSC was significantly large compared with that of Gelatin-sponge with other media.

Figure 5 shows the Ca deposition of hMSC cultured in gelatin sponges for 21 days. The Ca deposition amount of hMSC cultured in Gelatin-sponge with OM and OM-D_3^+ was significantly large compared with that with NM. The Ca deposition amount of hMSC cultured in Gelatin-sponge with OM-D_3^+ was significantly large compared with that with OM. The Ca deposition of hMSC cultured in Gelatin-sponge with OM and Dex-sponge with OM-Dex^- was not significantly different. The Ca deposition of hMSC cultured in Gelatin-sponge with OM-D_3^+ and D_3-sponge with OM was not significantly different. The amount of Ca deposition for hMSC cultured in the Dex-D_3-sponge with OM+D_3 was significantly large compared with that of cells cultured with other media.

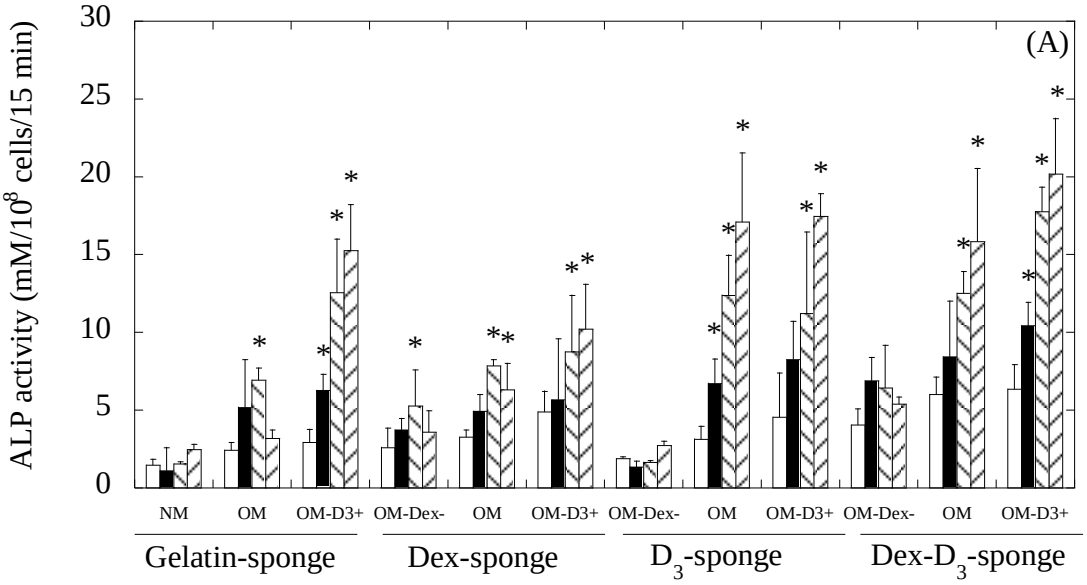
(A)
ALP activity (mM/10^8 cells/15 min)
30
25
20
15
10
5
0
NM
OM
OM-D3+
OM-Dex-
OM
OM-D3+
OM-Dex-
OM
OM-D3+
OM-Dex-
OM
OM-D3+
Gelatin-sponge
Dex-sponge
D3-sponge
Dex-D3-sponge

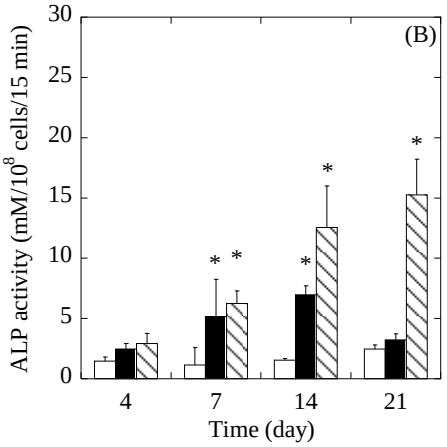
(B)
ALP activity (mM/10^8 cells/15 min)
30
25
20
15
10
5
0
4
7
14
21
Time (day)

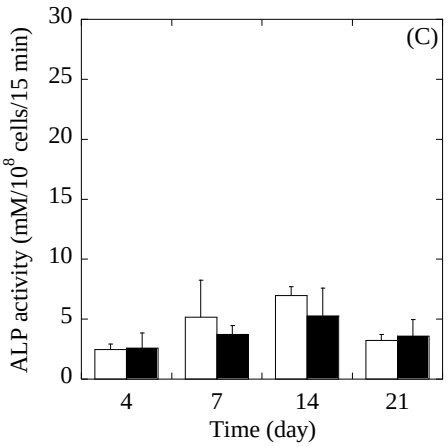
(C)
ALP activity (mM/10^8 cells/15 min)
30
25
20
15
10
5
0
4
7
14
21
Time (day)

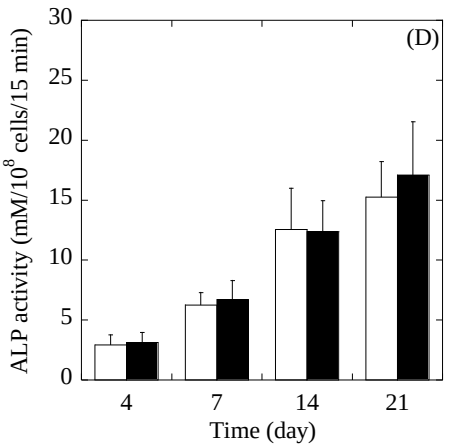
(D)
ALP activity (mM/10^8 cells/15 min)
30
25
20
15
10
5
0
4
7
14
21
Time (day)

Figure 4. (A) The ALP activity of hMSC cultured in Gelatin-sponge, Dex-sponge, D_3-sponge, and Dex-D_3-sponge for 4 (□), 7 (■), 14 (▨), and 21 days (▨).
*, P<0.05; significant against the ALP activity of hMSC cultured for 4 days.
(B) The ALP activity of hMSC cultured in Gelatin-sponge with NM (□), OM (■), and OM-D_3^+ (▨).
*, P<0.05; significant against the ALP activity of hMSC cultured in the corresponding sponge with NM
. †, P<0.05; significant against the ALP activity of hMSC cultured in the corresponding sponge with OM
(C) The ALP activity of hMSC cultured in Gelatin-sponge with OM (□), and in Dex-sponge with OM-Dex^- (■).
(D) The ALP activity of hMSC cultured in Gelatin-sponge with OM+D_3^+ (□), and in D_3-sponge with OM (■).

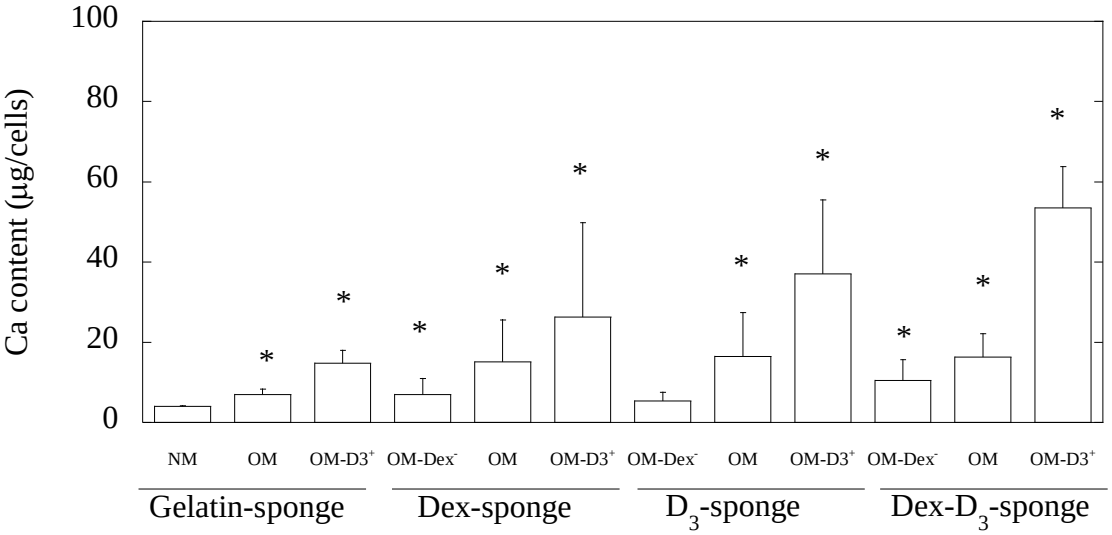

Figure 5. The Ca deposition of hMSC cultured in Gelatin-sponge, Dex-sponge, D_3-sponge, and Dex-D_3-sponge for 21 days.
*, P<0.05; significant against the ALP activity of hMSC cultured in Gelatin-sponge with NM

Histological observation of gelatin sponges

Figures 6A-C show the histological sections of cells-seeded Gelatin-sponge cultured with NM at different magnifications. **Figures 6D-N** show the histological sections of cells-seeded gelatin sponges cultured with different media at the highest magnification. The hMSC attached were observed in the all types of gelatin sponges. And the Ca deposition was detected sponges with the exception of Gelatin-sponge with NM, Dex-sponge with OM-Dex^-, and D_3-sponge with OM-Dex^-.

Figure 7 shows the ARS positive area of cells-seeded Gelatin-sponge, Dex-sponge, D_3-sponge, and Dex-D_3-sponge. No positive area was seen for cells-seeded Gelatin-sponge cultured with NM. On the contrary, the cells-seeded Gelatin-sponge cultured with OM and OM-D_3^+ was stained, and the ARS positive area of the cells-seeded Gelatin-sponge cultured with OM-D_3^+ was higher than that of OM (**Figure 7A**). The cells-seeded Dex-sponge (**Figure 7B**) and D_3-sponge (**Figure 7C**) cultured with OM and OM-D_3^+ was stained. However, the area was lower than that of Gelatin-sponge (**Figure 7A**). The cell-seeded Dex-D_3-sponge cultivated with OM-Dex^-, OM and OM-D_3^+ was stained, and the ARS positive area of the cell-seeded Dex-D_3-sponge cultivated with OM-D_3^+ was higher than that of OM-Dex^- and OM (**Figure 7D**).

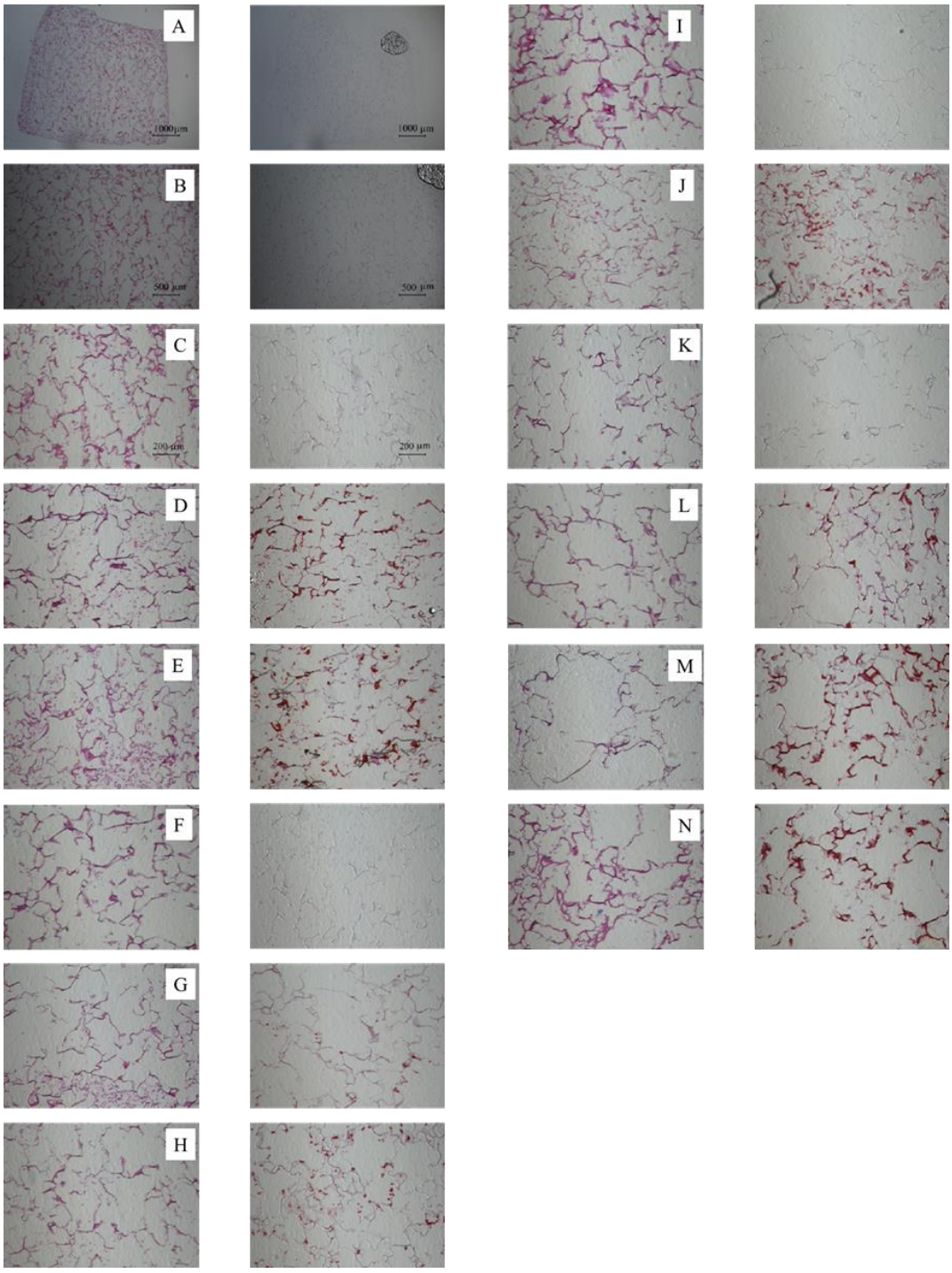

Figure 6. Histological sections (H&E and ARS staining) of cells-seeded Gelatin-sponge cultured with NM (A-C) at different magnifications. Histological sections (H&E and ARS staining) of cells-seeded Gelatin-sponge (D and E), Dex-sponge (F-H), D3-sponge (I-K), and Dex-D_3-sponge (L-N) cultured with OM-Dex (F, I, and L), OM (D, G, J, and M), and OM+D_3 (E, H, K, and N).

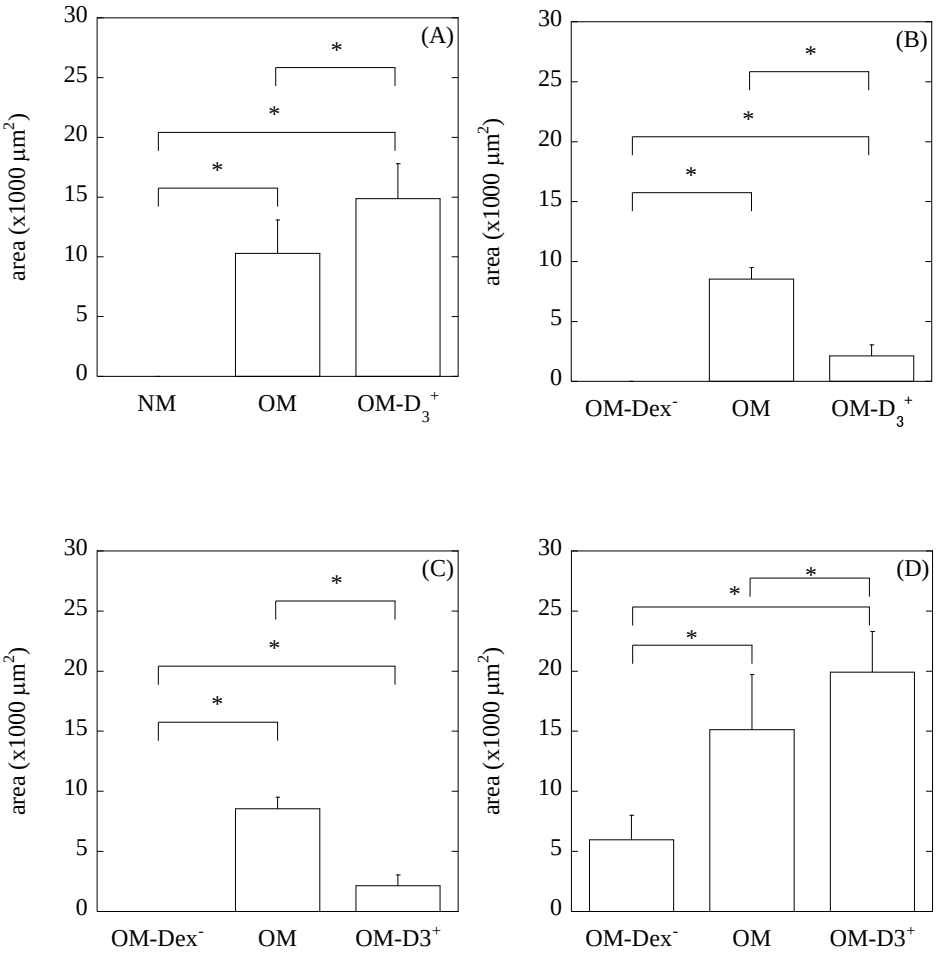

Figure 7. ARS positive area of cells-seeded Gelatin-sponge (A), Dex-sponge (B), D3-sponge (C), and Dex-D3-sponge (D) cultured with different culture media for 21 days.

*, P<0.05; significant against the two groups.

DISCUSSION

This study demonstrates that gelatin sponges can release water-insoluble Dex and 1,25-D_3 in PBS and DMEM containing 10 vol% FBS. The Dex and 1,25-D_3 were water-solubilized through the micelles formation with LA-Gelatin. The percentage of water-solubilized Dex and 1,25-D_3 was changed by altering the molecular weight and the grafted ratio of LLAo. In addition, when the micelles are formed, the mixing ratio of Dex and 1,25-D_3 to LA-Gelatin modified the efficiency of Dex and 1,25-D_3 water-solubilization. The low amount of the Dex and 1,25-D_3 mixed for micelle formation resulted in the high efficiency of water-solubilization. It is possible that the micelle stabilization and the amount of Dex and 1,25-D_3 solubilized in water are influenced by the state of hydrophobic core in micelles. It is demonstrated that the gelatin hydrogels could release water-insoluble drugs water-solubilized by the micelles of LA-Gelatin [34-36]. For the release test, the High-Dex-sponge and High-D_3-sponge were used because the drugs amount of Low-Dex-Sponge and Low-D_3-sponge were too low to allow the detection. Both the Dex and 1,25-D_3 were released from the gelatin sponges, irrespective of the type of release solution. Since the Dex-micelle and D_3-micelle were homogeneously incorporated into gelatin molecules, it is likely that the drugs release profile of Low-Dex-Sponge and Low-D_3-sponge is similar to that of High-Dex-Sponge and High-D_3-sponge. The Dex and 1,25-D_3 release in DMEM was faster than that in PBS. It is conceivable that both the Dex and 1,25-D_3 can be release in culturing with hMSC.

Our previous report shows the osteogenic differentiation of mesenchymal stem cells can be enhanced by the hydrogel sponges composed of 50 wt% of gelatin and 50 wt% of β-tricalcium phosphate (β-TCP) granules [33]. In this study, β-TCP is not used

to prepare gelatin sponges because the dual release of Dex and 1,25-D_3 shows a synergized effect to induce Ca deposition (i.e. matrix mineralization) [12]. The total amount of Dex and 1,25-D_3 added in the medium was 900 pmole (1.0 ml of 100 nM medium by 9 times the changing) for 21 days. The amount of Dex and 1,25-D_3 in the Dex-sponge, D_3-sponge, and Dex-D_3-sponge were fixed at approximately 900 pmole of Dex and/or 1,25-D_3.

There was no significant difference in the ALP activity of hMSC cultured in Gelatin-sponge with OM, and in Dex-sponge with OM-Dex^- for 21 days (Figure 4C). In the early phase, the Dex-sponge with OM-Dex^- showed the same ability of osteogenic differentiation as Gelatin-sponge with OM. The ALP activity of hMSC cultured in Gelatin-sponge with OM-D_3^+ was similar that cultured in D_3-sponge with OM (Figure 4D). In the early phase, the D_3-sponge with OM showed the same ability of osteogenic differentiation as Gelatin-sponge with OM-D_3^+. The presence of 1,25-D_3 in the medium and/or sponges tended to increase the ALP activity for 21 days (**Figures 4B** and **D**). On the other hand, the absence of 1,25-D_3 in the medium and/or sponges decreased the ALP activity at a later phase. This would be due to the biological function of 1,25-D_3. The osteogenic differentiation of hMSC occurred in the presence of 1,25-D_3 accompanied with cells proliferation [22]. Figure 5 shows that the combination of Dex-D_3-sponge and OM-D_3^+ showed the highest matrix mineralization. It is because that the 1,25-D_3 increases the protein expression for osteogenic differentiation at a later phase [12, 22].

To check the mineralization of sponges inside, their ARS staining was performed. In the case of the hMSC cultured with OM-Dex^- (i.e. supplement with Asc2P (300 μM) and β-GP (10 mM)), The ARS-stained area was observed only for the cells-seeded Dex-D_3-sponge (**Figures 6L** and **7D**). This indicates that the

Dex-D_3-sponge is useful for the osteogenic differentiation of hMSC. ARS positive area of the cells-seeded Dex-sponge (**Figure 7B**) and D_3-sponge (**Figure 7C**) cultured with OM and OM-D_3^+ was stained lower than that of Gelatin-sponge (**Figure 7A**). It suggests that the excessive quantity and un-balance ratio of Dex and 1,25-D_3 show a side effect to suppress the osteogenic differentiation of MSC. The ARS positive area of cells-seeded Dex-D_3-sponge cultured with OM-D_3^+ was the highest among other groups. This system may be useful bone regeneration in vivo. The further optimization of system for the application of bone regeneration is needed. Because the appropriate dose of Dex and 1,25-D_3 is not always same between the in vitro osteogenic differentiation of MSC and their in vivo bone regeneration.

REFERENCES

[1] De Coppi P, Bartsch G, Jr., Siddiqui MM, Xu T, Santos CC, Perin L, et al. Isolation of amniotic stem cell lines with potential for therapy. Nature biotechnology. 2007;25:100-6.

[2] Kruse C, Kajahn J, Petschnik AE, Maass A, Klink E, Rapoport DH, et al. Adult pancreatic stem/progenitor cells spontaneously differentiate in vitro into multiple cell lineages and form teratoma-like structures. Annals of anatomy = Anatomischer Anzeiger : official organ of the Anatomische Gesellschaft. 2006;188:503-17.

[3] Meng X, Ichim TE, Zhong J, Rogers A, Yin Z, Jackson J, et al. Endometrial regenerative cells: a novel stem cell population. Journal of translational medicine. 2007;5:57.

[4] Tovey ER, Kemp AS, Almqvist C, Sharland A, Marks GB. Do immune responses to inhaled skin flakes modulate the expression of allergic disease? Clinical and experimental allergy : journal of the British Society for Allergy and Clinical Immunology. 2007;37:1199-203.

[5] in 't Anker PS, Noort WA, Scherjon SA, Kleijburg-van der Keur C, Kruisselbrink AB, van Bezooijen RL, et al. Mesenchymal stem cells in human second-trimester bone marrow, liver, lung, and spleen exhibit a similar immunophenotype but a heterogeneous multilineage differentiation potential. Haematologica. 2003;88:845-52.

[6] Mackay AM, Beck SC, Murphy JM, Barry FP, Chichester CO, Pittenger MF. Chondrogenic differentiation of cultured human mesenchymal stem cells from marrow. Tissue engineering. 1998;4:415-28.

[7] Pittenger MF, Mackay AM, Beck SC, Jaiswal RK, Douglas R, Mosca JD, et al. Multilineage potential of adult human mesenchymal stem cells. Science.

1999;284:143-7.

[8] Drost AC, Weng S, Feil G, Schafer J, Baumann S, Kanz L, et al. In vitro myogenic differentiation of human bone marrow-derived mesenchymal stem cells as a potential treatment for urethral sphincter muscle repair. Annals of the New York Academy of Sciences. 2009;1176:135-43.

[9] Oswald J, Boxberger S, Jorgensen B, Feldmann S, Ehninger G, Bornhauser M, et al. Mesenchymal stem cells can be differentiated into endothelial cells in vitro. Stem Cells. 2004;22:377-84.

[10] Gong Z, Calkins G, Cheng EC, Krause D, Niklason LE. Influence of culture medium on smooth muscle cell differentiation from human bone marrow-derived mesenchymal stem cells. Tissue engineering Part A. 2009;15:319-30.

[11] Chamberlain G, Fox J, Ashton B, Middleton J. Concise review: mesenchymal stem cells: their phenotype, differentiation capacity, immunological features, and potential for homing. Stem Cells. 2007;25:2739-49.

[12] Jorgensen NR, Henriksen Z, Sorensen OH, Civitelli R. Dexamethasone, BMP-2, and 1,25-dihydroxyvitamin D enhance a more differentiated osteoblast phenotype: validation of an in vitro model for human bone marrow-derived primary osteoblasts. Steroids. 2004;69:219-26.

[13] Hildebrandt C, Buth H, Thielecke H. Influence of cell culture media conditions on the osteogenic differentiation of cord blood-derived mesenchymal stem cells. Annals of anatomy = Anatomischer Anzeiger : official organ of the Anatomische Gesellschaft. 2009;191:23-32.

[14] Friedman MS, Long MW, Hankenson KD. Osteogenic differentiation of human mesenchymal stem cells is regulated by bone morphogenetic protein-6. Journal of

cellular biochemistry. 2006;98:538-54.

[15] Stiehler M, Bunger C, Baatrup A, Lind M, Kassem M, Mygind T. Effect of dynamic 3-D culture on proliferation, distribution, and osteogenic differentiation of human mesenchymal stem cells. Journal of biomedical materials research Part A. 2009;89:96-107.

[16] Herbertson A, Aubin JE. Dexamethasone alters the subpopulation make-up of rat bone marrow stromal cell cultures. Journal of bone and mineral research : the official journal of the American Society for Bone and Mineral Research. 1995;10:285-94.

[17] Hong D, Chen HX, Xue Y, Li DM, Wan XC, Ge R, et al. Osteoblastogenic effects of dexamethasone through upregulation of TAZ expression in rat mesenchymal stem cells. The Journal of steroid biochemistry and molecular biology. 2009;116:86-92.

[18] Chang YL, Stanford CM, Keller JC. Calcium and phosphate supplementation promotes bone cell mineralization: implications for hydroxyapatite (HA)-enhanced bone formation. Journal of biomedical materials research. 2000;52:270-8.

[19] Prockop DJ, Kivirikko KI. Collagens: molecular biology, diseases, and potentials for therapy. Annual review of biochemistry. 1995;64:403-34.

[20] Hata R, Senoo H. L-ascorbic acid 2-phosphate stimulates collagen accumulation, cell proliferation, and formation of a three-dimensional tissuelike substance by skin fibroblasts. Journal of cellular physiology. 1989;138:8-16.

[21] Maehata Y, Takamizawa S, Ozawa S, Kato Y, Sato S, Kubota E, et al. Both direct and collagen-mediated signals are required for active vitamin D3-elicited differentiation of human osteoblastic cells: roles of osterix, an osteoblast-related transcription factor. Matrix biology : journal of the International Society for Matrix Biology. 2006;25:47-58.

[22] Fromigue O, Marie PJ, Lomri A. Differential effects of transforming growth factor

beta2, dexamethasone and 1,25-dihydroxyvitamin D on human bone marrow stromal cells. Cytokine. 1997;9:613-23.

[23] Meng X, Leslie P, Zhang Y, Dong J. Stem cells in a three-dimensional scaffold environment. SpringerPlus. 2014;3:80.

[24] Kohara H, Tabata Y. Enhancement of ectopic osteoid formation following the dual release of bone morphogenetic protein 2 and Wnt1 inducible signaling pathway protein 1 from gelatin sponges. Biomaterials. 2011;32:5726-32.

[25] Ikeda T, Ikeda K, Yamamoto K, Ishizaki H, Yoshizawa Y, Yanagiguchi K, et al. Fabrication and characteristics of chitosan sponge as a tissue engineering scaffold. BioMed research international. 2014;2014:786892.

[26] Tajima S, Tabata Y. Preparation and functional evaluation of cell aggregates incorporating gelatin microspheres with different degradabilities. Journal of tissue engineering and regenerative medicine. 2013;7:801-11.

[27] Charlton DC, Peterson MG, Spiller K, Lowman A, Torzilli PA, Maher SA. Semi-degradable scaffold for articular cartilage replacement. Tissue engineering Part A. 2008;14:207-13.

[28] Solorio LD, Dhami CD, Dang PN, Vieregge EL, Alsberg E. Spatiotemporal regulation of chondrogenic differentiation with controlled delivery of transforming growth factor-beta1 from gelatin microspheres in mesenchymal stem cell aggregates. Stem cells translational medicine. 2012;1:632-9.

[29] Mi HY, Palumbo S, Jing X, Turng LS, Li WJ, Peng XF. Thermoplastic polyurethane/hydroxyapatite electrospun scaffolds for bone tissue engineering: Effects of polymer properties and particle size. Journal of biomedical materials research Part B, Applied biomaterials. 2014.

[30] Jose MV, Thomas V, Xu Y, Bellis S, Nyairo E, Dean D. Aligned bioactive multi-component nanofibrous nanocomposite scaffolds for bone tissue engineering. Macromolecular bioscience. 2010;10:433-44.

[31] Atala A, Kasper FK, Mikos AG. Engineering complex tissues. Science translational medicine. 2012;4:160rv12.

[32] Okamoto T, Aoyama T, Nakayama T, Nakamata T, Hosaka T, Nishijo K, et al. Clonal heterogeneity in differentiation potential of immortalized human mesenchymal stem cells. Biochemical and biophysical research communications. 2002;295:354-61.

[33] Takahashi Y, Yamamoto M, Tabata Y. Osteogenic differentiation of mesenchymal stem cells in biodegradable sponges composed of gelatin and beta-tricalcium phosphate. Biomaterials. 2005;26:3587-96.

[34] Tanigo T, Takaoka R, Tabata Y. Sustained release of water-insoluble simvastatin from biodegradable hydrogel augments bone regeneration. J Control Release. 2010;143:201-6.

[35] Oka S, Matsumoto T, Kubo S, Matsushita T, Sasaki H, Nishizawa Y, et al. Local administration of low-dose simvastatin-conjugated gelatin hydrogel for tendon-bone healing in anterior cruciate ligament reconstruction. Tissue engineering Part A. 2013;19:1233-43.

[36] Hokugo A, Saito T, Li A, Sato K, Tabata Y, Jarrahy R. Stimulation of bone regeneration following the controlled release of water-insoluble oxysterol from biodegradable hydrogel. Biomaterials. 2014;35:5565-71.

SUMMARY

Chapter 1

The objective of this chapter is to design biodegradable hydrogels for the controlled release of deferoxiamine (DFO) and evaluate their biological activity. When the DFO was added to human umbilical vein endothelial cells cultured in 5.0% O_2, the level of hypoxia-inducible factor-1α and vascular endothelial growth factor significantly increased compared with that without DFO. The expression of angiogenesis-related genes was accordingly increased by the DFO addition. An aqueous solution of mixed gelatin and DFO was freeze-dried, and dehydrothermally treated to prepare a gelatin hydrogel incorporating DFO. After the hydrogel incorporating DFO was injected intramuscularly into a mouse model of hind limb ischemia, the number of new blood vessels formed was significantly higher than that with free DFO and DFO-free hydrogel. It is concluded that the DFO-containing hydrogel shows promising for inducing angiogenesis locally.

Chapter 2

The objective of this chapter is to design biodegradable hydrogels of gelatin for the controlled release of bioactive small interfering RNA (siRNA). Gelatin was cationized by chemically introducing ethylene diamine into the carboxyl groups in different conditions to obtain cationized gelatins (CGs). The CG was mixed with siRNA at various mixing ratios of amino groups of gelatin to the phosphate groups of siRNA in aqueous solution to form the siRNA-CG nano-complex. Gelatin together with the complex of siRNA and CG was chemically crosslinked to prepare the gelatin hydrogel incorporating the complex. In this release system, the siRNA was released as a result of

hydrogel degradation. The siRNA released showed an activity to specifically suppress the expression of the corresponding gene. The hydrogel is promising to release siRNA and also elicit biological activity for a longer time.

Chapter 3

The objective of this chapter is to design biodegradable hydrogels for the controlled release of low-molecular-weight heparin (LMWH) and evaluate the biological activity. Gelatin was cationized by chemically introducing ethylene diamine into the carboxyl groups in different conditions to obtain cationized gelatins. The cationized gelatin was mixed with the LMWH in aqueous solution to form the complex. Gelatin, together with the complex of LMWH and cationized gelatin, was dehydrothermally cross-linked for different time periods to prepare the gelatin hydrogel-incorporating complex. The half-life period of LMWH release was in good correspondence with that of hydrogel degradation. It is possible that the LMWH was released as the result of hydrogel degradation. When applied to the mouse model of abdominal membrane fibrosis, the hydrogel system of LMWH release showed a promising anti-fibrotic effect.

Chapter 4

The objective of this chapter is to design a drug delivery system (DDS) for the in vivo promotion of macrophage recruitment. As the drug, a water-insoluble agonist of sphingosine-1-phosphate type 1 receptor (SEW2871) was selected. SEW2871 (SEW) was water-solubilized by micelle formation with gelatin grafted by L-lactic acid oligomer. SEW micelles were mixed with gelatin, followed by dehydrothermal

crosslinking of gelatin to obtain gelatin hydrogels incorporating SEW micelles. When implanted into the back subcutis or the skin wound defect of mice, the hydrogel incorporating SEW micelles promoted macrophage migration toward the tissue around the implanted site to a significantly great extent compared with SEW-free hydrogel and that mixed with SEW micelles. The hydrogel is a promising DDS to enhance macrophage recruitment in vivo.

Chapter 5

The objective of this chapter is to design hydrogel sponges for the controlled release of dexamethasone (Dex) and active vitamin D_3 (1,25-D_3). The Dex and 1,25-D_3 were water-solubilized by the micelle formation with gelatin grafted by L-lactic acid oligomer. Three-dimensional sponge scaffolds of gelatin hydrogel incorporating Dex- and 1,25-D_3-micelle were prepared. The human mesenchymal stem cells (hMSC) were seeded into the sponge by an agitated seeding method. When the Dex and 1,25-D_3 were added to an osteogenic differentiation medium, the level of alkaline phosphatase (ALP) activity and the amount of mineralization of hMSC significantly increased compared with those of 1,25-D_3-free medium. Moreover, gelatin sponges incorporating Dex- and 1,25-D_3-micelle showed the highest amount of mineralization compared with other sponges.

LIST OF PUBLICATIONS

Chapter 1. **T. Saito**, Y. Tabata, Hypoxia-induced angiogenesis is increased by the controlled release of deferoxiamine from gelatin hydrogels, Acta biomaterialia, 10 (2014) 3641-3649.

Chapter 2. **T. Saito**, Y. Tabata, Preparation of gelatin hydrogels incorporating small interfering RNA for the controlled release, Journal of drug targeting, 20 (2012) 864-872.

Chapter 3. **T. Saito**, Y. Tabata, Preparation of gelatin hydrogels incorporating low-molecular-weight heparin for anti-fibrotic therapy, Acta biomaterialia, 8 (2012) 646-652.

Chapter 4. M. Murakami, **T. Saito**, Y. Tabata, Controlled release of sphingosine-1-phosphate agonist with gelatin hydrogels for macrophage recruitment, Acta biomaterialia, 10 (2014) 4723-4729.

Chapter 5. In preparation.

OTHER PUBLICATIONS

T. Okamoto, T. Saito, Y. Tabata, S. Uemoto, Immunological tolerance in a mouse model of immune-mediated liver injury induced by 16,16 dimethyl PGE2 and PGE2-containing nanoscale hydrogels, Biomaterials, 32 (2011) 4925-4935.

T. Fukui, M. Ii, T. Shoji, T. Matsumoto, Y. Mifune, Y. Kawakami, H. Akimaru, A. Kawamoto, T. Kuroda, T. Saito, Y. Tabata, R. Kuroda, M. Kurosaka, T. Asahara, Therapeutic effect of local administration of low-dose simvastatin-conjugated gelatin hydrogel for fracture healing, Journal of bone and mineral research : the official journal of the American Society for Bone and Mineral Research, 27 (2012) 1118-1131.

S. Oka, T. Matsumoto, S. Kubo, T. Matsushita, H. Sasaki, Y. Nishizawa, T. Matsuzaki, T. Saito, K. Nishida, Y. Tabata, M. Kurosaka, R. Kuroda, Local administration of low-dose simvastatin-conjugated gelatin hydrogel for tendon-bone healing in anterior cruciate ligament reconstruction, Tissue engineering. Part A, 19 (2013) 1233-1243.

A. Hokugo, T. Saito, A. Li, K. Sato, Y. Tabata, R. Jarrahy, Stimulation of bone regeneration following the controlled release of water-insoluble oxysterol from biodegradable hydrogel, Biomaterials, 35 (2014) 5565-5571.

T. Matsuzaki, T. Matsushita, Y. Tabata, T. Saito, T. Matsumoto, K. Nagai, R. Kuroda, M. Kurosaka, Intra-articular administration of gelatin hydrogels incorporating rapamycin-micelles reduces the development of experimental osteoarthritis in a murine model, Biomaterials, 35 (2014) 9904-9911.

P. Thitiwuthikiat, M. Ii, T. Saito, S. Kanokpanont, Y. Tabata, A Vascular Patch Prepared from Thai Silk Fibroin and Gelatin Hydrogel Incorporating Simvastatin-Micelles to Recruit Endothelial Progenitor Cells, Tissue engineering. Part A, (2014).

ACKNOWLEDGEMENTS

The present research was carried out under the continuous guidance of Dr. Yasuhiko Tabata, Professor of the Institute for Frontier Medical Sciences, Kyoto University. The author is deeply indebted to Professor Tabata for his constant guidance, encouragement, valuable discussion, and detailed criticism on the manuscript throughout the present work. The completion of the present research has been an exciting project and one which would not have been possible without his guidance.

The author wishes to express his special thanks to Dr. Masaya Yamamoto, Associate Professor of the Institute for Frontier Medical Sciences, Kyoto University, for his thoughtful guidance, helpful suggestions, and intimate advice.

The author wishes to express his special thanks to Dr. Jun-ichiro Jo, Assistant Professor of the Institute for Frontier Medical Sciences, Kyoto University, for his thoughtful guidance, helpful suggestions, and intimate advice.

The author is much indebted to Mr. Masahiro Murakami for his contribution to the present studies.

The author likes to take an opportunity to extend his heartily thanks to Mrs. Kyoto Bamba, Mrs. Hisako Yoshida, Ms. Yui Iwane, Ms. Nami Yoshioka, Mrs. Kaori Takahashi, Secretary to Professor Yasuhiko Tabata and other members of Professor Tabata's Laboratory for their kind help and kindness.

Finally, the author is deeply indebted to his parents, Tsuyoshi and Yuko.

January, 2015

Kyoto

Takashi Saito